

Master's Thesis – Master Water Science and Management

Modelling Alternative Drinking Water Extraction Strategies for the Sandy Pleistocene Regions of the Netherlands

A northern Achterhoek case-study towards hydro-environmental sustainability

//

- Alternatieve winningsstrategieën voor een duurzame drinkwatervoorziening -

By

J. C. van Lieshout

In partial fulfillment of the requirements for the degree of

Master of Science

Water Science and Management
at the Faculty of Geosciences
Utrecht University

11 July 2021

Word count: 12,982



Universiteit Utrecht

KWR Watercycle
Research
Institute

AUTHOR INFORMATION

Jasper Christiaan van Lieshout
5726786
MSc Water Science and Management
(J.c.vanlieshout@students.uu.nl, tel. 06 42093180)

EDUCATIONAL INFORMATION

Utrecht University
Faculty of Geosciences
Copernicus Institute of Sustainable Development
Heidelberglaan 8, 3584 CS Utrecht

Supervisor: dr. Jaivime Evaristo
(J.evaristo@uu.nl, tel. 030 2533147)
Second reader: prof. dr. Stefan Dekker
(S.c.dekker@uu.nl, tel. 030 2532260)

INTERNSHIP INFORMATION

KWR Water Research Institute
Groningenhaven 7, 3433 PE Nieuwegein

Supervisor: dr. Marjolein van Huijgevoort
(Marjolein.van.Huijgevoort@kwrwater.nl, tel. 06 54294367)
Second reader: dr. Klaasjan Raat
(Klaasjan.Raat@kwrwater.nl, tel. 06 53190810)

Abstract

Sufficient provision of high-quality drinking water is vital to a healthy society and the prosperity of local industries, agriculture, and energy sectors. For the sandy Pleistocene regions of the Netherlands, phreatic aquifers are the primary sources of drinking water. However, future socio-economic and climatological stresses increasingly exert pressure on the sustainable utilization of these sources; resulting in an onset of groundwater depletion, drought enhancement, and degradation of groundwater-dependent ecosystems. To ensure adequate water availability whilst maintaining hydro-environmental functioning, the strategic and sustainable management of groundwater is crucial. Changing to alternative manners of exploitation (i.e. strategies) of these regional groundwater sources could help to reduce impacts. However, which alternative strategies are viable, and how they affect the regional hydro-environment remains poorly understood

This thesis presents an explorative regional study in pursuit of a sustainable drinking water provision system from groundwater for these regions. The approach followed the identification and conceptualization of two innovative alternative extraction strategies: decentralized extractions and seasonal extractions. By a comprehensive quantitative scenario analysis, specified to the northern Achterhoek as case-study, both strategies were evaluated by their impacts on regional groundwater levels, soil moisture content, and evapotranspiration. The hydrological and environmental effects were quantified using the novel developed geohydrological model AMIGO (v3.1) and compared to a reference scenario for the period 01-04-2004 to 31-12-2019.

The results showed that decentralization, and to less extent seasonal extractions, can have a beneficial effect on regional groundwater levels. Decentralized extractions indicated a positive relation to the reduction of local drawdown, increasing under higher quantities of decentralized volumes (0 – 15%). Both the extent and intensity outweighed the adverse effects at decentral locations. Seasonal extractions were found slightly less effective (0 – 5%), except when applied in large volumes (5 – 15%), but showed potential to optimize annual water containment on a regional-scale. The positive effects of both strategies, however, only locally propagated to soil moisture content (0 – 10%) and minimally enhanced regional evapotranspiration (< 1%). The deep groundwater tables prohibited effective interactions ensuing changes in groundwater level, indicating that hydro-environmental functioning could only limitedly be improved under both strategies.

Whilst the results were bilateral, the implications are likely valuable to water managers assessing strategies from a multi-directional perspective. Inevitably, a transdisciplinary approach is required to meet demand and achieve a sustainable drinking water provision. This explorative work thereby contributes by paving the road to more detailed studies and hinting at rough directions of potential future sustainability.

Keywords: Drinking water, Sustainability, Groundwater, Extraction strategies, Pleistocene uplands

Acknowledgments

This master's thesis completes the final requirements of the masters program Water Science and Management at Utrecht University. During the last 21 weeks, I have worked on this thesis project with high enjoyment as part of a simultaneous internship at KWR Water Research Institute. As my five-year period at Utrecht University hereby comes to an end, I would like to acknowledge some individuals whose contributions were vital during this last phase.

Foremost, I would like to thank dr. Marjolein van Huijgevoort (KWR) for her extensive and enthusiastic guidance during this thesis and internship. Without our thorough weekly discussions and her support to secure accurate model functioning and results, this thesis would not have been possible. I would also like to thank KWR Water Research Institute, specifically teams eco- and geo-hydrology and dr. Klaasjan Raat, for their open welcome and willingness to assist at any time during the last five months.

Furthermore, I would like to thank my Utrecht University supervisor, dr. Jaivime Evaristo, for his critical feedback, reflectance, and support to achieve an academically sound thesis during COVID-19 restricted times. Additional gratitude goes to the second reader, prof. dr. Stefan Dekker (UU), for his time and feedback on the research proposal.

I would like to thank dr. Jelle van Sijl (Vitens), dr. Jan Jaap Buyse (Vitens), and dr. ir. Gijsbert Cirkel (KWR) for their time and feedback on preliminary results and swift responses to provide a suitable alternative model after initial ideas midway got unavoidably unobtainable. Thereby thank goes to Arcadis NV for permission to use their novel developed version of the hydrogeological model AMIGO.

Lastly, but most heartily, I would like to thank my family for their continuous love and support.

Table of Contents

CHAPTER 1 INTRODUCTION.....	7
1.1 INTRODUCTION AND PROBLEM DEFINITION	7
1.2 KNOWLEDGE GAP	8
1.3 RESEARCH AIM AND QUESTIONS	9
1.4 READING GUIDE.....	9
CHAPTER 2 THE SANDY PLEISTOCENE REGIONS OF THE NETHERLANDS.....	10
2.1 GEOMORPHOLOGICAL BACKGROUND	10
2.2 HYDROGEOLOGICAL CHARACTERISTICS	10
2.3 CASE-STUDY: THE NORTHERN ACHTERHOEK.....	12
2.3.1 <i>The natural system</i>	12
2.3.2 <i>Current groundwater extractions</i>	14
CHAPTER 3 THEORETICAL FRAMEWORK.....	15
3.1 GROUNDWATER DEPLETION	15
3.2 HYDRO-ENVIRONMENTAL SUSTAINABILITY	16
CHAPTER 4 METHODOLOGY	18
4.1 CONCEPTUAL MODEL	18
4.1.1 <i>Alternative strategy 1: Decentralized extractions</i>	18
4.1.2 <i>Alternative strategy 2: Seasonal extractions</i>	18
4.2 HYDROGEOLOGICAL MODEL SETUP	19
4.2.1 <i>Actueel Model Instrument Gelderland Oost (AMIGO)</i>	19
4.2.2 <i>Parameterization, boundary conditions, and meteorological data</i>	20
4.2.3 <i>Calibration and justification</i>	23
4.3 SCENARIO DEVELOPMENT	23
4.3.1 <i>Baseline scenario</i>	24
4.3.2 <i>Alternative scenarios</i>	24
4.4 SCENARIO ANALYSIS	27
CHAPTER 5 RESULTS.....	28
5.1 GROUNDWATER.....	28
5.1.1 <i>Baseline scenario</i>	28
5.1.2 <i>Decentralized scenarios</i>	30
5.1.3 <i>Seasonal scenarios</i>	33
5.2 SOIL MOISTURE CONTENT	36
5.2.1 <i>Baseline scenario</i>	36
5.2.2 <i>Decentralized scenarios</i>	38
5.2.3 <i>Seasonal scenarios</i>	41
5.3 EVAPOTRANSPIRATION	44
5.3.1 <i>Baseline scenario</i>	44
5.3.2 <i>Decentralized scenarios</i>	45
5.3.3 <i>Seasonal scenarios</i>	48

CHAPTER 6 DISCUSSION.....	50
6.1 LIMITATIONS, ASSUMPTIONS, AND UNCERTAINTIES	50
6.1.1 <i>Model limitations</i>	50
6.1.2 <i>Scenario assumptions</i>	51
6.1.3 <i>Uncertainty analysis</i>	51
6.2 DISCUSSION OF THE RESULTS	51
6.2.1 <i>Noteworthy results</i>	51
6.2.2 <i>Evaluation of the alternative strategies</i>	52
6.3 RESEARCH IMPLICATIONS	53
6.4 RECOMMENDATIONS AND FUTURE RESEARCH.....	54
CHAPTER 7 CONCLUSION	55
CHAPTER 8 REFERENCES.....	56
CHAPTER 9 APPENDICES	65
APPENDIX A	65
APPENDIX B	68
APPENDIX C	73
APPENDIX D	75
APPENDIX E.....	78
APPENDIX F.....	81
APPENDIX G	82

Chapter 1 Introduction

1.1 Introduction and problem definition

Sufficient provision of high-quality drinking water is one of the building blocks of a healthy functioning society (Glavan, 2018; Sachs et al., 2020). As defined by the United Nations (UN), access to an adequate supply of clean drinking water is a human right, and both the quantitative and qualitative components have obtained a prominent role in the novel Sustainable Development Goals (SDG6; Sachs et al., 2020). In addition to meeting humanitarian needs, drinking water provision is imperative to the prosperity of local industries, agricultural businesses, and energy sectors (Klijn et al., 2012). To avoid water scarcity for all sectors, available water sources must be strategically managed for both present-day and future scenarios (Castilla-Rho et al., 2019; McDonald et al., 2011; Sahoo & Jha, 2017).

In the Netherlands, aquifers are the primary sources of drinking water, and several provinces solely depend on groundwater extractions for their drinking water supply (e.g. Brabant, Drenthe, Overijssel; van Engelenburg et al., 2021). The utilization of groundwater as principal source is often preferred due to the high water quality, low exploitation costs, and generally widespread availability (Dinica, 2014; Vandenbohede et al., 2009). To meet socio-economic demand, groundwater is pumped continuously from preferably centralized locations. However, large-scale aquifer exploitation has exposed the realistic threat of groundwater depletion, and academics increasingly pose questions concerning the sustainability of the demand-based groundwater extractions (Aeschbach-Hertig & Gleeson, 2012; Bierkens & Wada, 2019; Gleeson et al., 2020). Groundwater is currently treated as a non-renewable resource. Consequently, extractions exert pressure on the equilibrium between groundwater levels and natural environmental recharge (Lóaiciga & Leipnik, 2001). Groundwater depletion does not only diminish the water availability; impacts also include regional land subsidence, deterioration of water quality through increased saline lenses, soil drought enhancement, and degradation of groundwater-dependent ecosystems (Bierkens & Wada, 2019; Sahoo & Jha, 2017). The latter is defined as detrimental to the sustainability of the regional environment and agriculture.

Additionally, future climatological trends and socio-economic developments are expected to further threaten groundwater sources (Klijn et al., 2012). The Royal Netherlands Meteorological Institute (KNMI) has projected the consequences of an intensified hydrological cycle: indicating a more frequent drought risk and higher precipitation intensities (Bruggeman et al., 2011). Moreover, abiding population growth and economic prosperity will increase freshwater demand up to 35% by the year 2050 (Wolters et al., 2018). Combined with an increasingly overloaded subsurface (e.g. geothermal energy) and rising groundwater pollution (e.g. agricultural, industrial), the sustainable management of groundwater (i.e. meeting anthropogenic water demand without deteriorating the hydro-environment) constitutes a growing body of both fundamental and applied water research (Aeschbach-Hertig & Gleeson, 2012; Mays, 2013).

The phreatic aquifers in the sandy Pleistocene regions of the Netherlands are exemplary of particularly vulnerable groundwater sources. The sand-dominated highly permeable subsurface prohibits effective water containment and enhanced rapid infiltration. Moreover, in these higher elevated regions surface water infiltration is limited, and precipitation is often the sole source of replenishment to local groundwater reserves (Doorn & Jalink, 2017).

To still achieve sustainable drinking water provision from groundwater for these regions, structural improvements are imperative (Spek et al., 2010). Local governments and scientific institutes have identified the need for a 'climate-robust water transition', corresponding to a structurally redesigned system equipped to meet socio-economic demand whilst preserving hydro-environmental functioning (Chan et al., 2014; Jeuken et al., 2015; Klijn et al., 2012). Transitioning towards sustainability requires the introduction of supplementary sources or alternative groundwater extraction strategies. This thesis focuses on the latter as a crucial explorative pathway.

As local groundwater exploitation is often still preferred, it is vital to understand the effects of alternative extraction strategies. An extraction strategy is defined as the spatial and temporal manner of utilization of a groundwater source (e.g. pumping timing, proportioning, depth, location). Alternative extraction strategies by alterations to these characteristics in both space and time (e.g. decentralization, deep-groundwater extractions, seasonal extractions) are progressively identified as potentially viable (Jansen et al., 2021; van Alphen & Frijns, 2014). However, to implement structural alternatives, comprehensive knowledge is required beforehand on both the effectiveness of a strategy and its impact on the hydro-environmental system (Bartholomeus et al., 2021). Which alternative strategies are effective and to what extent they affect the local hydro-environment remains yet unclear.

1.2 Knowledge gap

KWR Water Research Institute has made significant progress in its research towards a sustainable drinking water supply for the sandy Pleistocene regions of the Netherlands (e.g. Bartholomeus et al., 2020, 2021; van Loon et al., 2014). Moreover, research on sustainable aquifer extractions strategies to combat future climatological and socio-economic stresses has been executed in multiple studies (e.g. Roumasset & Wada, 2010; Sahoo & Jha, 2017; Vandenbohede et al., 2009). However, accurate predictions on the impacts of alternative strategies on local hydro-environmental functioning have been scarce, and strong supporting quantitative data analyses are often lacking (Aeschbach-Hertig & Gleeson, 2012; Custodio et al., 2005).

Furthermore, structural improvements to groundwater extractions in the form of spatial and temporal adjustments are only sporadically explored. Particularly, the concepts of decentralization and seasonal extractions lack a fundamental literary basis as significant practical interest is relatively novel. Most commonly, studies explored compensational strategies such as artificial recharge (Kumar et al., 2008; van Engelenburg et al., 2020), deep-well injections (Page et al., 2018), or temporal sub-surface storage (Khan et al., 2008; Rambags et al., 2013). Whilst promising results are periodically observed, their effectiveness is firmly embedded in the local technical, environmental, and socio-economic characteristics (van Engelenburg et al., 2019). Case-specific circumstances dominate concluding findings, requiring unique extraction strategies per region. Consequently, the uniform application of established strategies in the Pleistocene regions of the Netherlands is obstructed, and more region-specific research is needed.

1.3 Research aim and questions

The main objective of this thesis is to test to what extent spatial and temporal adjusted extraction strategies could enhance the sustainable utilization of regional groundwater sources for the Pleistocene regions of the Netherlands. This study aims to contribute to both the practical (i.e. societal) field and the academic field by expanding scientific knowledge on sustainable aquifer extractions. Consequently, the following research question is formulated guiding this thesis:

To what extent can implementation of local alternative drinking water extraction strategies by spatial and temporal adjustments contribute to the sustainable utilization of regional groundwater sources for the sandy Pleistocene regions of the Netherlands?

The main research question is answered by a division into two sub-questions, collectively providing an integrated result:

- I. *What is the effect of implementation of local alternative drinking water extraction strategies by spatial and temporal adjustments on the regional groundwater levels?*
- II. *What is the effect of implementation of local alternative drinking water extraction strategies by spatial and temporal adjustments on the regional soil moisture content and evapotranspiration?*

1.4 Reading guide

This thesis contains the following chapters. First, the hydrological functioning of the sandy Pleistocene regions of the Netherlands and the selected case-study are described in Chapter 2. Hereafter, a brief theoretical framework is presented in Chapter 3, elaborating on sustainability in groundwater extractions. Chapter 4 consists of two sections. The first sub-chapter conceptualizes the evaluated alternative strategies. The following sub-chapters present the quantitative methodology, including hydrological model set-up, scenario development, and analysis methods. Chapter 5 presents the results of this thesis, structured alongside the research questions. Chapter 6 discusses the results against the current body of literature and critically examines the reliability, limitations, and applicability of the applied approaches and outcomes. Chapter 7 finalizes this thesis by presenting the main conclusions.

Chapter 2 The sandy Pleistocene regions of the Netherlands

2.1 Geomorphological background

The sandy Pleistocene regions of the Netherlands comprise the elevated North-East to South-East of the Netherlands (Figure 1; Zoetwatervoorziening Oost-Nederland, 2017). While the spatial extent of these uplands is widespread, they predominantly comprise the provinces Overijssel, Drenthe, Gelderland, Noord-Brabant, and Limburg. The landscape is characterized by its unique geomorphology and dominant sand and loam deposits, originating from the Pleistocene epoch [2.6 ma – 11,7 ka] (Stouthamer et al., 2020; Wesselingh, n.d.). Fluctuating interglacial warm periods during the early-to-mid Pleistocene induced an alteration of riverine valley erosion and fluvial deposition (Berendsen, 2015; Stouthamer et al., 2020). Consequently, various fine-to-course sand-characterized layers were deposited throughout the Netherlands (e.g. Kreftenheye formation, Stramproy formation, Peize formation; Berendsen & Stouthamer, 2008). Scandinavia's subsequent glacial frontiers pushed the sandy deposits, including other unconsolidated materials, into high ridges (Berendsen, 2015). These moraines (*stuwwallen*) remained after deglaciation. Ultimately, as the late Pleistocene was characterized by its strong polar winds, sandy materials continuously eroded from the dried-up unvegetated oceanic floors. Consequently, fine aeolian sand deposits (cover sands; *dekzanden*) can be found ubiquitous in the uplands of the Netherlands (e.g. Bostel formation; Stouthamer et al., 2020). Naturally, however, the exact sedimentological structure is location-dependent.

2.2 Hydrogeological characteristics

The moraines, cover sands, and stream valleys define the current functioning of the groundwater system in the Pleistocene uplands. In general, the Pleistocene sandy topsoil and subsurface are characterized by their high conductive nature and often overlay a deep thin aquitard layer of Miocene clay (Stouthamer et al., 2020). The high permeability of the sandy soils results in a high infiltration capacity, low moisture containment, and reduced residence times of water in the unsaturated zone (Doorn & Jalink, 2017). As local groundwater recharge often relies solely on precipitation due to limited surface water availability, rapid drainage hampers the quantitative buffer capacity of the soil. Consequently, the groundwater system is susceptible to changes in precipitation regimes associated with both seasonality and enhanced climate change (Doorn & Jalink, 2017; Hendriks, 2010).

However, the effect of fluctuating precipitation volumes depends on local factors. Important parameters herein are the thickness of the unsaturated zone, infiltration rates, interactions between infiltration regions and seepage faces, and groundwater extractions (Bartholomeus et al., 2020). Specifically in areas containing cover sand dominated soils, precipitation excess is discharged through the shallow soil towards creeks. Here, the unsaturated zone acts as a highly dynamic system and leads to low residence times (Doorn & Jalink, 2017). The thickness of the aquiferous top sand layer primarily defines the soil residence times (Hendriks, 2010). Observations state an average thickness of 10 meters, roughly corresponding to a ten-year residence time. Due to deep groundwater levels and limited capillary rise, elevated cover sands are often vegetated with non-groundwater dependent vegetation, whilst lower-elevated stream valleys function as agricultural grounds (Bakel et al., 2008; Doorn & Jalink, 2017).

In contrast, moraines contain relatively deep groundwater levels and thereby predominantly fulfill a groundwater recharging function in the long-term. Characterized by a thick unsaturated layer, moraines evoke a less dynamic system and enhance residence times in the order of 50 years (Doorn & Jalink, 2017; Hendriks, 2010). Consequently, these regions are less vulnerable to fluctuations in precipitation (van Engelenburg et al., 2020). The geomorphologic origin of moraines however hampers effective predictions due to highly varying local lithologies. Furthermore, infiltration is highly vegetation-dependent and can vary significantly on a local basis (Doorn & Jalink, 2017).

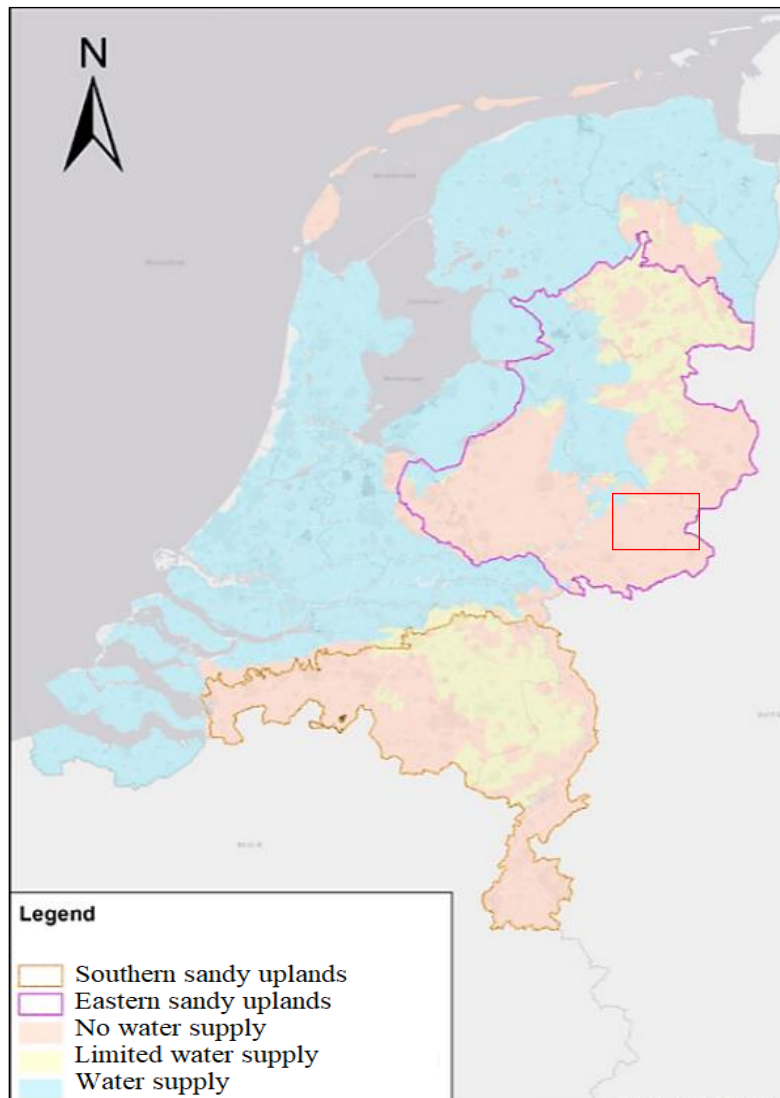


Figure 1. Schematic overview of the spatial extent of the Southern and Eastern sandy Pleistocene regions of the Netherland (Zoetwatervoorziening Oost-Nederland, 2017). The red borders are indicative of the location of the northern Achterhoek region used as detailed case-study for this thesis (see Chapter 2.3).

2.3 Case-study: The northern Achterhoek

The northern Achterhoek (52.01 °N, 6.39 °E) in the province of Gelderland was selected as a representative case-study (Figure 2). The spatial extent stretches approximately 50,000 ha from the German border (20 – 30 m NAP) to the floodplain of the IJssel river (0 – 10 m NAP).

2.3.1 The natural system

The geological subsurface inclines towards the West, with the hydrological base present at the Miocene clay of the Breda formation (Figure 3; Hummelman et al., 2019; TNO, 2021). Whilst an additional layer of deep marine deposits of the Oosterhout formation is present in the eastern section, the near-surface morphology of this region predominantly consists of Pleistocene sands. Fine-grained highly-permeable fluvial sands from the Urk, Drenthe, and Kreftenheye formation form the first phreatic aquifer layer of approximately 20 to 40 meters thick. Regionally thin impermeable aquitard layers of boulder clays act as confining elements (TNO, 2021). The lithology of the topsoil is defined by loamy to fine-grained cover sands from the Boxtel formation, present amongst the first 5 – 10 m in the whole cross-section (Stouthamer et al., 2020; TNO, 2021). In North-South direction, the geohydrological structure corresponds to the linear horizontal extension of the presented West-East cross-section. Furthermore, a hydraulic flow gradient is present in South-East to North-West direction, consequent to the elevation disparity. The groundwater drainage direction varies locally based on moraines presence, land use, and groundwater extractions (Berendsen & Stouthamer, 2008; van Beek et al., 2007).

Natural hydrological recharge comprises precipitation predominantly. Annual precipitation varies between 825 – 850 mm, with monthly minima defined at 52 mm in April (Beersma et al., 2019). During summer months, regional evaporation exceeds precipitation, thereby inducing monthly net precipitation deficits from April to August (Bakel et al., 2008; Witte et al., 2020). Surface waters are limitedly present and restricted to local tributaries of the IJssel river (e.g. Baakse Beek, Berkel, Slinge). Respectively, the seasonally averaged discharges of these streams are 2.1, 10, 12, and 0.7 m³/s. Spek et al. (2010) concluded that over 80% of the surface waters fall dry during the summer months. The IJssel river (340 m³/s) functions as primary surface water drainage outlet for the northern Achterhoek (van Beek et al., 2007).

Agricultural grasslands dominate land cover in the northern Achterhoek. In particular, around extraction locations (< 100-year zone), 70 – 95% of the total area comprises agricultural fields (Breman et al., 2013; van Beek et al., 2007). Forested areas regionally prevail on the elevated cover sands and moraines. Furthermore, a variety of biodiverse nature areas are located in local stream valleys. Herein groundwater-dependent environments, like wet meadows (*blauwgrasland*) and peat remnants (*hoogveenrestanten*), are widely present (Breman et al., 2013; P. C. Jansen et al., 2013). Within these low-lying environments, stable groundwater levels are vital to ensure vegetation prosperity. Moreover, agricultural grasslands contain high evaporation rates and are vulnerable to lowered groundwater levels (Witte et al., 2020).

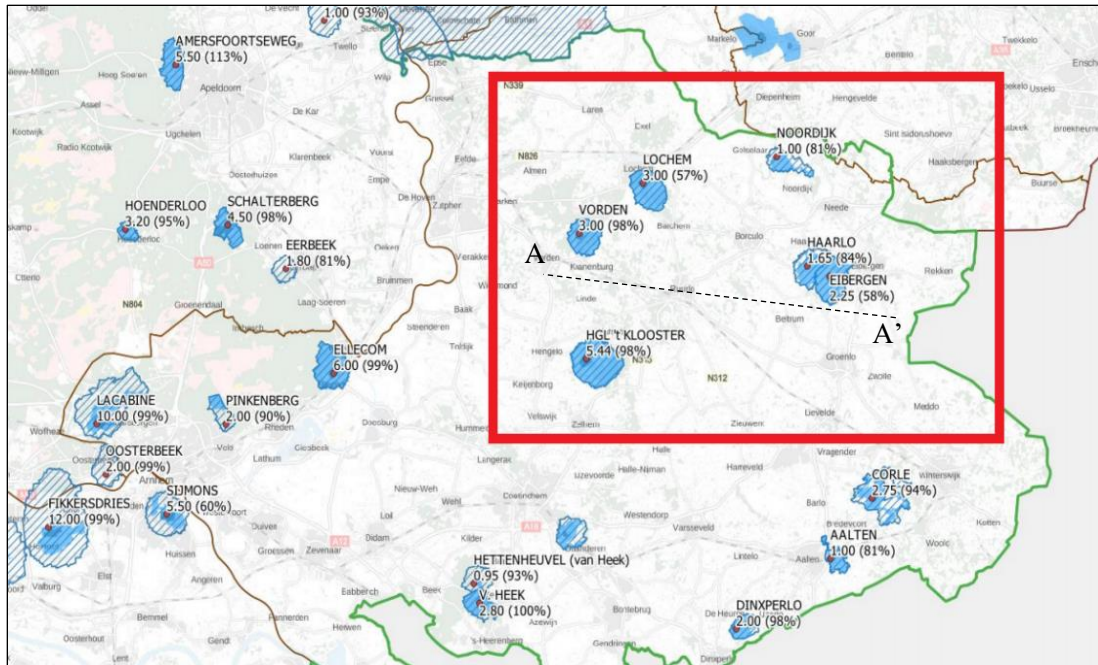


Figure 2. Overview of the northern Achterhoek region (red border). Groundwater extraction locations of Vitens are presented by name, annual extraction [10^6 m^3], utilized percentage of permitted annual extraction, and recharge area [blue shaded regions] (van Sijl & Giesbers, 2020). The black dashed line represent the cross-section taken (See Figure 3).

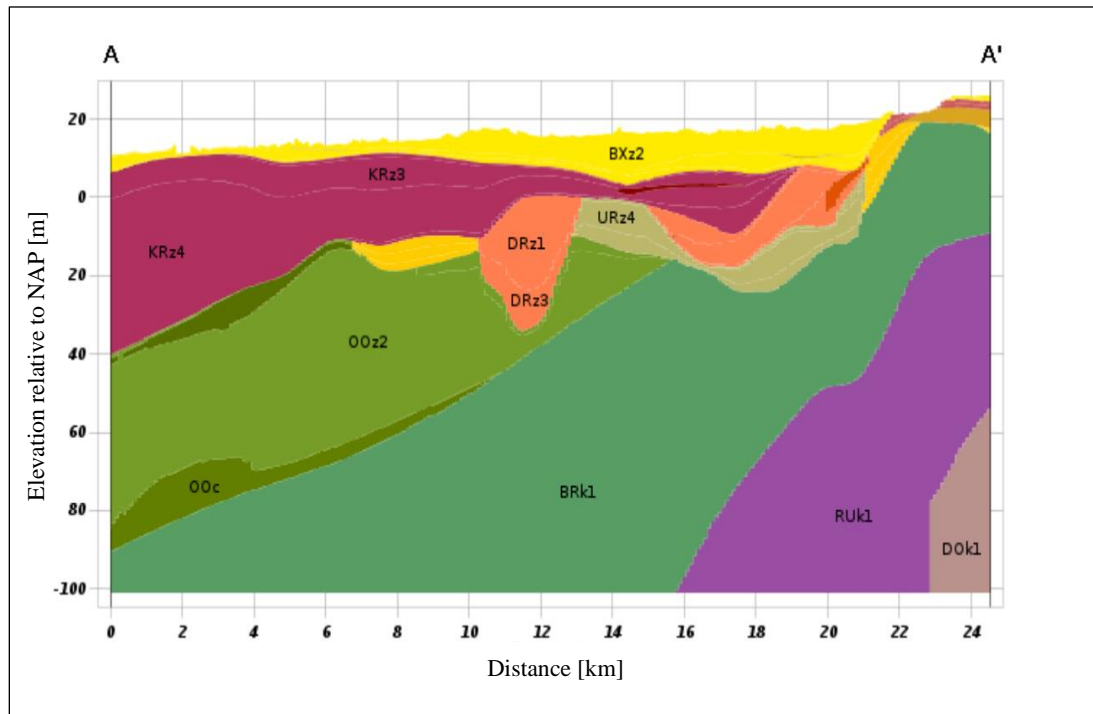


Figure 3. Geohydrological cross-section of the northern Achterhoek region in West-East direction (Hummelman et al., 2019; TNO, 2021). Hydrogeological layers according to Regis II v2.2: BxZ = Boxtel formation (sand), KRz = Kreftenheye formation (sand), URz = Urk formation (sand), DRz = Drenthe formation (sand), OOz = Oosterhout formation (sand), OOc = Oosterhout formation (clay), BRk = Breda formation (clay). Note: a vertical exaggeration is applied on the y-axis.

2.3.2 Current groundwater extractions

The present-day extractions are characterized by their centralized location and demand-based pumping. Groundwater extractions take place at six locations proprietary to Vitens (resp. drinking water company): 't Klooster, Lochem, Vorden, Noordijk, Haarlo, and Eibergen (Figure 2: van Sijl & Giesbers, 2020). Collectively the six sites acquire approximately $13.48 \cdot 10^6 \text{ m}^3$ groundwater annually. 't Klooster and Vorden, respectively 5.33 and $2.93 \cdot 10^6 \text{ m}^3$, act as the most significant contributors (Table 1; Folmer et al., 2012a, 2012b). Lochem, Noordijk, Haarlo and Eibergen contribute in lesser quantities. Within the region, three supply circuits are present. Groundwater extracted from 't Klooster and Vorden is individually distributed and treated, whilst water from Lochem, Noordijk, and Haarlo is transported to Eibergen for water treatment processing before further redistribution (Vergouwen et al., 2016).

Table 1. Characteristics of the six well-systems in the northern Achterhoek. Constructed based on Folmer et al. (2012a, 2012b), van Sijl & Giesbers (2020), van Vugt et al. (2017), and Verhagen et al. (2011). ¹Summer = $\sum(\text{Apr-Sep})$, Winter = $\sum(\text{Oct-Mar})$.

Well system	Location [latitude, longitude]	Permitted yield [m ³ / yr]	Utilization [%]	Net yield [m ³ / yr]	Seasonality [Summer / Winter] ¹	Elevation [m +NAP]	Well depths [m]
't Klooster	52.05, 6.35	$5.44 \cdot 10^6$	98	$5.33 \cdot 10^6$	1.09	15	-18 – -35
Vorden	52.12, 6.35	$3.00 \cdot 10^6$	98	$2.93 \cdot 10^6$	1.25	13	-20 – -38
Lochem	52.15, 6.48	$3.00 \cdot 10^6$	57	$1.72 \cdot 10^6$	1.00	15	-20 – -50
Noordijk	52.16, 6.55	$1.00 \cdot 10^6$	81	$0.81 \cdot 10^6$	1.04	15	-15 – -30
Haarlo	52.11, 6.58	$1.65 \cdot 10^6$	84	$1.38 \cdot 10^6$	1.61	18	-15 – -30
Eibergen	52.09, 6.61	$2.25 \cdot 10^6$	58	$1.31 \cdot 10^6$	1.13	20	-15 – -30

Interseasonal trends in extractions volumes are present amongst all locations, exempting Lochem. To meet demand, summer extractions exceed winter extractions by limited to considerable margins (4 to 61%; Table 1). Moreover, while 't Klooster and Vorden operate near their permitted yield, Lochem only extracts around half its permitted yield. (van Sijl & Giesbers, 2020; Verhagen et al., 2011). The cluster Haarlo and Eibergen has an additional superimposed combined maximum permitted yield of $2.8 \cdot 10^6 \text{ m}^3/\text{yr}$. Vergouwen et al. (2016) determined furthermore that Lochem reached its maximum technological capacity.

The western locations, 't Klooster, Vorden, and Lochem, extract at relatively deep depths from the phreatic aquifer, utilizing the local Kreftenheye or Oosterhout layers (Table 1). For the higher-elevated locations in the North-East, the presence of sand-filled Pleistocene gullies is essential. Haarlo, Noordijk, and Eibergen exploit this morphological structure to extract from the aquiferous layers of the Drenthe and local Urk formation (Verhagen et al., 2011; Waterschap Rijn en IJssel, 1998). For Haarlo and Eibergen, a local thin clay aquitard layer acts as a partly-confining element (Vergouwen et al., 2016).

Supplementary site-specific and geohydrological information can be found in Appendix A.

Chapter 3 Theoretical framework

3.1 Groundwater depletion

Understanding whether alternative strategies could enhance the sustainability of the groundwater system prerequisites knowledge on the theory behind groundwater depletion. The continuous pumping of groundwater provokes changes in flow regimes and the development of horizontal hydrological gradients in the local subsurface (Figure 4; Brozović et al., 2006; House of Water and Environment, n.d.). Consequently, piezometric drawdown is induced, forming a depression cone around the extraction well. Theim's well equation theorizes the concept drawdown in unconfined aquifers for steady radial flow:

$$S = (h_r^2 - h_w^2) = \frac{Q}{\pi k} \ln \left(\frac{r}{r_w} \right) \quad (\text{Fitts, 2013})$$

With S = drawdown, h_r and h_w = hydraulic head at distance r and the well location, respectively, Q = extraction rate, k = permeability coefficient, r = distance from well, and r_w = well radius.

The extent of the drawdown at distance r thereby is defined as the critical relation between (1) the extraction volume, (2) soil permeability, and (3) the well's distance (Brozović et al., 2006; Essink, 2001). Higher extraction volumes consequently result in a more substantial drawdown. As a system contains a multitude of wells, interactions between overlapping regions could occur. The total drawdown for these systems can be estimated by linear superposition (Brozović et al., 2010; Neuman, 1972). Additionally, Brozović et al. (2010) argued the theoretical optimization of extractions based on further distances from neighbouring wells due to the linear logarithmic correlation of drawdown to the well distance. Furthermore, Fitts (2013) established the high site-specific influence of permeability through soil heterogeneity on groundwater velocities and drawdown. All three parameters are hereby imperative to the quantitative extent of the total drawdown.

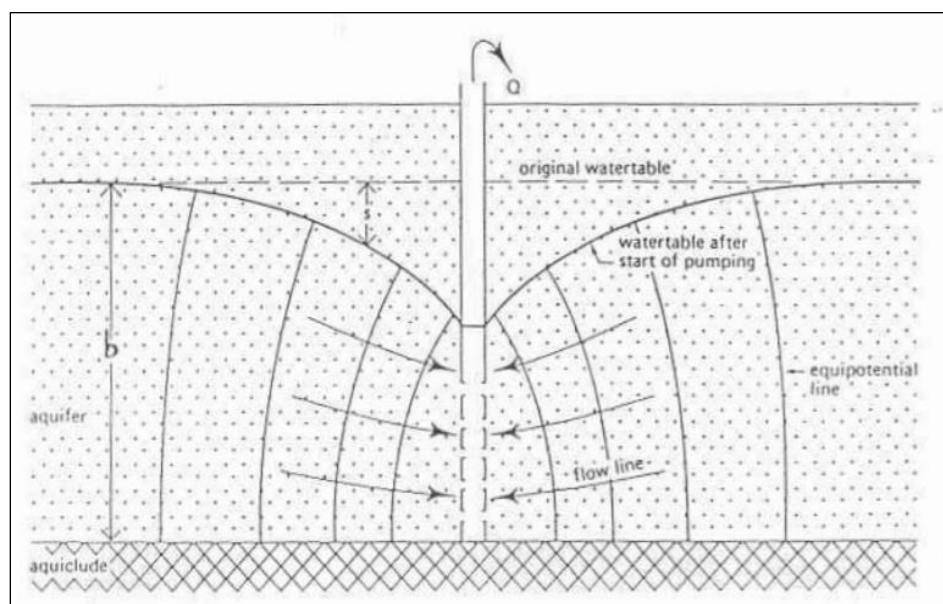


Figure 4. Schematic overview of the theoretical principle behind phreatic aquifer extractions through a fully penetrating well, and the effects on the regional groundwater hydraulics and resulting depression cone (House of Water and Environment, n.d.).

The local drawdown depends on antecedent conditions and changes in the pumping regime. Groundwater fluctuations are observed lagging pumping regime changes, and even though the majority of drawdown occurs simultaneously, an S-shaped curve more accurately defines this phenomenon (Brozović et al., 2006; Mao et al., 2011). Both papers additionally identified the spatial interdependence of the drawdown lag. Neighbouring locations experience drawdown primary from relatively new pumping regime changes, whilst an increasing distance induces a complex interaction between antecedent pumping regimes. The conceptualization of drawdown is of importance when considering spatial or temporal adjustments to current extraction strategies, as their effectiveness is embedded in this simplified theoretical framework.

3.2 Hydro-environmental sustainability

Sustainable groundwater management, whilst often defined regarding groundwater depletion, however is not unilateral as a concept (García-Cáceres et al., 2019; van Engelenburg et al., 2021). Focussing solely on groundwater depletion for 'sustainable' extraction neglects the complex interactions between hydrology and ecology. The unsaturated zone (i.e. vadose zone) is of critical importance as it acts as the integrative link between groundwater and vegetation through soil moisture (Lowry & Loheide, 2010; Wang et al., 2018). Hasiotis et al. (2007) have schematized this system's primary fluxes and stores (Figure 5).

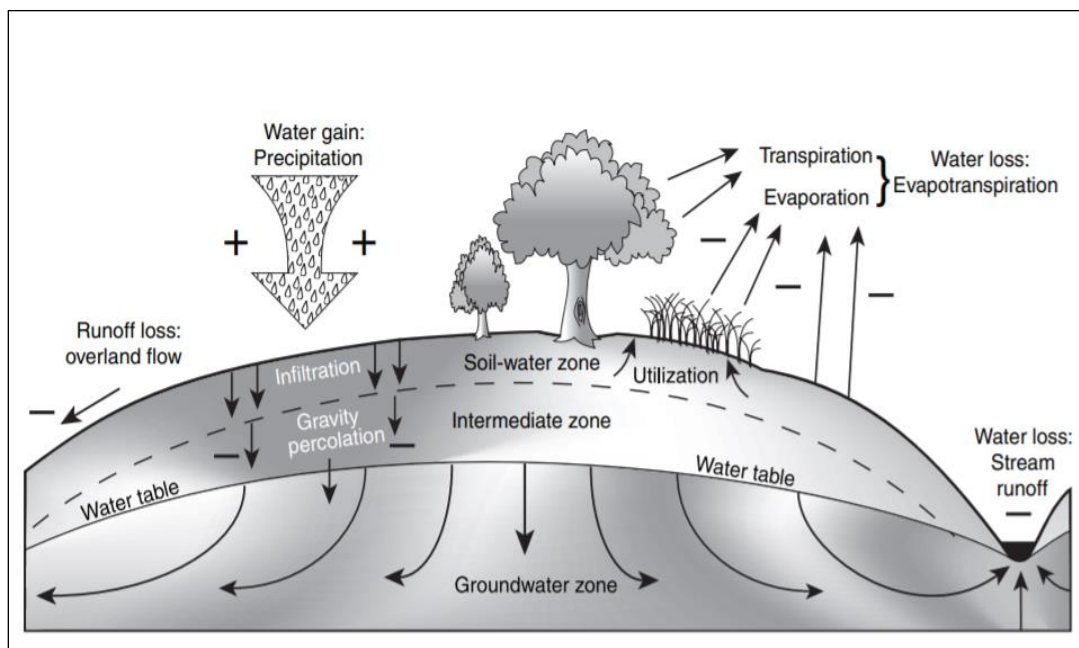


Figure 5. Schematic overview of the hydrological stores and fluxes in the land-based water balance from the perspective of soil moisture as integrative link (Hasiotis et al., 2007).

Decreases in groundwater levels propagate into decreased soil moisture content by reduced capillary rise. Consequently, water supply to groundwater-dependent vegetation is hampered. Soil moisture deficits directly affect ecological growth, development, and establishment (Hasiotis et al., 2007). Contrariwise, the local vegetation characteristics also determine the spatial and temporal soil moisture patterns and infiltration rates (Kim & Jackson, 2012; Sulis et al., 2017). Furthermore, gross precipitation in practice hardly equals natural groundwater recharge due to infiltration and evapotranspiration (Bergkamp & Cross, 2006). The extent of soil moisture utilization by plants however depends on the plant density, phenological phase, and transpiration rates (Wang et al., 2018). The interaction between soil moisture and vegetation contributes

significantly to nutrient exchange, photosynthesis, and local ecological activity and is vital to the system's sustainability (Lowry & Loheide, 2010; Wang et al., 2018). Furthermore, phreatic environments relate to the ecological value of a region, agricultural functioning, and, debatably most important, the natural capacity of microbiological purification of infiltrating groundwater (Bergkamp & Cross, 2006; Larned, 2012).

The vast agricultural areas and groundwater-dependent nature in the northern Achterhoek put particular importance on hydro-environmental interactions. The interactive nature of the system requires an integrated but holistic view of the concept of sustainability. To assess the sustainability of alternative extractions, it is vital to not only confine to groundwater levels but explore the connection to soil moisture.

Chapter 4 Methodology

4.1 Conceptual model

4.1.1 Alternative strategy 1: Decentralized extractions

The decentralization of groundwater extractions was evaluated as first alternative strategy. The concept of decentralized extractions focuses on the spatial redistribution of the socio-economic water demand over an extended area. By detachment of (partial) consumer volumes towards decentralized locations, central production plants require less intensive pumping regimes. The required (partial) demand of decentralized consumers is regained by locally extracted and produced groundwater. Decentralization proportionally distributes the piezometric drawdown over a multitude of fractionalized lower-intensity extraction locations, compared to the current high-intensity central points. Consequently, changes to the pumping regime propagate to fluctuations in the local drawdown. The conceptual implementation of this strategy requires local infrastructural developments by positioning individual extraction wells at various locations. Which locations are suitable for decentralization varies depending on the used definition. Within this thesis, decentralization solely concerns larger consumers ($Q_{\text{annual}} > 3,000 \text{ m}^3$) to ensure infrastructural practicality.

Decentralization increasingly gains practical viability due to local technological advancements (e.g. smart monitoring sensors, advanced purifications technics, independent operational systems). As water often remains as a residual product in agricultural, industrial, and energy-generative processes, decentralization also contains integrative potential between the hydrological and energy chains (Houtsma, 2015). Whilst optimizing usages and costs for both chains is a key-benefit, the latter is primarily defined as promising driver of socio-economic interest needed to implement this strategy on a local level (Giezen et al., 2017). Decentralization has furthermore proven to increase water supply reliability on a local scale due to the lower occurrence of infrastructural disturbances (Piratla & Goverdhanam, 2015). The limitations of this strategy comprise the higher initial and operative expenditures, required multilevel legislation, and limited quantitative and qualitative monitoring possibilities.

4.1.2 Alternative strategy 2: Seasonal extractions

The seasonal extraction of groundwater was evaluated as second alternative strategy. This temporally adjusted strategy is based on bridging socio-economic water demand and natural availability. The seasonal availability of groundwater in the northern Achterhoek negatively correlates to the drinking water demand. Natural groundwater levels are highest in the winter months, whilst demand and extractions peak during summer. The available excess groundwater in the winter however is not retained as a strategy and often drains from the system (Chan et al., 2014). Consequently, the timing of current extractions is not optimized for seasonal hydraulic regimes (Ramaker et al., 2006). The concept of seasonal extractions aims to improve this imbalance by extracting groundwater based on natural supply instead of socio-economic demand. The implementation is conceptualized by the additional extraction of groundwater during winter months, combined with interseasonal (subsurface)-storage, to meet demand during summer. When summer demand remains constant, potential for decreased summer extractions exists; depressurizing the groundwater system during vulnerable months.

Seasonal extractions require limited adjustments to the current infrastructure. As Vitens preserves complete property and distribution control, no stakeholder interference occurs, and constant water quality monitoring is assured. However, seasonal extractions' potential depends on the availability of local interseasonal (subsurface)-storage. Viable methods comprise large-scale reservoirs or established principles as Aquifer Storage and Recovery (ASR; Rambags et al., 2013). Explorative research towards suitable subsurface layers (e.g. Drenthe formation) is required but was excluded due to time constraints.

4.2 Hydrogeological model setup

4.2.1 Actueel Model Instrument Gelderland Oost (AMIGO)

The hydro-environmental impacts of alternative extraction strategies were quantified using AMIGO v3.1. AMIGO is a detailed numerical geohydrological model covering the province of Gelderland, developed by Arcadis in 2021 (de Weme et al., 2019). AMIGO encompasses various high-resolution geodatabases, further specified in Chapter 4.2.2, to execute hydrological simulations for management purposes. The primary application of AMIGO comprises climatological and policy-related scenario analyses regarding the regional water balance. The model operates on a maximum spatial and temporal resolution of respectively 25x25 m and 1-day. iMOD v5.1 functioned as executive program (Vermeulen et al., 2020). AMIGO couples two hydrological modules: the finite-difference groundwater module MODFLOW, and the Soil Vegetation Atmosphere Transfer (SVAT) module MetaSWAP (Langevin et al., 2017; van Walsum et al., 2014). The structure of MODFLOW is quasi 3-D, referring to the subdivision into aquiferous layers, containing horizontal flow, and separating layers, containing vertical flow. Groundwater flow is simulated by the partial differential Darcy equation for saturated transient 3-D flow:

$$\frac{\partial h}{\partial x}(K_{xx}) + \frac{\partial h}{\partial y}(K_{yy}) + \frac{\partial h}{\partial z}(K_{zz}) - Q = S \frac{\partial h}{\partial t} \quad (\text{Langevin et al., 2017})$$

With h = hydraulic head, K = hydraulic conductivity alongside the respective x , y , or z -Cartesian plane, Q = volumetric flux per unit volume per corresponding source and flux, t = time.

MetaSWAP however lacks horizontal flow. The unsaturated zone is therefore simulated per vertical soil column by the steady-state Richards' equation for 1-D flow:

$$\frac{\partial}{\partial z} \left[K(\psi) \left(\frac{\partial \psi}{\partial z} + 1 \right) \right] - \tau(\psi, z) = 0; \quad 0 \geq z \geq b \quad (\text{van Walsum et al., 2014})$$

With z = elevation (negative in downward direction), K = hydraulic conductivity, ψ = pressure head, τ = root water uptake, b = groundwater elevation.

Vertical columns are positioned parallel and linked to MODFLOW to obtain horizontal coverage (van Walsum et al., 2014). Individual dynamic processes in MetaSWAP are hereafter derived using extensive time-variable water balances, combined with environmental soil physics (e.g. transpiration, evaporation, rootzone moisture). Detailed computational theories and assumptions behind MODFLOW, MetaSWAP, and AMIGO can be found in respectively Langevin et al. (2017), van Walsum et al. (2014), and de Weme et al. (2019).

4.2.2 Parameterization, boundary conditions, and meteorological data

4.2.2.1 Parameterization

The subsurface model was based on REGIS II v2.2. Fifteen geological layers were included in the model, starting at the hydrological base of the Breda formation. Minimal layer thickness was set at 0.01 m. The subsurface of the German section was obtained through linear extrapolation. Subsurface data contained gridded information [.idf] for all 15-layers on horizontal and vertical hydraulic conductivity, c-values (hydraulic resistance), and transmissivity. Conductivity varied per cell and layer but generally confined to 5 to 25 m/d horizontally, and 0.005 to 0.0003 m/d vertically (TNO, 2021). Regionally, Kd and c-values were preferred by GeoTOP v1.3 due to higher accuracy. Minimum Kd values were set to 0.1 m²/d. The minimum c-value was set at 0.1 d. Horizontal flow barriers were locally defined for layers 3, 4, 5, and 6; however, their location exceeded the study area. Horizontal anisotropy values were set to 1.0 for all layers, exempting moraines where values varied between 0.25 and 1 (de Weme et al., 2019). Furthermore, confined storage coefficients were set to 0.15 for layer 1, and 0.0001 for layer 2 to 14 to simulate phreatic aquifer functioning (Vermeulen et al., 2020).

The ground level was defined by the Actueel Hoogtebestand Nederland (AHN) on a 5x5 m resolution. Initial groundwater heads and boundary conditions were derived on a 25x25 m resolution by a stabilization-run of four consecutive years. Overland flow was set to occur onwards of 0.05 m above ground level (de Weme et al., 2019).

Physical soil parameters for the MetaSWAP unsaturated zone module were obtained through LHM2016 v1. Land cover, land use, and rootzone thickness and depth were derived from the WUR LGN/CORINE database on a gridded 25x25 m resolution (Heinen et al., 2021). Soil characterization was derived from the 72-units version of BOFEK2012 (de Weme et al., 2019). Relevant input maps are included in Appendix B.1.

The WUR provided agricultural pipe drainage, resistance, and depth on a 25x25 m resolution through the buisdrainagekaart developed by Massop & Schuiling (2016). Drainage depth varied locally between 0.8 to 1.20 m, dependent on land use and soil type. Resistance was put at 70 days for the whole dataset. Furthermore, urban drainage was neglected to prevent overestimation.

Current well locations and extraction volumes were derived from the database (*onttrekkingenbestand v2021*) of the Water board Rijn en IJssel. Available data contained daily extraction volumes per well per individual subsurface layer for a temporal range of 31-01-1990 to 31-01-2020. Distinction was made between five extraction purposes: drainage, agricultural, drinking water, other, and unknown (de Weme et al., 2019). Relevant wells characteristics and applied alterations are further discussed in Chapter 4.3.

The surface waters characteristics were derived from Rijkswaterstaat and SOBEK2014 for respectively primary rivers and regional water systems. Information was obtained on a 1-day resolution comprising location, water level, bottom elevation, and conductance. Infiltration factors were set at 1.0 for primary rivers, and 0.3 for local streams (de Weme et al., 2019).

An overview of the utilized packages and parameters can be found in Appendix B.2

4.2.2.2 Boundary conditions

To ensure temporal feasibility for this thesis, the construction of a localized model cut-out was required. A spatial minima criterion was enforced to prevent discontinuities between the model boundaries and the radial region influenced by groundwater pumping. Model boundaries were set to differentiate at least three times the length of the leakage factor (*spreidingslengte*) from extraction locations to ensure neglectable hydraulic interference [$<5\%$] (Hoogvliet et al., 2014; van der Gaast & Massop, 2003). Computation of the leakage factor follows the Mazure equation:

$$\lambda = \sqrt{\sum K_h D * \sum c} \quad (\text{Fitts, 2013})$$

With λ = leakage factor [m], $\sum K_h D$ = summed horizontal transmissivity of aquiferous layers [m^2/d], $\sum c$ = summed resistance of aquiferous layers [d].

Based on the subsurface dataset of DINOloket (TNO, 2021), λ -values were determined between 400 to 1400 m for the northern Achterhoek. Detailed studies differentiated between 500 to 750 m at lower-elevated regions, and 1500 to 2500 m at high ridges (Gaast & Massop, 2008; Hoogvliet et al., 2014). Conservatively, high uncertainty values ($\lambda = 1400$ m, $3\lambda = 4200$ m respectively) were chosen to inhibit underestimation. Definite model boundaries corresponded to Cartesian xy;xy coordinates: 214337.71, 447686.52; 241461.51, 468053.07 (Figure 6; Figure 7).

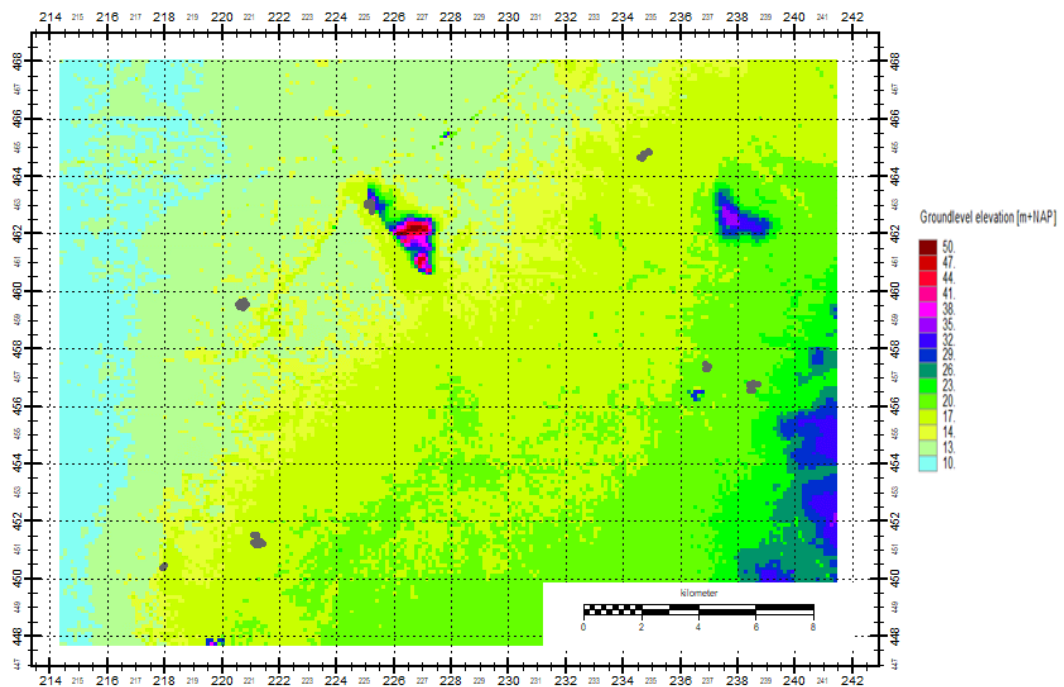


Figure 6. Two-dimensional overview of the modelled area in AMIGO: top-view display of the surface level elevation [m +NAP] including the local distribution of all current active well systems (one individual grey dot per active well).

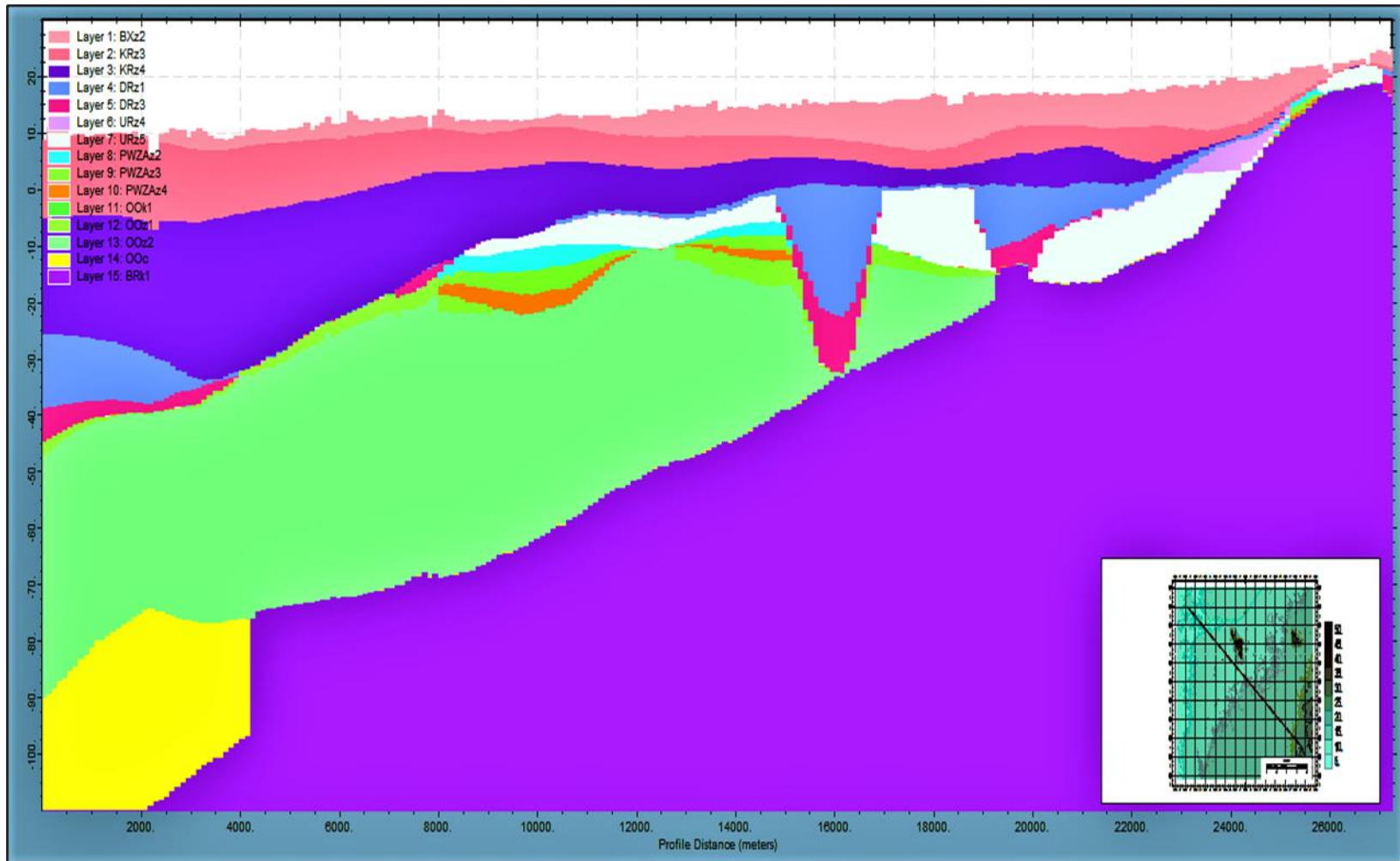


Figure 7. Cross-sectional subsurface structure of the modelled area in AMIGO. Identifying layer coding is in accordance to BRO REGIS II v2.2 (TNO, 2021). The Y-axis present the elevation in m +NAP. Note a vertical exaggeration is of 1:60,000 is applied on the y-axis.

4.2.2.3 Meteorological data

Meteorological input comprised daily precipitation and reference crop evaporation. Daily gridded precipitation data were obtained from the KNMI Data Platform for 16 years onwards of January 2004 (<https://dataplatform.knmi.nl>). The gathered data consisted of cumulative interpolated daily precipitation over 24-hours, starting at 08:00, measured for 294 locations in the Netherlands. Data interpolation done by the KNMI was based on Kriging regression (KNMI, n.d.; Sluiter, 2009). Precipitation data was provided in tenth of millimeter waterslice per day [0.1 mm/d]. The data collection was manually checked for errors and updated by supplementary data by Arcadis due to missing grids for the year 2009.

The reference crop evaporation was obtained similarly from the KNMI Data Platform. Reference crop evaporation was estimated based on Makkink's equation and gathered for the equivalent temporal range of 16-years. The Makkink reference evaporation is defined and computed as the empirical relation between incoming solar radiance and the latent heat of vaporization (Tabari, 2010; Wang et al., 2019). Reference evaporation data were obtained as a grid file interpolated from 7-35 weather stations containing a 1-day temporal resolution (KNMI, n.d.). Data interpolation applied by the KNMI was by the Thin Plate Spline method (Hiemstra & Sluiter, 2011). Reference evaporation was directly obtained in suitable units [mm/d]. Similar to precipitation data, evaporation data were checked for errors and adjusted accordingly.

4.2.3 Calibration and justification

Arcadis has calibrated the complete model upon development by partial-automatic parameter analysis or both stationary and non-stationary runs for the period 2008-2016. Calibration was based on the Representer calibration method using primary groundwater measurements and fluctuating K_d and c -values, respectively factored with 0.1, 1, 10, and 100 (Przybysz-Jarnut et al., 2007). Following calibration, the drainage resistance was increased to optimize the groundwater results. Arcadis validated the model by two case-study assessments (i.e. Baakse Beek, Haarlo-Eibergen), affirming application (de Weme et al., 2019).

Justification for the model selection and input data applicability is obtained through comparative literature. Previous versions of AMIGO have been routinely tested and used for regional scenario simulations (de Weme et al., 2019), and MODFLOW and MetaSWAP have been applied in a multitude of high-detailed explorative regional hydrological studies (e.g. Ehtiat et al., 2018; Sahoo & Jha, 2017). As data coverage within Gelderland is extensive, the spatial and temporal resolution accurately suits the scope of the research objective at a broader regional scale. Consequently, no up-scaling had to be applied.

4.3 Scenario development

The impact of alternative strategies was evaluated by comprehensive scenario analysis. As by Kosow & Gaßner (2008), scenario analysis provides a powerful method to comparatively assess future-orientated measures and their consequences. First, a baseline scenario was constructed to represent the current state of practice. Hereafter, three scenarios were developed to evaluate decentralization. Additionally, five scenarios contemplated seasonal extractions and optimization. An overview is presented in Table 2. All scenarios were run for 5753 1-day stress periods, corresponding to a transient time discretization from 01-04-2004 to 31-12-2019. The spatial resolution was set to 100x100 m. An exemplative scenario runfile can be found in Appendix B.3

Table 2. Overview of all constructed scenarios.

Scenario	Type	Description	Characteristics
Sb	Baseline	Reference	Six centralized systems, current extractions
Sd1	Spatial	Decentralized	Disconnected consumers $Q_{\text{annual}} > 10,000 \text{ m}^3$
Sd2	Spatial	Decentralized	Disconnected consumers $Q_{\text{annual}} > 5,000 \text{ m}^3$
Sd3	Spatial	Decentralized	Disconnected consumers $Q_{\text{annual}} > 3,000 \text{ m}^3$
St1	Temporal	Seasonal	For all wells winter extraction +10%; summer extraction $-\Delta Q_{\text{winter}}$
St2	Temporal	Seasonal	For all wells winter extraction +20%; summer extraction $-\Delta Q_{\text{winter}}$
St3	Temporal	Seasonal	For all wells winter extraction +30%; summer extraction $-\Delta Q_{\text{winter}}$
Sst1	Temporal	Interlocational	Winter extractions +15% for Noordijk & Haarlo; summer extractions $-\Delta Q_{\text{winter}}$ for 't Klooster & Vorden
Sst2	Temporal	Interlocational	Winter extractions +15% for Lochem & Eibergen; summer extractions $-\Delta Q_{\text{winter}}$ for 't Klooster & Vorden

4.3.1 Baseline scenario

The baseline scenario was developed to represent current extraction strategies. Available well systems and their respective number of individual wells stated: 't Klooster (12), Vorden (9), Lochem (9), Noordijk (9), Haarlo (9), and Eibergen (7) (see Figure 6). The in total 55 wells were placed in sub-surface model layer 4 for 't Klooster and Vorden, layer 6 and 9 for Lochem, layer 8 for Noordijk, layer 6 and 8 for Haarlo, and layer 9 and 10 for Eibergen. Extraction volumes and their distribution within a well-system were enforced as within the described extraction databases.

4.3.2 Alternative scenarios

4.3.2.1 Decentralized extractions

The decentralized extraction scenarios were constructed by the disconnection of industrial consumers from the current supply systems, combined with the implementation of decentralized wells. Localized consumer data was requested from Vitens and obtained on a postcode spatial resolution (Vitens, 2021). Gathered data comprised annual consumption, provided in m^3 , per industrial consumer per individual supply system based on 2020 measured reference volumes. The original dataset listed 89 local consumers.

As postcode resolution data provision was paramount due to privacy considerations, no information was present on exact locations. Therefore, postcodes were converted into applicable Rijksdriehoek (RD) xy-coordinates by assuming central localization within each postcode area. Dataset reduction occurred by eliminating consumers outside the model boundaries. Consequently, 50 consumers remained. Extraction wells were hereafter implemented at each decentralized consumer. To fit model input, temporal homogeneity for summer and winter was assumed to convert annual consumptions into monthly and daily values. Furthermore, yearly extractions were assumed constant for the entire simulation period. The well-depth and subsurface layer were assumed to correspond to the nearest located well of the current supply system. An overview of the supplemented datafile characteristics can be found in Appendix C.

Based on the prepared datafile, three scenarios were developed (Table 2). Decentralization was tested in gradual steps by detachment of solely major consumers ($Q_{\text{annual}} > 10,000 \text{ m}^3$), semi-large consumers ($Q_{\text{annual}} > 5,000 \text{ m}^3$), and all gathered consumers ($Q_{\text{annual}} > 3,000 \text{ m}^3$). Respectively, this comprised 16, 27, and 50 decentralized locations for scenarios Sd1, Sd2, and Sd3. The spatial distribution of decentralized consumers and the new well system is presented in Figure 8.

The initial extraction volumes of current supply systems were reduced per scenario with the redistributed decentralized volumes (Table 3). Reductions were assumed temporally linear, both interseasonal and interannual, and kept uniformly distributed over the active wells within a system at each time-step. For the Lochem well system, only well-files 0255, 0256, 0257, 0260, and 0261 were adjusted due to the frequent occurrence of hiatus in extraction volumes within the remainder of well-files. In the sporadic case a daily extraction volume subceeded zero, values were set to zero.

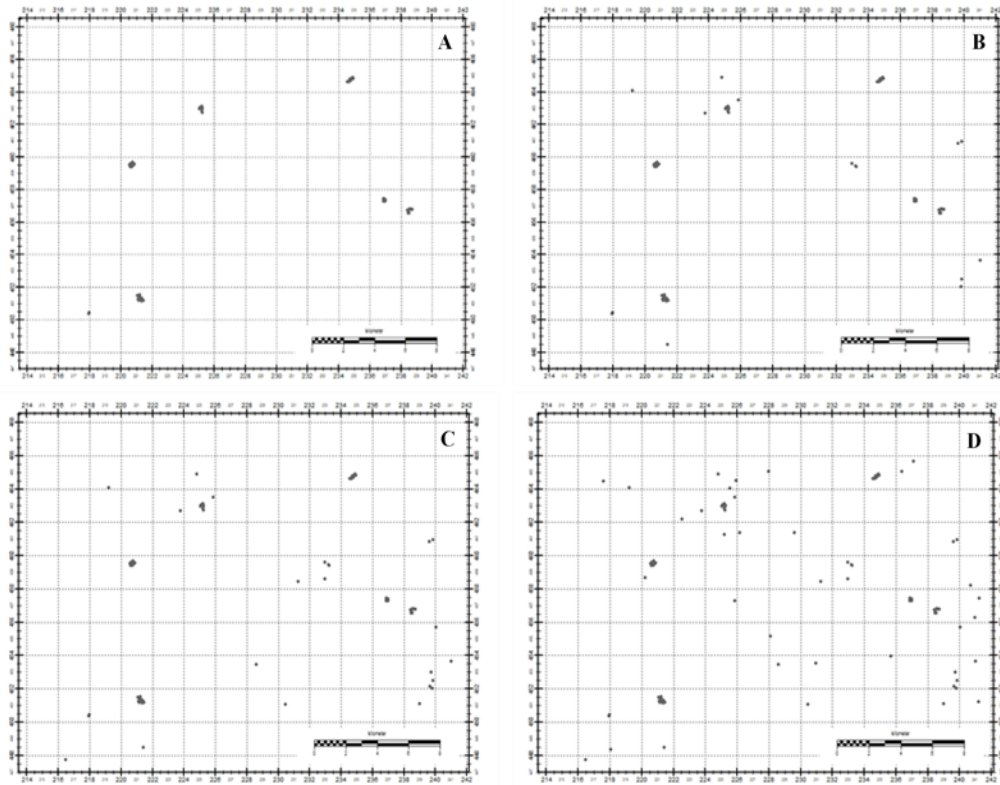


Figure 8. New (privatized) distribution of the regional well systems as a result of decentralization. Distribution maps in order: a) Baseline, b) Sd1, c) Sd2, d) Sd3. Individual grey points represent an active well location.

Table 3. Quantitative net decreases in current extraction volumes per supply system per spatial scenario. Extraction volumes [Q] in total m³/period. Percentages as the relative decrease in extraction volumes compared to current total extraction volumes.

Supply system	Period	Sd1 [Q]	Sd2 [Q]	Sd3 [Q]
't Klooster	Year	-1.33 10 ⁶	-1.37 10 ⁶	-1.39 10 ⁶
	Day	-3.69 10 ³	-3.82 10 ³	-3.85 10 ³
Percentage to baseline	-	-24.9%	-25.7%	-26.1%
Vorden	Year	-1.04 10 ⁵	-1.04 10 ⁵	-1.45 10 ⁵
	Day	-287	-288	-403
Percentage to baseline	-	-3.55%	-3.55%	-4.95%
Eibergen	Year	-3.04 10 ⁵	-3.34 10 ⁵	-3.71 10 ⁵
	Day	-844	-929	-1.03 10 ³
Percentage to baseline	-	-5.82%	-6.39%	-7.12%

4.3.2.2 Seasonal extractions

The seasonal extraction scenarios were developed in two phases. Phase one comprised three scenarios testing the conceptual theory (St1, St2, St3; Table 2). For these scenarios, winter extractions were increased for all well systems by 10, 20, and 30%. Simultaneously, reductions to the local summer extractions were applied by the corresponding obtained winter volumes. Winter months were defined, as by the hydrological year, as October-March. Summer months corresponded to April-August. Extraction volumes were reduced and amplified linearly per season on a daily resolution (Table 4). Temporal uniformity was assumed between months and days within a season. Alterations to extractions volumes were applied on all active well-files per timestep. Lochem well-files were treated as previous. Furthermore, no additional interannual variations were enforced as water demand was enforced as within reference extractions. The alterations to the seasonal extraction ratios of all individual well systems were based on the assumption of local interseasonal storage availability.

Phase two focused on specific alignments between current well-systems based on local characteristics. To ameliorate the highest pressurized locations (i.e. 't Klooster and Vorden), two scenarios contemplated interlocal seasonal extractions (Sst1 & Sst2; Table 2). For Sst1, winter extractions were increased by 15% for the locations Noordijk and Haarlo. Selection was based on the criteria: low current extractions and elevated geography. Winter volumes were determined by consideration of not exceeding local permitted yields. Summer extractions of 't Klooster and Vorden were reduced linearly with the extracted volumes (Table 4). Equal division between the latter two locations was applied. For Sst2, winter extractions were increased by 15% for the locations Lochem and Eibergen. Here, conformity is found in the criterion: low current utilization of permitted yield. Again, linear reduction of summer extractions of 't Klooster and Vorden was applied. Alternations to extractions under both scenarios were applied coherently to the procedure and assumptions as under phase one.

Table 4. Quantitative net shifts in daily extraction volumes per supply system per temporal scenario. Extraction volumes [Q] in m³/day. Percentages as the relative shift in extraction volumes compared to current extraction volumes.

Well system	Period	St1 [Q]	St2 [Q]	St3 [Q]	Sst1 [Q]	Sst2 [Q]
't Klooster	Summer	-1.42 10 ³	-2.84 10 ³	-4.25 10 ³	-433	-602
	Winter	1.42 10 ³	2.84 10 ³	4.25 10 ³	-	-
Percentage to baseline	-	±10%	±20%	±30%	-2.84%	-3.92%
Vorden	Summer	-723	-1.45 10 ³	-2.17 10 ³	-433	-602
	Winter	723	1.45 10 ³	2.17 10 ³	-	-
Percentage to baseline	-	±10%	±20%	±30%	-4.79%	-6.67%
Lochem	Summer	-478	-956	-1433	-	-
	Winter	478	956	1433	-	730
Percentage to baseline	-	±10%	±20%	±30%	-	+ 15%
Noordijk	Summer	-283	-566	-850	-	-
	Winter	283	566	850	425	-
Percentage to baseline	-	±10%	±20%	±30%	+15%	-
Haarlo	Summer	-294	-587	-881	-	-
	Winter	294	-587	881	441	-
Percentage to baseline	-	±10%	±20%	±30%	+15%	-
Eibergen	Summer	-315	-630	-945	-	-
	Winter	315	630	945	-	473
Percentage to baseline	-	±10%	±20%	±30%	-	+15%

4.4 Scenario analysis

Modelled scenario outcomes have been analyzed by both spatial and temporal analysis. The spatial analysis comprised top-view pattern analysis. Regional differences, pattern developments, and parameter extent and intensity fluctuations were compared between alternative scenarios and the baseline for summer and winter. Winter representation was taken on 15-12-2011. The summer situation was taken on 24-07-2012. Seasonal averages were taken for October – March (winter) and April – August (summer) over the entire simulation period. The temporal analysis comprised point data comparison of individual scenarios to the baseline for the period 01-04-2004 to 31-12-2019 on a 1-day resolution. Timeseries were obtained by 20 observation wells (Figure 9). Observation wells were placed prior, amid, and behind current well sites, respectively to the natural hydraulic gradient. Placement was based on a distance of $\pm 0.8x$ the length of the total leakage factor. Supplementary wells were uniformly distributed to obtain regional coverage; however were mainly excluded from the results due to neglectable values.

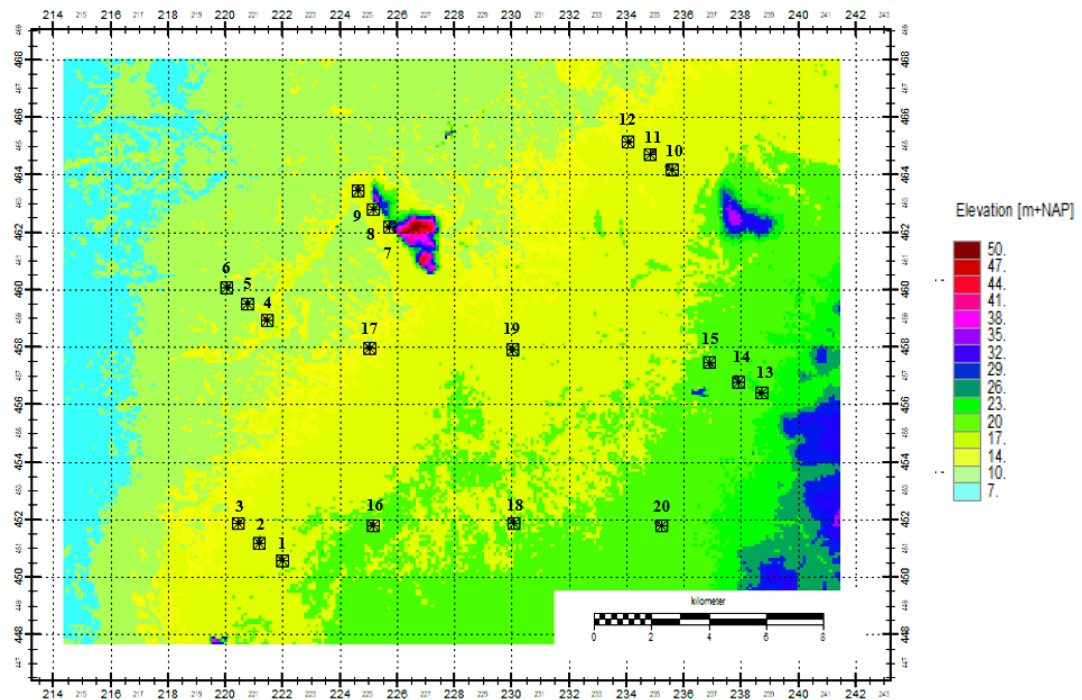


Figure 9. Local distribution and coding of all placed observations wells within the study area. Surface level elevation is taken as uniform background.

The research questions were answered by three specific output parameters amid the complete regional water balance. Output computation conformed to Kriging interpolation. Groundwater functioning was analyzed by the parameters groundwater level (*Head*). Head was defined as groundwater level elevation in m +NAP (Vermeulen et al., 2020). Hydro-environmental impacts were analyzed by soil moisture saturation deficit (*SsdTot*) and actual evapotranspiration (*ETact*). *SsdTot* was defined as the net total deficit in soil moisture to saturation over n-layers of the unsaturated zone cell in m^3/m^2 . *ETact* was defined, conform Makkink, as the total net evapotranspiration as negative flux direction in m^3/m^2 (van Walsum et al., 2014).

Chapter 5 Results

5.1 Groundwater

5.1.1 Baseline scenario

Regional groundwater levels varied in space and time. Spatial characteristics showed that groundwater levels followed the natural gradient in South-East to North-West direction (Figure 10). Noticeable distortions mainly were found at extraction locations and elevated ridges, respectively, as negative and positive effects. The spatial extent of the distorted gradient lines was found corresponding to higher extraction volumes, ranging between 1.4 – 2 km for the larger extractions (i.e. 't Klooster, Vorden, Lochem), and up to 1 km for Noordijk Haarlo and Eibergen.

Temporal trends indicated a seasonal harmonic oscillation based on meteorological input. Seasonal values for observation wells 2 and 5 varied approximately 1.5 – 2.0 m (Figure 11). Remaining extraction locations (resp. wells 8, 11, 13, and 15) indicated seasonal variations between 1.0 – 1.5 m, both peaking in winter. The effect of season variations was higher at further distances from extraction sites (e.g. well 1 and 3, compared to well 2). On a multiple-year scale, a slight decrease in heads is observed for all wells, indicative of the climatological and socio-economic depletion of groundwater under current regimes (Figure 11).

Observation well 8 showed a local peak in groundwater head following a 6-month period (1-10-2007 to 1-03-2008) without active extractions. This directly indicated the significant influence of extractions on the local groundwater table. This same principle was found when looking at the groundwater depth compared to surface level elevation. Without interference, regional groundwater depths primarily fluctuated between 0.5 – 2.5 m below the ground level. Under current extractions, the depth to the groundwater table increased with ranges varying between 1.0 – 1.5 m for observation wells 2, 11, and 13, and 0.5 – 1.0 m for wells 5, 8, and 15. The groundwater increased in a roughly similar distribution around the extraction sites (i.e. equal impacts below or before the natural flow gradient).

Table 5. Averaged groundwater table depth [-m] below the surface level for relevant observation wells under the baseline scenario for summer and winter.

Observation well	1	2	3	4	5	6	7	8	9	10	11	12	13	14	15
Winter groundwater table depth [-m]	3.1	4.5	2.6	2.8	3.1	2.3	7.1	4.6	4.2	2.1	3.3	2.0	2.8	1.0	1.1
Summer groundwater table depth [-m]	3.8	5.2	3.4	3.4	3.6	2.5	7.6	4.9	4.6	2.5	3.7	2.6	3.4	1.5	1.5

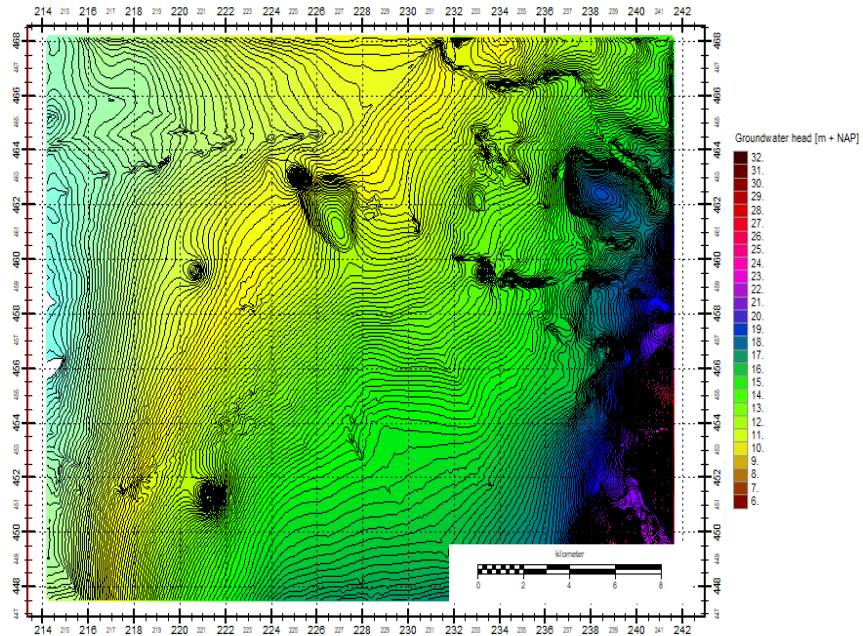


Figure 10. Regional groundwater head [m +NAP] of the northern Achterhoek under the baseline scenario during summer representation. Summer representation was taken on 24-07-2012. Gradient lines are set to at 0.2 m resolution.

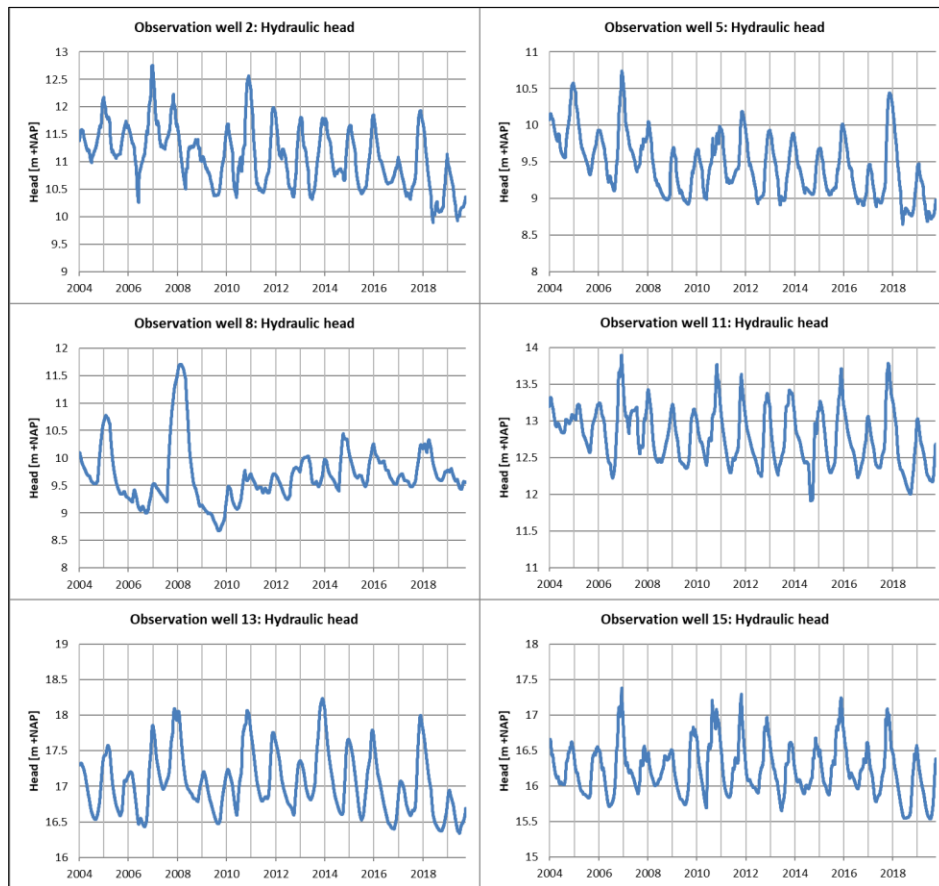


Figure 11. Timeseries of the local groundwater levels [m + NAP] for the entire simulation period for all six extraction locations. Observation wells 2, 5, 8, 11, 13, and 15 correspond to extraction locations 't Klooster, Vorden, Lochem, Noordijk, Eibergen, and Haarlo.

5.1.2 Decentralized scenarios

The model results showed that all three decentralized scenarios positively affected the regional groundwater levels at extraction locations (Figure 12; Table 6). Most significant effects were observed at observations wells 1, 2, and 3, corresponding to high decentralized volumes for 't Klooster system (See Table 3). Seasonal averages under Sd1, Sd2, and Sd3, respectively, reduced groundwater depletion with 0.74 – 0.86 m, 0.84 – 1.04 m, and 0.8 – 1.06 m for observation well 2. Further away from extraction wells (i.e. well 1; well 3), positive effects declined to ranges between 0.18 – 0.36 m and 0.22 – 0.35 m, respectively. For the Vorden and Eibergen systems, decentralized scenarios showed less pronounced effects (resp. 0.01 – 0.12 m; Table 6). Findings indicated a highly-local character, as effects at surrounding observations wells (± 0.8 leakage factor) abruptly declined to changes below 0.05 m. Furthermore, results showed local seasonal fluctuations with prevalent winter effects (resp. 5 – 20%) during increased groundwater recharge. Interestingly, the influence of seasonal changes decreased in proximity to well-fields; induced by dominant extraction regimes. Figures for all observations wells are included in Appendix D.1.

Limited differences were found between individual decentralized scenarios (e.g. Figure 12). As most significant consumers were already included in Sd1, advanced scenarios did not indicate additional effects; whilst practical requirements increased (i.e. number of wells). Results for Vorden (well 4, 5, 6) were identical under Sd1 and Sd2 as no annual consumers were present between 10,000 and 5,000 m³. For observation well 8, groundwater differences diminished compared to the baseline scenario during 2007. Missing extraction data explained this 6-month period.

The regional patterns were presented on a 0.05 m contour resolution as lower values were deemed unreliable (Figure 13). Results indicated that most spatial effects accumulated around observation well 2. The spatial distribution of total positive effects around location 2 increased from 3031 – 5025 ha to 3271 – 5281 ha, and 3849 – 6161 ha under Sd1, Sd2, and Sd3 for summer and winter. Similar to local effects, the maximum extent was enhanced during winter with a factor of 1.2 – 1.5. Interestingly, most contour lines were found at consistent distances to extractions wells, with only the 0.05 m contours significantly expanding under different scenarios. For the remaining locations, limited effects were found. For observations wells 5, 8, 11, 13, and 15 solely highly-local influences were observed, restricted to the vicinity of the well-fields (< 500m). Furthermore, minimal distinguishments could be made between spatial impacts per decentralized scenario. Results thereby demonstrated that decentralization is predominantly effective in larger volumes.

Under all three scenarios, positive changes were found to exceed negative trends by considerable margins. Adverse effects confined to few local sites (total: 572 ha – 602 ha), with the largest decentralized location stretching 2337 – 2021 ha for summer and winter, respectively (Figure 13). Results indicated that most decentralized wells, exempting the few largest, did not induce significant (> 0.05 m) impacts on the regional groundwater levels. Consequently, the net regional effect was positive, implying a positive relation between groundwater levels and the concept of decentralization. Findings thereby advocated the effectiveness of decentralized extractions by minimal adverse impacts compared to the net benefits. Interesting findings furthermore showed the buffering effect of river systems in the results (e.g. Berkel river; 232500, 459000). Adjacent to rivers, reduced differences were observed compared to the near surroundings (up to 1.5 m); benefiting the local groundwater after placement of decentralized wells.

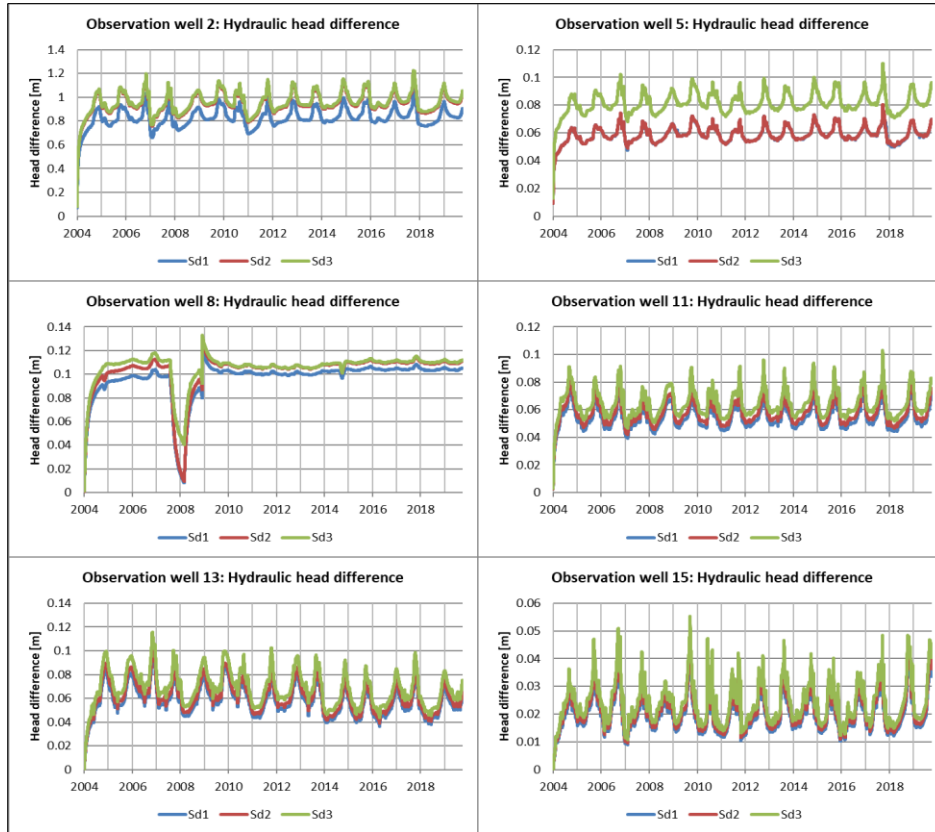


Figure 12. Timeseries of the local difference in phreatic groundwater head [m] under all decentralized scenarios compared to the baseline scenario for the six current extraction locations. Positive values indicate an increased groundwater head under decentralized scenarios. Negative values indicate a reversed situation.

Table 6. Net averaged seasonal differences in phreatic groundwater head [m] between alternative scenarios and the baseline at individual observation wells during summer and winter. Positive values indicate a higher groundwater level elevation for alternative scenarios compared to the baseline. Negative values indicate an inversed situation. Values below 10^{-7} are set to zero. Colour scheme: percentage change compared to current groundwater depths: >15% (dark green), 15 – 5% (green), 5 – 1% (light green), 1 – 0% (white), 0 – -1% (Grey), -1 – -5% (light blue), -5 – -10% (blue). ¹S = summer, W=winter.

Season	Sd1		Sd2		Sd3		St1		St2		St3		Sst1		Sst2	
	s	w	s	w	s	w	S	W	s	w	s	w	s	w	s	w
1	0.18	0.28	0.20	0.35	0.21	0.36	< 0.05	< -0.05	0.06	< -0.05	0.11	-0.07	< 0.05	< 0.05	< 0.05	< 0.05
2	0.74	0.86	0.84	1.04	0.85	1.06	0.09	< -0.05	0.31	-0.25	0.70	-0.43	< 0.05	0.0	< 0.05	0.0
3	0.22	0.31	0.23	0.34	0.23	0.35	< 0.05	< -0.05	0.07	< -0.05	0.10	-0.09	< 0.05	< 0.05	< 0.05	< 0.05
4	< 0.05	< 0.05	< 0.05	< 0.05	< 0.05	< 0.05	< 0.05	< -0.05	< 0.05	< -0.05	0.06	-0.05	< 0.05	< 0.05	< 0.05	< 0.05
5	0.05	0.07	0.05	0.07	0.07	0.09	0.07	-0.05	0.17	-0.12	0.28	-0.16	< 0.05	< 0.05	< 0.05	0.05
6	< 0.05	< 0.05	< 0.05	< 0.05	< 0.05	< 0.05	< 0.05	-0.05	0.05	-0.05	0.08	-0.05	< 0.05	< 0.05	< 0.05	< 0.05
7	< 0.05	< 0.05	< 0.05	< 0.05	< 0.05	< 0.05	< 0.05	< -0.05	< 0.05	< -0.05	0.06	< -0.05	0.0	0.0	< -0.05	< -0.05
8	0.08	0.10	0.11	0.11	0.11	0.11	0.06	< -0.05	0.31	-0.18	0.55	-0.37	0.0	0.0	< -0.05	-0.12
9	< 0.05	< 0.05	< 0.05	< 0.05	< 0.05	< 0.05	< 0.05	< -0.05	0.05	< -0.05	0.09	-0.06	0.0	0.0	< -0.05	< -0.05
10	< 0.05	< 0.05	< 0.05	< 0.05	< 0.05	< 0.05	< 0.05	< -0.05	0.05	< -0.05	0.07	< -0.05	< -0.05	< -0.05	0.0	0.0
11	0.05	0.07	0.05	0.07	0.06	0.07	0.05	< -0.05	0.11	-0.07	0.17	-0.10	< -0.05	-0.06	0.0	0.0
12	< 0.05	< 0.05	< 0.05	< 0.05	< 0.05	< 0.05	< 0.05	< -0.05	0.05	< -0.05	0.07	< -0.05	< -0.05	< -0.05	0.0	0.0
13	0.05	0.08	0.06	0.08	0.06	0.09	0.06	< -0.05	0.09	-0.06	0.18	-0.10	0.0	0.0	< -0.05	0
14	< 0.05	< 0.05	< 0.05	< 0.05	< 0.05	< 0.05	< 0.05	< -0.05	0.05	< -0.05	0.09	-0.06	0.0	0.0	< -0.05	< -0.05
15	< 0.05	< 0.05	< 0.05	< 0.05	< 0.05	< 0.05	< 0.05	< -0.05	< 0.05	< -0.05	0.07	-0.05	0.0	< -0.05	0.0	0.0

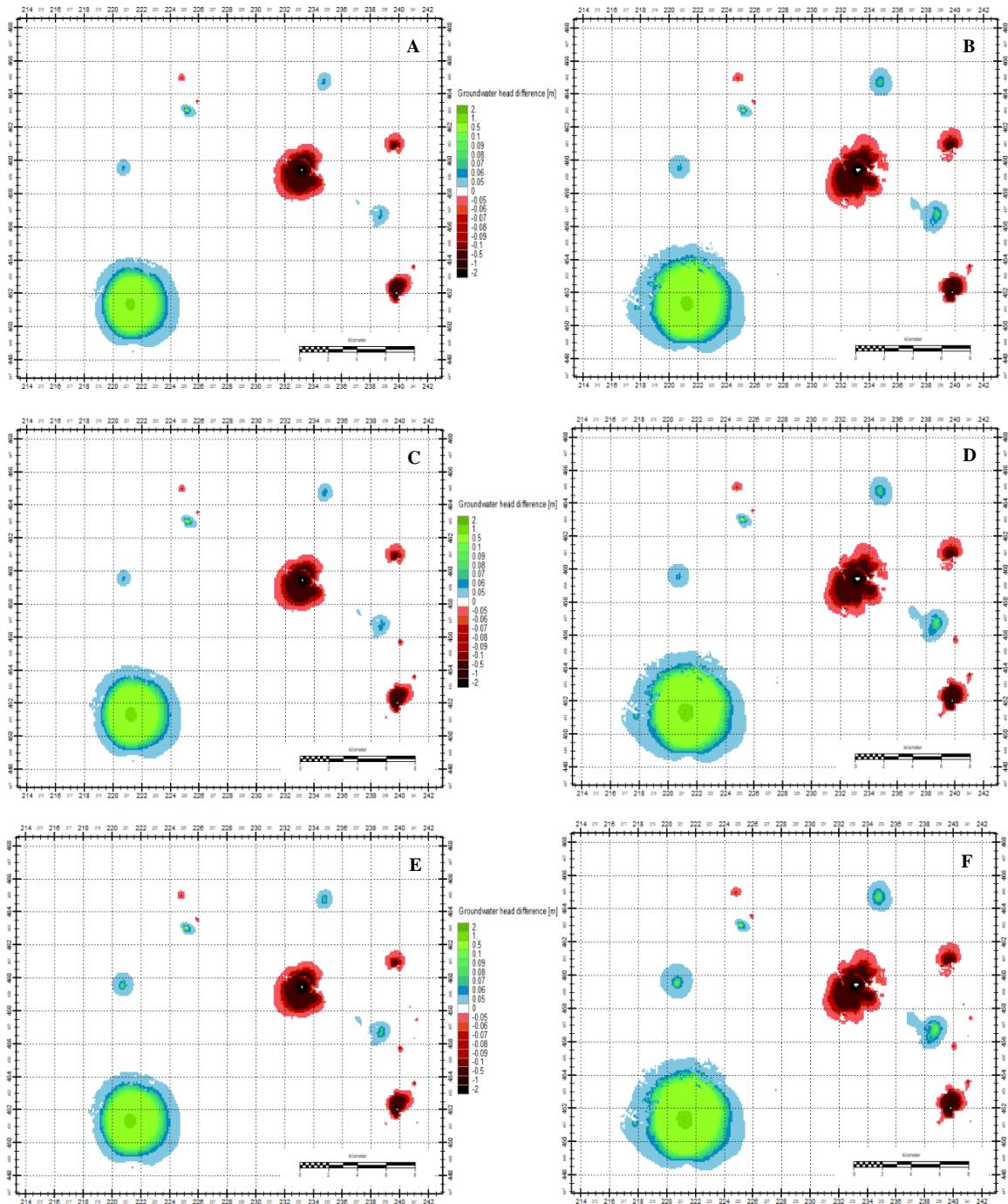


Figure 13. Regional difference maps of the phreatic groundwater head [m] under decentralized scenarios compared to the baseline scenario. Positive difference values indicate an increased groundwater head under decentralized scenarios. Negative difference values indicate a reversed situation. Difference maps in respective order: a) Sd1 summer, b) Sd1 winter, c) Sd2 summer, d) Sd2 winter, e) Sd3 summer, f) Sd3 winter. Summer representation was taken on 24-07-2012. Winter representation was taken on 15-12-2011.

5.1.3 Seasonal scenarios

All scenarios positively affected the regional groundwater levels (Table 6;

Figure 14). The extent of positive differences varied based on the degree of seasonal extractions (i.e. 10%, 20%, 30%); however, were found onwards of 1% compared to the baseline for most wells. The lowest impacts occurred under St1, stating average local effects between 0 – 0.09 m. Under St2 and St3, this respectively increased to 0.04 and 0.31 m, and 0.07 and 0.70 m (Table 6). The relation between the degree of seasonal extractions and their impacts seemed to be non-linear. Most notable differences were found at observations wells 2, 5, and 8. Respectively, groundwater levels increased with 0.09 – 0.70 m, 0.07 – 0.28 m, and 0.06 – 0.55 m compared to the baseline under St1, St2, and St3. The results indicated that seasonal scenarios were more effective when applied for higher volumes. The differences in groundwater under seasonal scenarios, as observed in Figure 14, followed a harmonic sinusoidal trend. Following positive summer effects, negative differences peaked after winter extractions. The intensity of these adverse impacts was consistently a factor 0.6 – 0.8 lower than the summer intensities. As its sharp peaks characterized the harmonic function, results deviated limited periods from seasonal averages (Table 6).

The spatial extent of relevant effects concentrated around extraction locations, increasing with applied seasonality and higher initial extractions (Figure 16). The 0.05 m difference contour for 't Klooster was observed to increase from 450 ha under St1 to 708 ha and 2131 ha under St2 and St3. Differences in groundwater level (> 0.1 m) primarily confined to local regions, indicated by sharp decreases with further distances to well-fields (Table 6). More clearly defined was again the relevance of initial volumes changes; wells 2 and 5 indicated consistent larger effects than the other extraction locations. The effective ranges of wells 11 and 13 overlapped due to their proximity. During winter, negative differences followed similar patterns. Like previous results, the extent of negative effects following increased winter extraction was consistently lower than summer benefits (resp. factor 0.8 – 0.85).

Seasonal extractions consequently demonstrated potential to increase groundwater levels on an annual scale (Figure 16). For St1, St2, and St3 yearly positive trends in phreatic head were found, sharply increasing per applied percentage of seasonality. The net effects mostly varied between 0 – 0.02 m; however, peaks (e.g. well 2, well 5) indicated annual positive effects between 0.02 – 0.09 m. At lower initial volumes, this effect was smaller (< 0.01 m). Whilst limited in lower volumes; results showed to be fairly effective in optimizing the natural water availability to socio-economic demand. Concrete, annually less unutilized water drained from the system using season extractions, positively affecting regional groundwater levels.

Both specific seasonal scenarios did not significantly affect the regional groundwater (Table 6; Figure 14). Most significant changes for Sst1 and Sst2 were found to be 0.04 and 0.05 m, respectively, for observation well 5. However, results primarily ranged between 0 and 10^{-3} m for both summer and winter. Even though high relative changes to winter extractions were applied (resp. 15% to 2 – 7%), the net effects were limited due to the low initial volumes at the specific well-fields compared to larger well-fields (e.g. 't Klooster). Results indicated that seasonal extractions in lower quantities do minimally enhance regional groundwater tables. As most net effects subsided 0.05 m, spatial patterns were restricted to a 100 m radius outside well-fields and did not indicate distinct patterns. The slight positive annual phreatic head trends under wells 2 and 5 (resp. 0.03 and 0.04 m) were therefore deemed highly-local (Figure 16). The same applied to negative

trends at wells 7 – 15. Regional difference maps for Sst1 and Sst2 are included in Appendix D.2 for transparency.

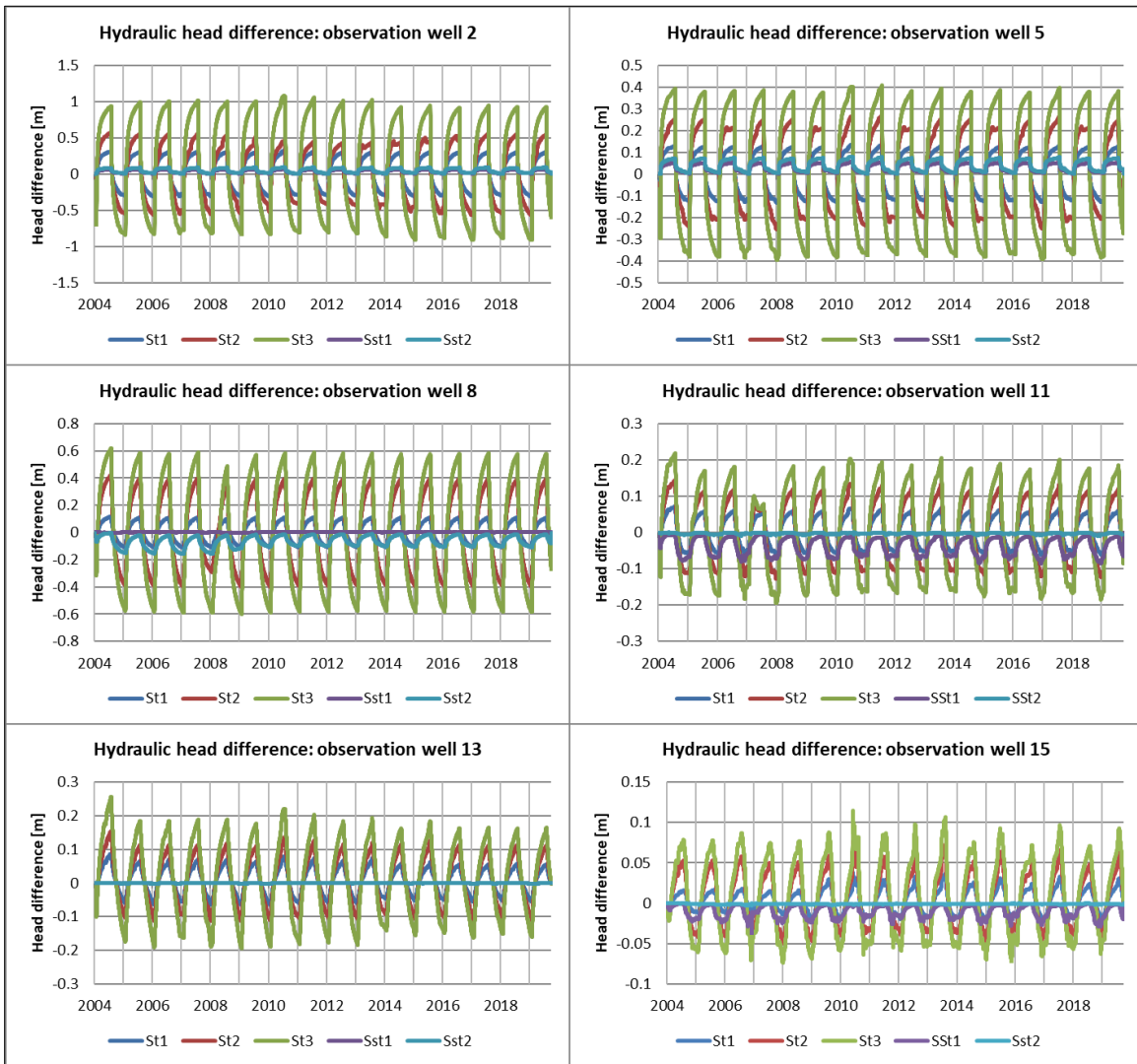


Figure 14. Timeseries of the local difference in phreatic groundwater head [m] under all seasonal scenarios compared to the baseline scenario for the six current extraction locations. Positive difference values indicate an increased groundwater head under seasonal scenarios. Negative difference values indicate a reversed situation.

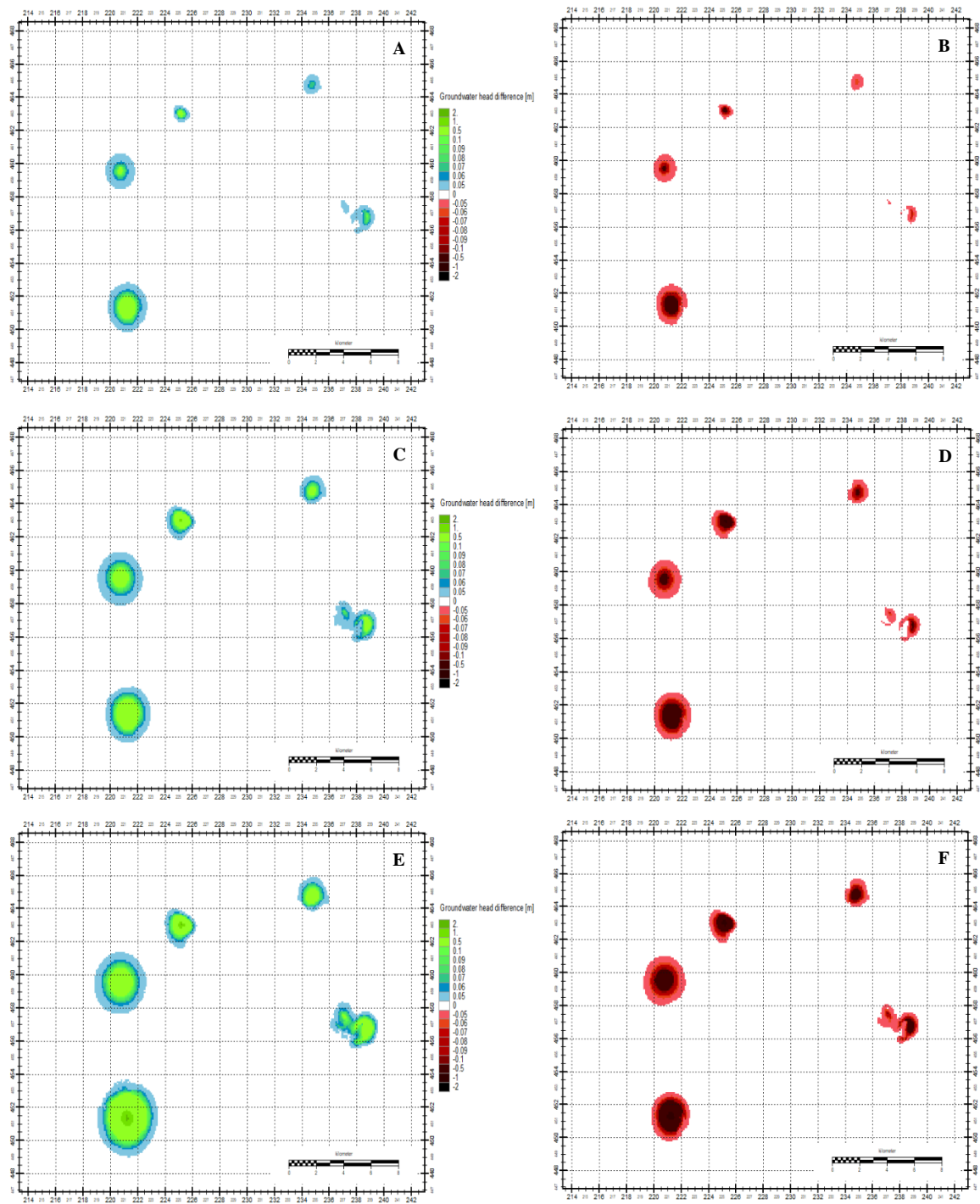


Figure 15. Regional difference maps of the phreatic groundwater head [m] under seasonal scenarios compared to the baseline scenario. Positive difference values indicate an increased groundwater head under seasonal scenarios. Negative difference values indicate a reversed situation. Difference maps in respective order: a) St1 summer, b) St1 winter, c) St2 summer, d) St2 winter, e) St3 summer, f) St3 winter. Summer representation was taken on 24-07-2012. Winter representation was taken on 15-12-2011.

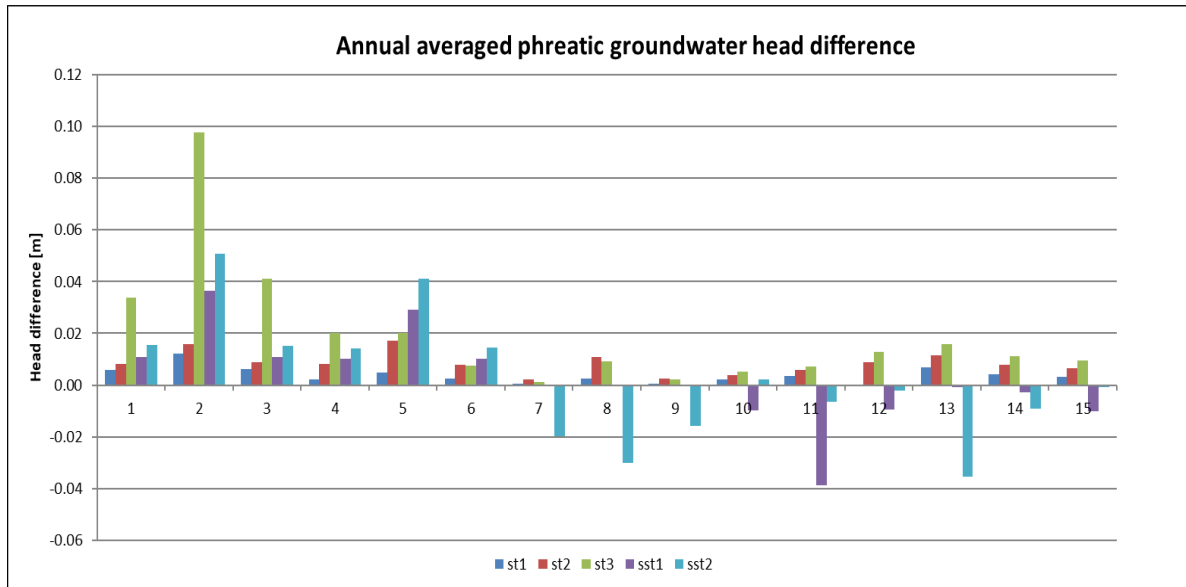


Figure 16. Yearly averaged phreatic groundwater head differences [m] under seasonal scenarios compared to the baseline for the relevant observation wells. Positive difference values indicate an increased groundwater head under seasonal scenarios. Negative difference values indicate a reversed situation. Individual numbers on the x-axis correspond to the respective observation well coding.

5.2 Soil moisture content

5.2.1 Baseline scenario

Under baseline conditions, regional soil moisture varied based on local characteristics, groundwater extractions, and seasonality. Regionally, soil moisture saturation deficits were found highest at forested areas and elevated ridges (resp. 450 – 850 mm/d; Figure 18). Similar deficits characterized urban regions. The widespread agricultural areas contained consistent deficits in the range of 100 – 250 mm/d. Around current well-fields, reduced soil moisture content was found (Figure 17). The most noticeable deficits were observed at locations 2 and 8. Soil water saturation deficits at these locations varied between 550 – 1250 and 750 – 1300 mm/d, based on seasonal precipitation. Similar seasonal variations were found at locations 5, 11, 13, and 15; however present in lower initial ranges (100 – 700 mm/d). Lower initial ranges were found corresponding to local extraction intensities (See also Table 1). The high extraction rates explained the high deficit under wells 2 and 8. Additionally, well 8 is adjacent to a locally elevated ridge (i.e. *Lochemse berg* [+30 m]). The missing extractions in 2007 at well 8, was also seen propagated in soil moisture content, indicated by a decrease of 200 mm/d in soil water saturation deficit compared to annual trends. Over the entire period, a slight increasing trend was observed, indicating consistent soil drying due to climatological trends. The highest deficiencies were found on well-fields, decreasing with further differences to extraction sites (e.g. net difference between well 2 to 1 and 3; or 11 to 10 and 12; Table 7). The soil water saturation deficits for all observation wells are summarized in Table 7.

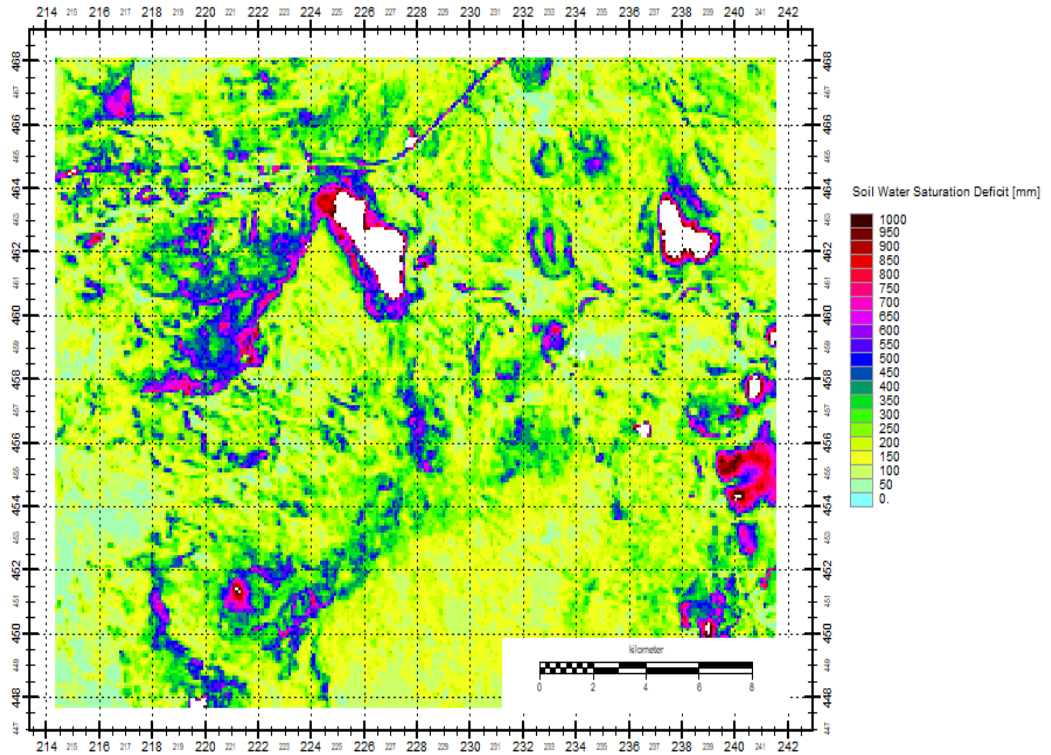


Figure 18. Daily soil water saturation deficit [mm] map of the northern Achterhoek during summer representation for the baseline scenario. Summer representation was taken on 24-07-2012. Note that higher elevated regions compared to the surface level (>30 m) have been masked (white) for readability purposes.

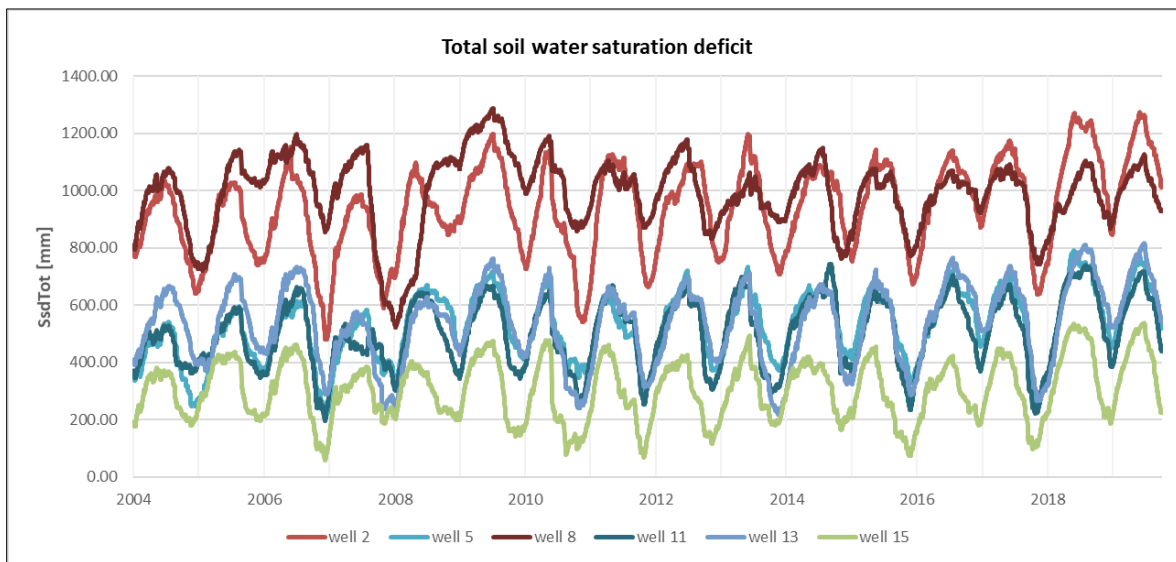


Figure 17. Timeseries of the total soil water saturation deficits [mm/d] for all six current extraction locations over the entire simulation period. Respective observation wells 2, 5, 8, 11, 13 and 15 correspond to extraction locations 't Klooster, Vorden, Lochem, Noordijk, Eibergen, and Haarlo

Table 7. Overview of the averaged daily soil water saturation deficits [mm] during summer and winter over the entire simulation period per relevant observation wells for the baseline scenario.

Observation well	1	2	3	4	5	6	7	8	9	10	11	12	13	14	15
Average summer deficit [mm/d]	584	1092	421	712	623	312	1726	991	808	274	750	566	642	102	394
Average winter deficit [mm/d]	121	805	94	590	412	175	1566	829	687	114	406	243	447	59	245

5.2.2 Decentralized scenarios

All three decentralized scenarios slightly reduced the soil water saturation deficits around extraction locations (Figure 19; Table 8). The differences in soil moisture were found to occur simultaneously to changes in groundwater head; however, the effects were less prominent. Differences were primarily found around locations 1, 2, and 3 (resp. 5 – 10%). Sd1, Sd2, and Sd3 locally decreased the average net soil water saturation deficits with 45 – 63 mm/d, 156 – 178 mm/d, and 45 – 51 mm/d in respective well order. Further relevant changes were found for observation well 11 during winter months (15 – 18 mm/d).

Only limited effects were found for the remaining locations under all scenarios (resp. 1 – 5%; Table 8). Results indicated a similar seasonal oscillation as under groundwater, with the highest peaks in winter. The seasonal variation consistently showed winter benefits exceeding summer benefits by 25 – 50%. On a multi-year level, differences were consistent with initial trends, the exception being well 8 as explained. Figures for all observation wells are included in Appendix E.1.

The spatial distribution of changes in soil water saturation deficits highly correlated to groundwater results (Figure 20). Primary differences accumulated around extraction locations. No clear relation was observed with current soil or vegetation types. Scenarios Sd1, Sd2, and Sd3 all showed similar patterns. The most noticeable differences (i.e. 10 – 100 mm/d) were solely found in proximity to current extraction locations (< 2 km). At further distances, differences restrained to a 1 – 10 mm/d range (resp. 0 – 5%). These smaller positive effects were found to reach up to 9103 - 9841 ha area around well 2 respectively for summer and winter under Sd2. For location 5, this respectively was 803 - 844 ha. The spread for locations 8, 11, 13, and 15 was less extensive and restricted to roughly 254 – 293 ha. Adverse effects, however, only stretched to a maximum of 3612 – 4003 ha, with most subceeding 251 ha. Consequently, general net positive results were found to outweigh adverse effects in both intensity and extent on a regional scale.

Findings concluded that the impacts on soil moisture under decentralized locations related to the net shifts in volume rather than local characteristics. However, the effects were moderate and identified as predominantly well-field specific; observed quickly reduced effects with increasing distance to current extractions. Interestingly, several local adverse extraction trends increased under higher decentralization rates (e.g. well 7, well 14; Figure 20). This phenomenon occurred where multiple smaller extraction wells exceeded the benefits from decentralized volumes, which were uniformly divided over the Eibergen system. Results showed that these smaller local effects were more frequently visible for soil moisture than groundwater (e.g. Sd3; Figure 20); however, the net impact compared to initial values remained limited (<10 mm/d). Furthermore, results demonstrated the effect of river systems (i.e. Berkel). Similar to groundwater, the negative impact on the primary decentral location was reduced by a 200 m wide incision of stable soil moisture contents.

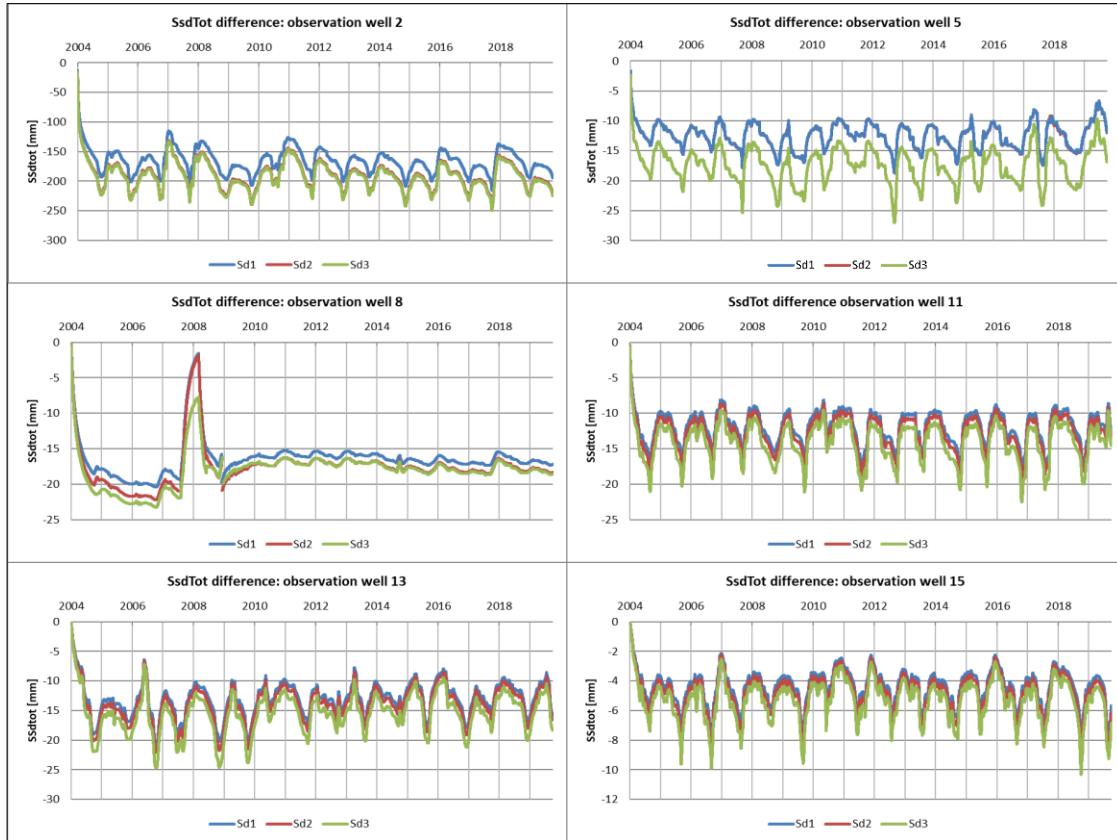


Figure 19. Timeseries of the local difference in soil water saturation deficits [mm/d] under decentralized scenarios compared to the baseline scenario for the six current extraction locations. Negative difference values indicate a decreased deficit under decentralized scenarios. Positive difference values indicate a reversed situation.

Table 8. Net averaged seasonal differences in soil water saturation deficits [mm/day] between alternative scenarios and the baseline at individual observation wells during summer and winter. Negative difference values indicate a lowered soil water saturation deficit for alternative scenarios compared to the baseline. Positive values indicate an inversed situation. Values below 10^{-7} are set to zero. Colour scheme: percentage change to baseline: 10 – 5% (dark green), 5 – 1% (light green), 1 – 0% (white), 0 – -1% (Grey), -1 – -5% (light blue), -5 – -10% (blue). ¹S = summer, W=winter.

Seas-on ¹	Sd1		Sd2		Sd3		St1		St2		St3		Sst1		Sst2	
	s	w	s	w	s	w	s	w	s	w	s	w	s	w	s	w
1	-56	-55	-62	-62	-63	-63	-8.0	4.5	-16	8.2	-23	14	-2.3	0.0	-2.7	0.0
2	-156	-181	-172	-210	-178	-213	-35	28	-55	52	-105	82	-7.9	-1.2	-8.3	-1.3
3	-45	-51	-51	-56	-51	-57	-9.8	4.8	-14	6.6	-27	12	-2.6	0.0	-2.8	-0.1
4	-3.5	-4.6	-3.5	-4.6	-4.7	-6.3	-4.1	2.1	-8.3	5.6	-12	9.4	-2.1	-0.1	-2.4	-0.4
5	-12	-12	-12	-12	-17	-17	-8.2	5.1	-35	13	-41	26	-5.3	-0.9	-7.3	-1.2
6	-4.7	-4.1	-4.7	-4.1	-6.4	-5.6	-3.1	2.5	-6.2	4.7	-11	7.4	-1.6	-0.5	-1.9	-0.7
7	-2.3	-2.5	-2.6	-2.8	-2.6	-2.8	-1.5	1.0	-3.9	2.4	-7.8	5.1	-1.4	-0.4	-1.8	-0.4
8	-12	-12	-12	-13	-13	-13	-12	5.3	-38	19	-51	26	0.0	0.0	1.1	1.3
9	-1.9	-1.9	-2.1	-2.2	-2.1	-1.9	-0.9	0.5	-2.7	1.8	-4.2	2.6	0.0	0.0	1.2	2.7
10	-4.8	-5.6	-5.0	-5.9	-5.4	-6.4	-2.6	1.4	-5.3	3.1	-7.5	4.7	0.5	1.7	0.0	0.0
11	-12	-15	-13	-16	-15	-18	-8.9	6.4	-16	11	-25	17	0.8	5.4	0.0	0.0
12	-4.3	-4.8	-4.5	-5.1	-5.0	-5.6	-2.6	0.4	-6.4	1.5	-8.3	2.7	0.6	0.8	0.0	0.0
13	-13	-1.7	-13	-18	-15	-20	-18	12	-31	21	-49	34	0.0	0.0	2.2	6.8
14	-3.1	-2.6	-3.3	-2.9	-3.7	-3.0	-2.9	1.3	-4.6	2.2	-8.1	3.9	0.0	0.0	0.5	2.2
15	-3.8	-5.1	-4.1	-5.5	-4.5	-6.2	-3.9	1.7	-7.8	3.5	-11	5.3	1.9	0.1	0.0	0.0

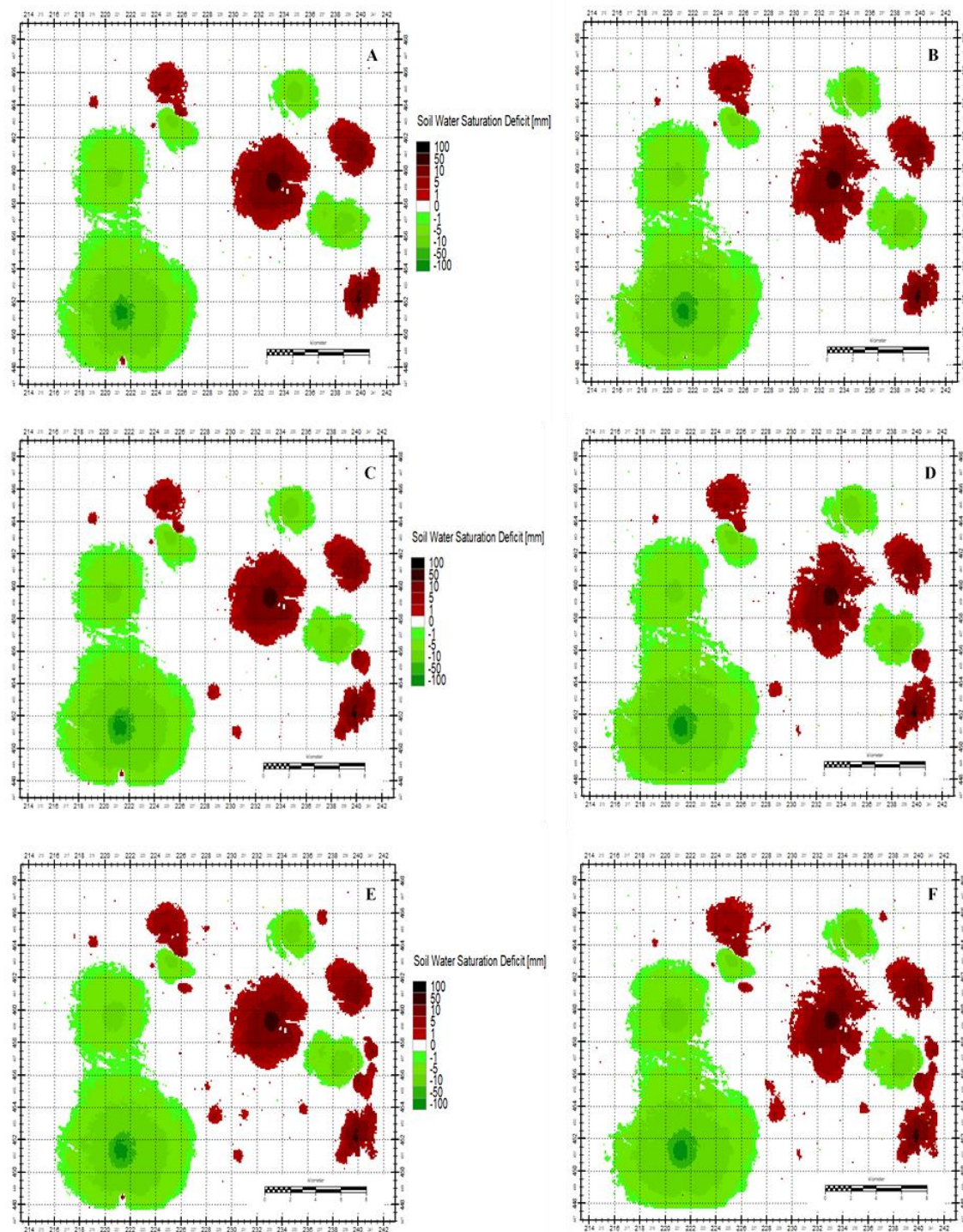


Figure 20. Regional difference maps of the daily soil water saturation deficits [mm/d] under decentralized scenarios compared to the baseline scenario. Negative difference values indicate a decreased deficit under decentralized scenarios. Positive difference values indicate a reversed situation. Difference maps in respective order: a) Sd1 summer, b) Sd1 winter, c) Sd2 summer, d) Sd2 winter, e) Sd3 summer, f) Sd3 winter. Summer representation was taken on 24-07-2012. Winter representation was taken on 15-12-2011.

5.2.3 Seasonal scenarios

Seasonal scenarios provoked lower effects on regional soil moisture (Table 8). All scenarios only decreased average summer soil moisture saturation deficits by 1 – 5% for most wells. Higher intensity effects were found for St2 and St3 (5 – 10%; resp. wells 11 and 13, and wells 2, 3, 5, 11, and 13), coinciding with high initial extractions. At further distances from well-fields, no changes were present (i.e. wells 16 – 20). Locally, results indicated more prominent effects (Figure 21; Appendix E.1). Noticeable peak results varied between -210 – 175 , -120 – 95 , and -56 – 43 mm/d for well 2 under St1, St2, and St3. The lowest fluctuations were found at observation well 14 (resp. -15 – 8, -9 – 5, -5 – 2 mm/d). These extremes represented the accumulated differences after 6-months of consecutive extractions. Whilst significant, these peaks in deficits only lasted several days and occurred at the ends of the respective season. Furthermore, averaged over the corresponding season, values were similar to decentralized scenarios (See Table 8).

In winter, soil moisture content decreased compared to the baseline. However, adverse soil moisture results were significantly lower in intensity (factor 0.5 – 0.8) than summer improvements (Table 8; Figure 21). Consequently, annual trends were positive (i.e. net decrease in deficits), indicating the effective containment of water in the unsaturated zone. The averaged net effect was related to the applied percentages and shifts in volumes under the seasonal scenarios. Surprisingly, this relation was non-linear and variable based on local characteristics.

The regional soil moisture differences strictly followed groundwater results (Figure 22). The extent of the effects showed conformity to higher initial extraction volumes and applied degree of seasonality. Positive effects were found up to 2.0 km around observation wells 2 and 5 for St2. For wells 8, 11, 13, and 15, this varied between 0.7 – 1.1 km. However, impacts mostly confined to well-fields, as results outside a 500 m radius often subceeded a 1% change compared to baseline values. Comparable patterns were found for St1 and St3 (Appendix E.2). Similar to Table 8, the positive influences during summer consistently exceeded adverse winter effects (resp. factor 1.15 – 1.25; Figure 22).

Additionally, results highlighted a delayed reaction for higher elevated ridges. At these locations (Figure 22), soil moisture replenishment and depletion lagged behind seasonal patterns. The effect increased slightly per scenario but was vastly-local. Overall, results indicated that seasonal extractions had only a moderate regional effect, particularly in lower applied volumes. Yet, seasonal scenarios slightly improved the current mismatch to seasonal demand and demonstrated potential for consistent local improvements in the long-term.

The specific seasonal scenarios (Sst1, Sst2) were minimally effective in improving regional soil moisture content (Table 8; Figure 21). Relative influences of either scenario did not exceed 1% compared to the baseline. The most noticeable differences (resp. 8.3 mm/d for well 2 under Sst2) only attained 23% of the effect as under the lowest seasonal scenario (resp. 35 mm/d for well 2 under St1); correlating to input ratios. These findings demonstrated the limited effectiveness of seasonal extractions in lower quantities on the regional soil moisture. The spatial differences were restricted to local well-fields and did not indicate influences outside a 300 m radius (Figure 22). At locations of increased winter extractions (i.e. well 11 and 15; 8 and 13), slight adverse effects on the soil moisture were found. Whilst adverse effects were of lower intensity (<1%), the spatial extent was significantly larger than their beneficial counterparts (resp. 78 – 631 ha) due to applied volume proportioning.

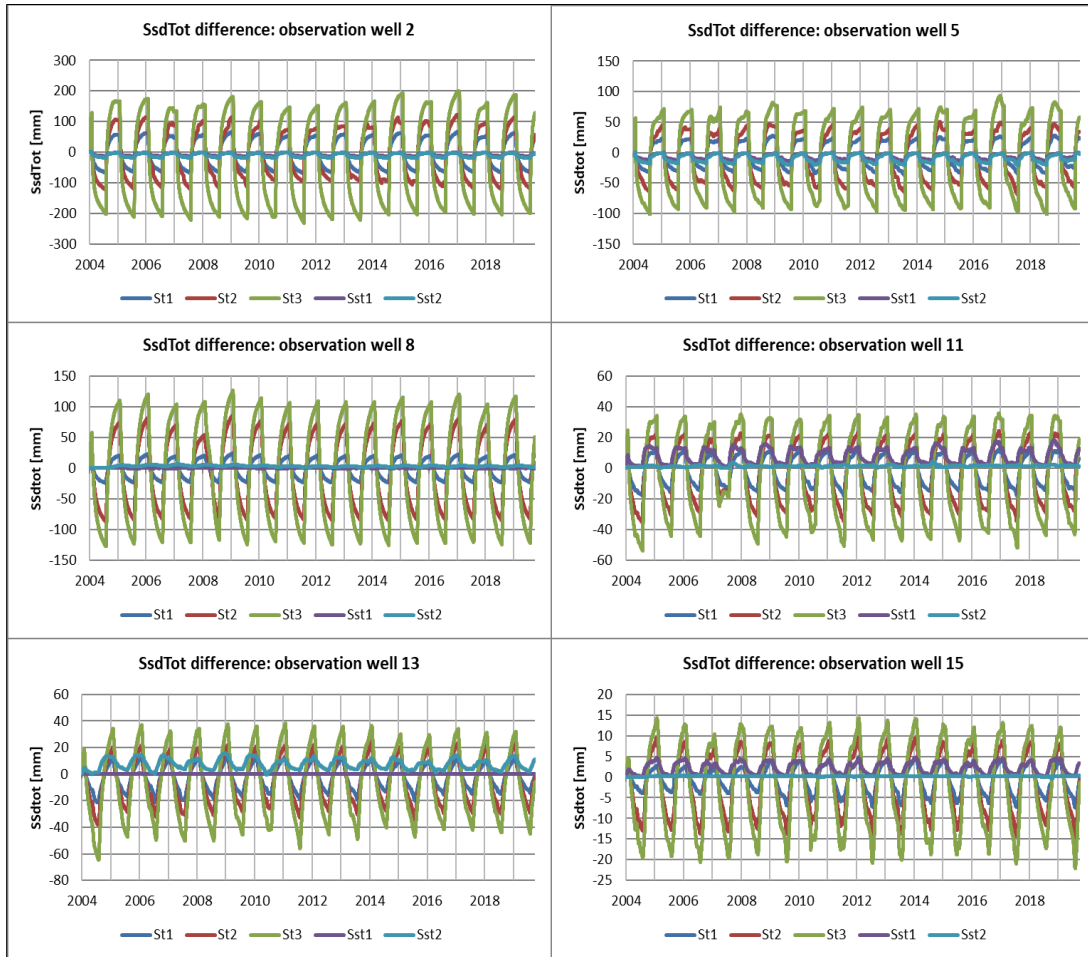


Figure 21. Timeseries of the local difference in soil water saturation deficits [mm/d] under seasonal scenarios compared to the baseline scenario for the six current extraction locations. Negative values indicate a decreased deficit under seasonal scenarios. Positive values indicate a reversed situation.

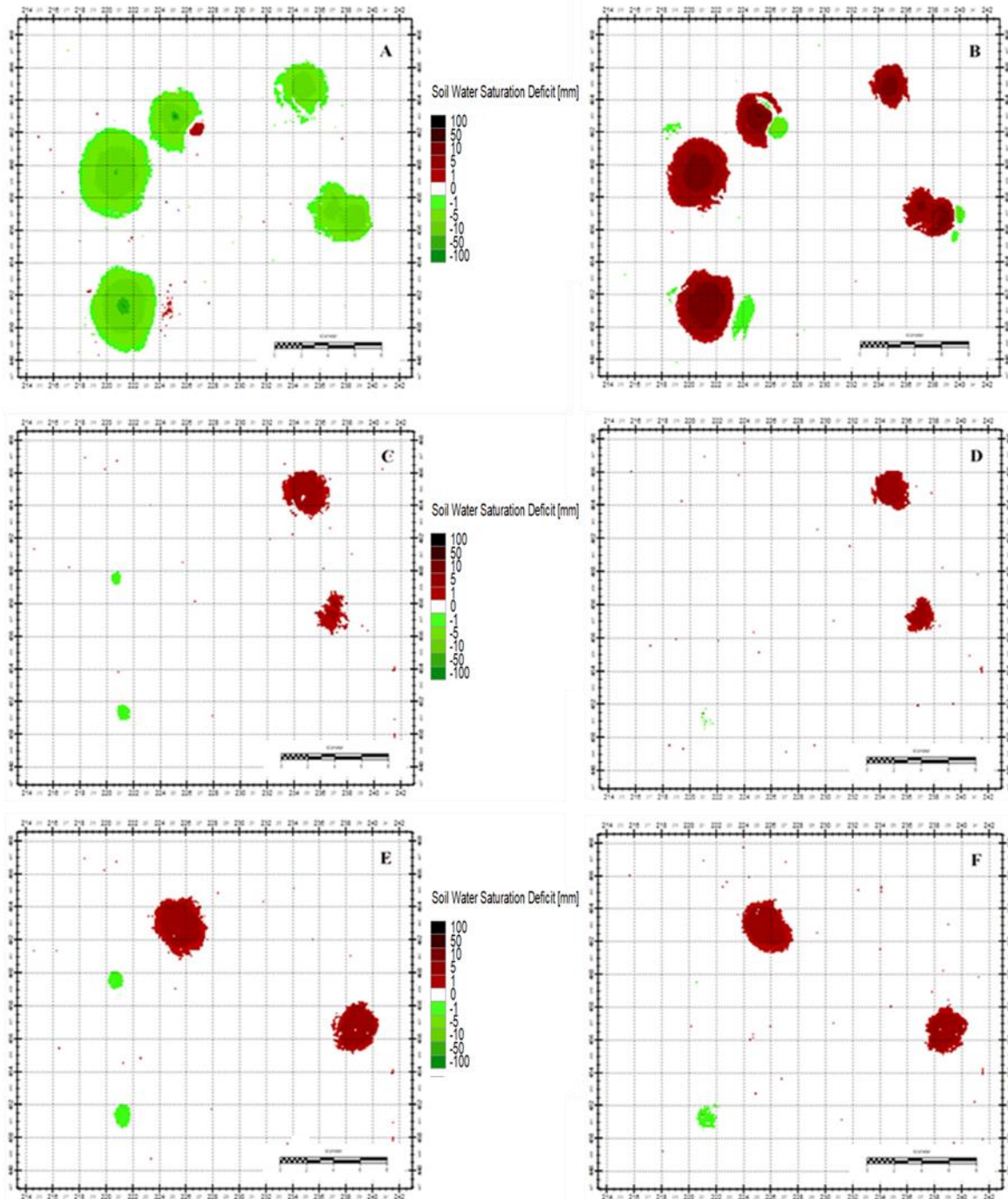


Figure 22. Regional difference maps of the daily soil water saturation deficit [mm/d] under relevant seasonal scenarios compared to the baseline for summer and winter. Negative values indicate a decreased deficit under decentralized scenarios. Positive values indicate a reversed situation. Difference maps in respective order: a) St2 summer, b) St2 winter, c) Sst1 summer, d) Sst1 winter, e) Sst2 summer, f) Sst2 winter. Summer representation was taken on 24-07-2012. Winter representation was taken on 15-12-2011.

5.3 Evapotranspiration

5.3.1 Baseline scenario

Evapotranspiration under the baseline scenario varied in both space and time (Figure 23; Figure 24). Actual evapotranspiration was found most significant in summer (e.g. observation well 2, 5, 8, and 13). During winter, evapotranspiration is climatological and phenological limited in the Netherlands, affirmed by low values (0 – 0.5 mm/d). Figures for all observation wells can be found in Appendix F. The lower elevated observations wells 2, 5, and 6 showed yearly fluctuating peak summer evapotranspiration between 6 to 9 mm/d. Observation well 13 showed peaks roughly between 5 and 6 mm/d (Figure 23). The remaining wells varied accordingly in-between these findings (Table 9). Peak evapotranspiration in summer only occurred for brief continuous periods within each year (< 14 days) and did not noticeably relate to local extraction regimes. Averaged summer values (April – August) were taken as more representative. Respectively, values varied between 2.5 – 3.0 mm/d at the lower end and 3.5 – 4.5 mm/d at the high end (Table 9). Yet again, little relation was found compared to local groundwater levels and extraction regimes.

Together, results indicated that current extraction regimes played a minimal role in local evapotranspiration patterns. Baseline evapotranspiration was instead observed to conform to regional land cover types and soil moisture content (Figure 24). Results indicated regional consistency around agricultural regions (3 – 4.5 mm/d: *green*). Slight differences were found distinguishing arable lands and grassland from crop (maize) production (resp. 3 – 3.5 mm/d; 4 – 4.5 mm/d). Further findings showed consistent evapotranspiration rates in urban areas (1.5 – 2 mm/d: *purple*) and forested regions (2.5 – 3 mm/d: *blue*). No significant differences were distinguished between coniferous and deciduous forests. The lower evapotranspiration under forested regions compared to grassland followed from the combination of agricultural irrigation and the applied methodology (i.e. Makkink crop factor; 0.8).

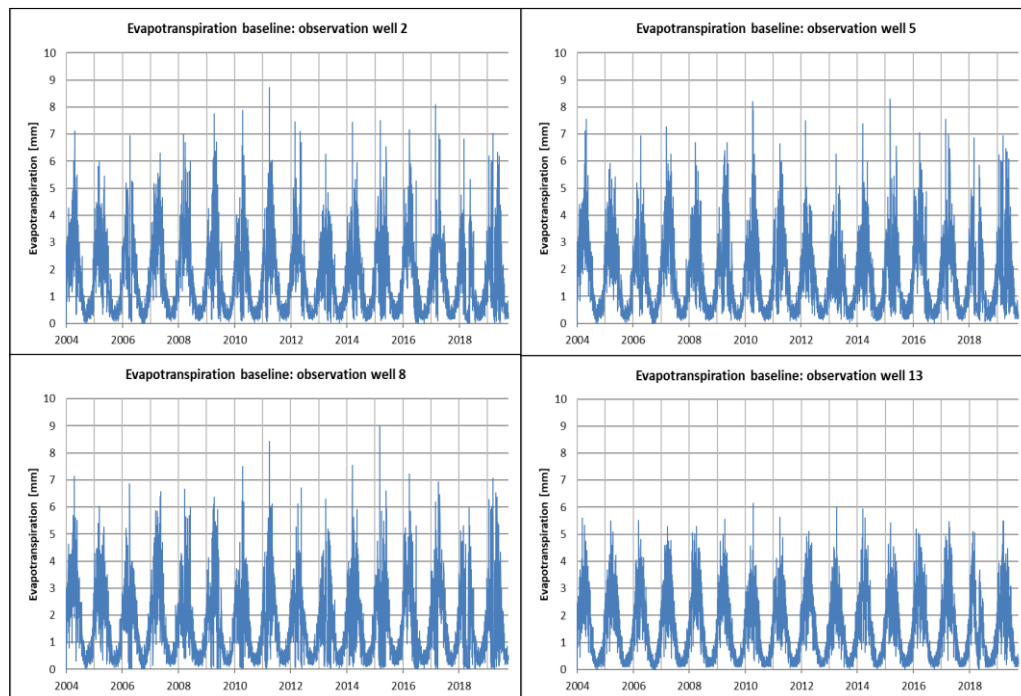


Figure 23. Timeseries of local evapotranspiration rates [mm/d] for the entire simulation period for four exemplary observation wells. Respectively observation wells 2, 5, 8, and 13 correspond to extraction locations 't Klooster, Vorden, Lochem, and Eibergen.

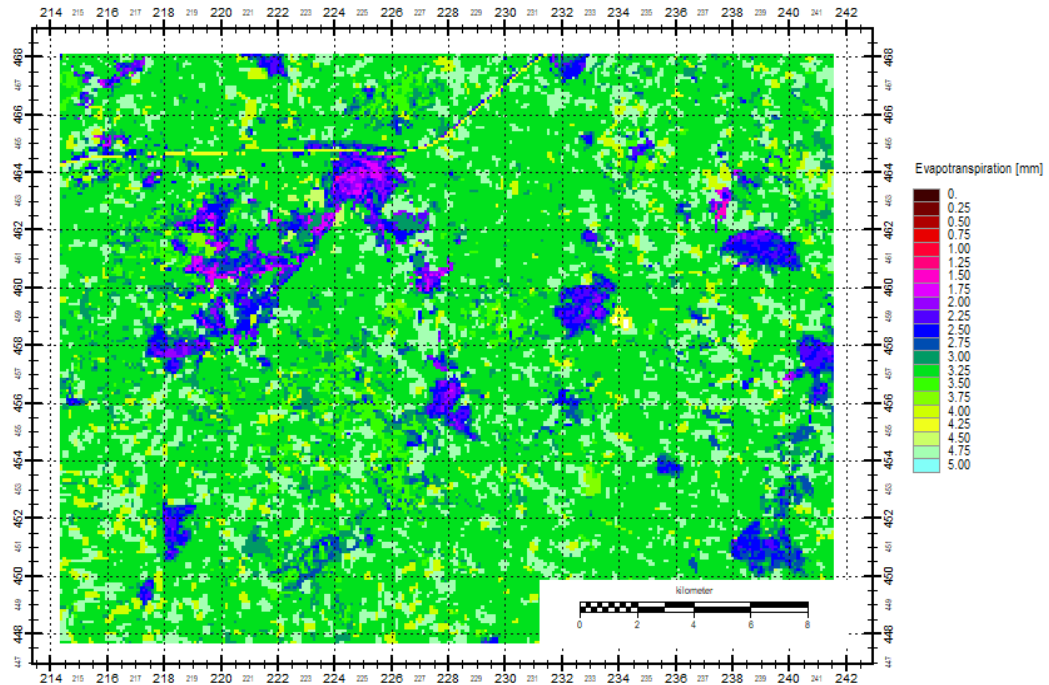


Figure 24. Daily evapotranspiration [mm] of the northern Achterhoek during summer representation for the baseline scenario.

Table 9. Averaged summer evaporation [mm/d] and peak summer evapotranspiration [mm/d] over the entire simulation period per relevant individual observation wells under the baseline scenario.

Observation well	1	2	3	4	5	6	7	8	9	10	11	12	13	14	15
Peak summer evapotranspiration [mm/d]	5.5	8.6	6.4	8.5	7.1	6.2	6.9	8.9	5.8	6.2	8.1	7.3	6.1	7.1	8.2
Averaged summer evapotranspiration [mm/d]	3.1	4.0	3.5	4.1	3.9	3.3	3.6	4.3	2.6	3.2	4.0	3.5	3.2	3.5	4.1

5.3.2 Decentralized scenarios

In contrast to previous results, all three decentralized scenarios only had a limited effect on the regional evapotranspiration; Appendix F). Net differences in evapotranspiration were solely observed during the summer months. Most noticeable changes were found at observation well 2 (0.21 – 0.23 mm/d) related to high decentralized reductions. Modest improvements (resp. 1 – 5%) to evapotranspiration rates were further only observed under Sd2 and Sd3. For locations 1, 11, and 14, Sd2 and Sd3 increased evapotranspiration with respectively 0.03, 0.04, and 0.03 mm/d. However, differences were defined as highly well-field specific. This finding was strengthened by the sharp decline of positive effects on evapotranspiration between observation wells 1 and 2. Similar trends were observed at the other well-fields (e.g. 4 and 5; 8 and 9).

Yet, most results for Sd1, Sd2, and Sd3 varied between 0 and 10^{-2} mm/d. Excluding the site-specific effects, minimal differences were observed between the three scenarios (Table 10). The results, therefore, indicated that all three tested scenarios were mostly ineffective (< 1%) in enhancing regional evapotranspiration. The lack of significant improvements hinted at the limited active interaction between groundwater under extraction regimes and regional vegetation. A potential explanation was found in the deep regional

groundwater tables (> 2 m). It is conceptualized that the tested scenarios were insufficiently able to enhance groundwater level and soil moisture by capillary rise to reach vegetation.

The regional distribution of evapotranspiration closely matched the initial land cover patterns rather than changes in groundwater regimes (Figure 25). The largest improvements were observed around observation wells 2 and 5 (resp. $0.01 - 0.05$ mm/d). These regions corresponded to the slightly elevated coniferous and deciduous forests, containing limited soil moisture and evapotranspiration under the baseline scenario. However, due to the deep local rootzone of forested regions, they benefit in an earlier stage to fluctuation in groundwater and soil moisture compared to the surrounding grasslands. The spatial extent of the positive effect on this area increased slightly per decentralized scenario.

Evapotranspiration declined in minor ranges around observation well 9 ($-0.001 - -0.005$ mm/d) after the placement of multiple concentrated wells. This phenomenon was similarly observed below Eibergen (well 13). Even for the largest decentralized location (232500; 459000), limited changes to the regional evapotranspiration were found ($-0.01 - -0.05$ mm/d). Moreover, the spatial extent at these locations was secondary compared to the positive trends seen around the current extraction locations (Figure 25). Results thereby advocated the beneficial effect of decentralization by the sparse occurrence of adverse effects; and demonstrated that these negative effects were relatively small. Caution however applies as all results were minimal in extent and intensity.

Table 10. Net averaged seasonal evapotranspiration differences [mm/day] between alternative scenarios and the baseline at individual observation wells during summer and winter. Positive difference values indicate higher evapotranspiration during alternative scenarios. Negative values indicate a reversed situation. Values below 10^{-7} are set to zero. Colour scheme: percentage change compared to baseline values: 10 – 5% (dark green), 5 – 1% (light green), 1 – 0% (white), 0 – -1% (light blue). ¹S = summer, W=winter.

Season ¹	Sd1		Sd2		Sd3		St1		St2		St3		Sst1		Sst2	
	s	w	s	w	s	w	s	w	s	w	s	w	s	w	s	w
1	0.02	0	0.03	0	0.03	0	$2.0 \cdot 10^{-4}$	0	$6.2 \cdot 10^{-3}$	0	0.03	0	$1.8 \cdot 10^{-4}$	0	$4.5 \cdot 10^{-4}$	0
2	0.21	0	0.21	0	0.23	0	0.04	0	0.07	0	0.13	0	0.01	0	0.02	0
3	0	0	0	0	0	0	0	0	0	0	0	0	0	0	0	0
4	$9.1 \cdot 10^{-3}$	0	$9.1 \cdot 10^{-3}$	0	0.02	0	$1.8 \cdot 10^{-3}$	0	$7.2 \cdot 10^{-3}$	0	$4.9 \cdot 10^{-3}$	0	$4.8 \cdot 10^{-3}$	0	$6.9 \cdot 10^{-3}$	0
5	0.02	0	0.02	0	0.03	0	0.03	0	0.04	0	0.07	0	0.02	0	0.02	0
6	0	0	0	0	0	0	0	0	0	0	0	0	0	0	0	0
7	0	0	0	0	0	0	0	0	0	0	0	0	0	0	0	0
8	$7.6 \cdot 10^{-3}$	0	$8.6 \cdot 10^{-3}$	0	$8.9 \cdot 10^{-3}$	0	$5.2 \cdot 10^{-3}$	0	0.03	0	0.03	0	0	0	$-5.5 \cdot 10^{-3}$	0
9	$5.1 \cdot 10^{-3}$	0	$5.8 \cdot 10^{-3}$	0	$5.8 \cdot 10^{-3}$	0	$2.5 \cdot 10^{-3}$	0	$1.3 \cdot 10^{-5}$	0	$1.9 \cdot 10^{-5}$	0	0	0	$-8.9 \cdot 10^{-3}$	0
10	0	0	0	0	0	0	0	0	0	0	0	0	0	0	0	0
11	0.02	0	0.04	0	0.04	0	$1.3 \cdot 10^{-5}$	0	$6.7 \cdot 10^{-3}$	0	$8.4 \cdot 10^{-3}$	0	$-5.8 \cdot 10^{-4}$	0	0	0
12	0	0	0	0	0	0	0	0	0	0	0	0	0	0	0	0
13	0	0	0	0	0	0	0	0	0	0	0	0	0	0	0	0
14	0.01	0	0.01	0	0.03	0	$7.3 \cdot 10^{-4}$	0	$1.3 \cdot 10^{-3}$	0	$2.2 \cdot 10^{-3}$	0	$-5.2 \cdot 10^{-4}$	0	$-1.9 \cdot 10^{-4}$	0
15	0	0	0	0	0	0	0	0	0	0	0	0	0	0	0	0

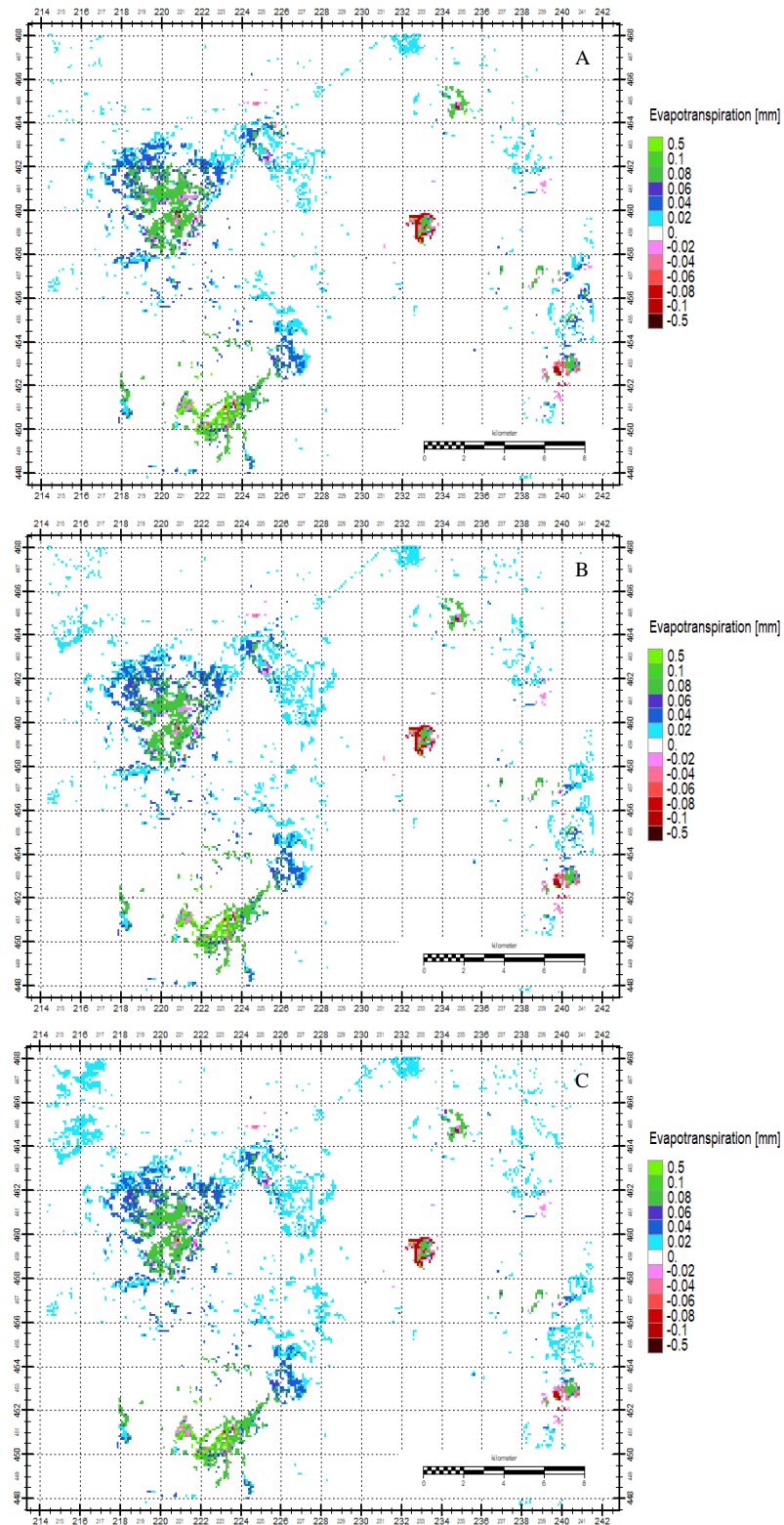


Figure 25. Daily evapotranspiration difference maps [mm] for decentralized scenarios compared to the baseline scenario during summer representation. Positive difference values indicate increased evapotranspiration under decentralized scenarios. Negative difference values indicate a reversed situation. Difference maps in respective order: a) Sd1, b) Sd2, c) Sd3. Summer representation was taken on 24-07-2012.

5.3.3 Seasonal scenarios

Seasonal scenarios minimally improved evapotranspiration (Table 10). Changes in evapotranspiration under St1, St2, and St3 were most noticeable at locations 2 and 5 (resp. 1 – 5%) due to high extractions. Similar positive differences were found at observation wells 1 and 8, roughly increasing evapotranspiration by 0.03 mm/d for both St2 and St3. However, mostly minor changes (< 1%) were found at individual locations, and no improvements were found outside the vicinity of current well-fields (i.e. observation wells 16 – 20). The degree of seasonal extraction showed a slight relation to evapotranspiration. Higher seasonal scenarios (e.g. St3) induced more favorable evapotranspiration rates compared to lower scenarios (factor 2 – 5, compared to St1); however, all net effects were highly local and relatively restricted in intensity (Table 10). None of the seasonal scenarios effectively increased the regional evapotranspiration by more than 5% for any individual location

The regional extent of evapotranspiration was similar to results under decentralized scenarios (Figure 26). Little resemblance to groundwater or soil moisture results was found, indicating restricted interactions between extraction regimes and evapotranspiration patterns. The forested regions near observation wells 2 and 5 were observed to show the most regional improvement (resp. 0.01 – 0.5 mm/d). Furthermore, slight positive effects were present around well 8 under St2 and St3 (resp. 0.02 – 0.03 mm/d). Both locations were characterized by low initial evapotranspiration and elevated surface levels. Between scenarios, only areas positively affected by at least 0.05 – 0.01 mm/d under St1 showed increased extents under St2 and St3. The distribution of lower intensity changes (0.001 – 0.01 mm/d) remained unchanged over all scenarios (Figure 26). Furthermore, larger regions did not contain positive changes in a similar range (> 1%), as significant results mostly confined to local well-fields (see also).

Both specific seasonal scenarios were observed with the lowest net effect (Table 10; Figure 26). Due to limited shifts in seasonal volumes (resp. 15, to 2 – 7%), minimal-to-no improvements (< 0.02 mm/d) were observed for all locations. Furthermore, lower positive effects in both extent and intensity were found at sites previously indicating dominant improvements under St1 to St3 (well 2, well 5; Figure 26). Interlocational distribution of volumes resulted in negative difference values at observation wells 11 and 14, and 8, 9, and 14, respectively, for Sst1 and Sst2 (Table 10). The presence of negative evapotranspiration differences indicated a slight relation to extraction regimes; however, observed values were of insignificant order (< 1%) to be reliably defining. Furthermore, negative differences propagated from winter to summer months.

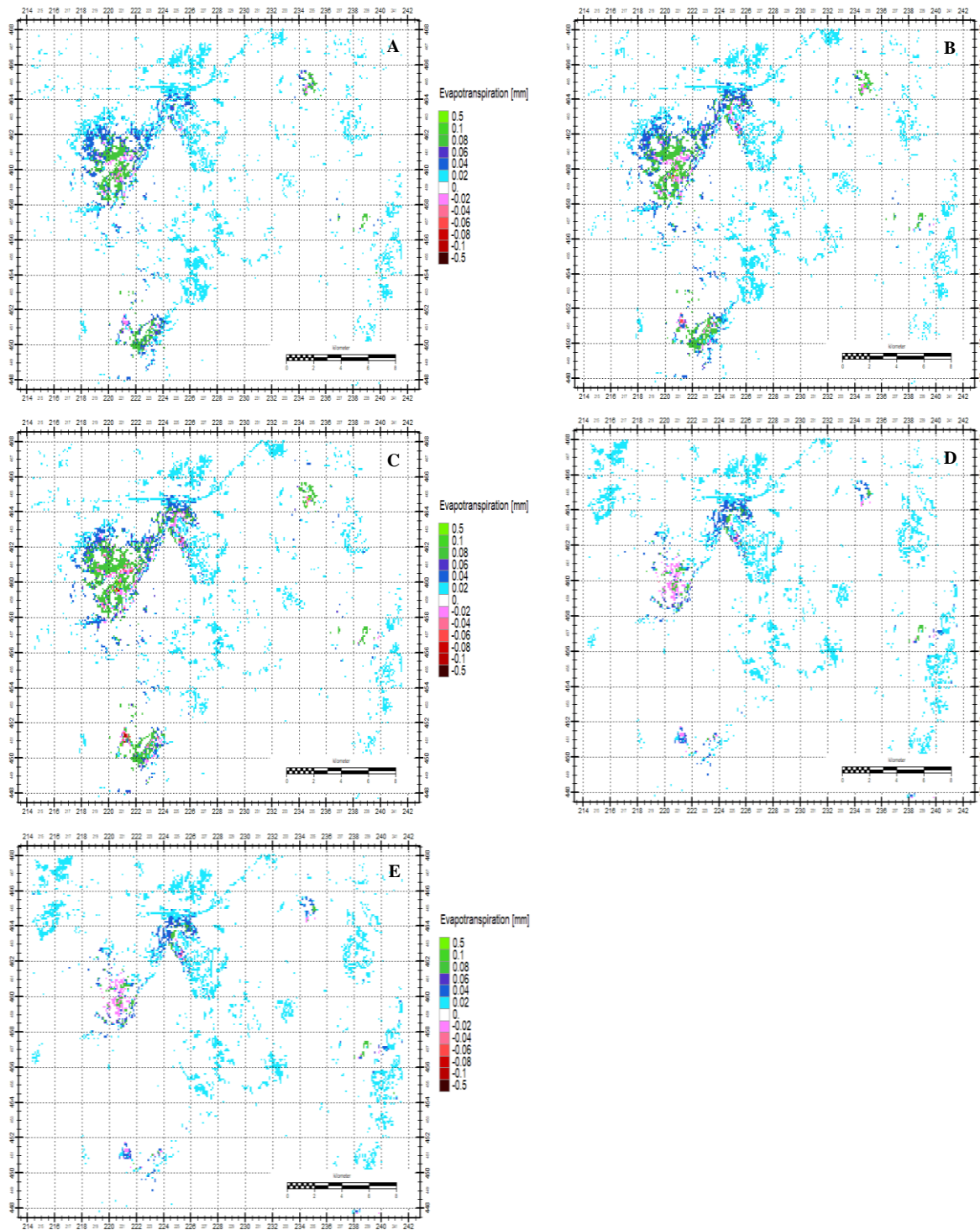


Figure 26. Daily evapotranspiration difference maps [mm] for seasonal scenarios compared to the baseline scenario during summer representation. Positive values indicate increased evapotranspiration under seasonal scenarios. Negative values indicate a reversed situation. Difference maps in respective order: a) St1, b) St2, c) St3, d) Sst1, e) Sst2. Summer representation was taken on 24-07-2012.

Chapter 6 Discussion

6.1 Limitations, assumptions, and uncertainties

6.1.1 Model limitations

Hydrogeological modelling as an approach relies on the fundamental propositions behind data availability, computational theories, calibration methods, and performance metrics (i.e. restricted estimation of physical phenomena; Biondi et al., 2012; Peel & Blöschl, 2011). The novelty of AMIGO v3.1 (Beta-version) during this thesis presented some specific limitations. Arcadis progressively identified small discontinuities in the model outputs (e.g. overestimation anisotropy at moraines; missing evaporation grids in 2009). Whilst currently adjusted by model re-runs with refitted data, the potential prevails that new inaccuracies will be discovered in the definite simulations. An example still present is the lack of multiple precipitation grids inside the German section of the model. The extent to which this disturbed the results is yet unclear, even to Arcadis. However, as the model cut-out, including buffer-zone, was located at a significant distance to this border, limited interference is expected.

Furthermore, by using Makkink's approach to fit data availability, evapotranspiration for local forested regions might be underestimated. Whilst a time-variable crop factor was applied enhancing daily accuracy by including phenological phases; crop factors vary amongst literature which can induce discontinuities (e.g. yearly averaged crop factor for coniferous forests: within the model: 0.85, Jansen et al. (2004): 0.9, Roelsma et al. (2008): 1.2, or de Bruin & Lablans (1998): 1.0. Moreover, yearly forest evapotranspiration firmly depends on temperature, vapour pressure, and aerodynamic resistance, rather than radiation (i.e. second term Penman-Monteith equation; Moors et al., 1996; Rácz et al., 2013). Makkink primarily simulates the dependency on the first Penman-Monteith term, dominated by radiation. This effect is less distorting for grasslands as the same principle mainly affects grasses during winter when evapotranspiration is minimal. Since this assumption overarches all scenarios, net differences are expected to contain little deviation. However, with low values in the results (i.e. 0.5 – 0.01 mm/d), it can be questioned whether exact results are reliable, or rather indicative of minimal trends.

Another limitation is the steady-state approach taken to model local surface water bodies. The stages of local waterways were approximated by fixed values per cell (25x25 m) for winter and summer, as full transient simulations would require detailed daily data: currently only available for major rivers (e.g. IJssel river; de Weme et al., 2019). By this simplification, natural climatological variances, often promptly affecting surface waters, were neglected (Geertsema et al., 2011). As a significant part of streams fall dry during summer (Massop, 2019), streamflow is overestimated, potentially propagating to local drainage flows, groundwater levels, and soil moisture. Similarly, high discharges during peak precipitation events were not considered, underestimating local parameters during winter. Moreover, few smaller water bodies (*infiltratieplassen*) were taken as infinite sources of infiltration and evaporation due to the constant surface water levels. Although not directly visible in the results, local overestimations were found by an in-depth analysis on transpiration and drainage fluxes, highest around regions with strong drawdown regimes.

Lastly, the spatial resolution of the model was set relatively coarse (100x100m) to retain feasible simulation times. Whilst still suitable for regional-scale studies (Schipper et al., 2015; Van Baaren et al., 2016), the reliability of local results in finer quantitative ranges is limited (van Daele & de Bie, 2015).

6.1.2 Scenario assumptions

Yearly consumer data had to be linearly extrapolated over the entire simulation period to fit model input. Hereby temporal variances and trends were neglected, causing a mismatch to the detailed extraction data. As no information was available on the consumers' characteristics, this research was unable to reconstruct these trends. In reality, seasonal-fitted extractions might be a more realistic representation of the strategy, depending on consumer type (e.g. industrial, energy, agricultural). For example, agrarian consumers might show a skewed seasonal water usage distribution, peaking during growth seasons or dry stretches, whilst industrial sectors require constant water provision for production (van der Meer, 2013).

Secondly, the assumption had to be made to place a single decentralized well amid the corresponding consumer postcode. Due to privacy considerations, it could not be identified whether consumer data represented a singular user or a multitude of users. The practical redistribution of extractions under multiple locations could reduce the strategies' effect. Furthermore, some postcodes comprised significant areas, hampering realistic well placement. As evapotranspiration and soil moisture results were highly-local and related to local characteristics, the inaccurate placement might have influenced both results based on present landcover type (e.g. urban, agricultural grasslands).

6.1.3 Uncertainty analysis

Model uncertainties were determined by de Weme et al. (2019) using residuals. Mean GHG and GLG results indicated limited residuals compared to measured observational data: respectively 0.23 m and 0.13 m (See Appendix G). Mean absolute residuals were found slightly higher (resp. 0.45 – 0.37 m). However, regional differences were leading; around 't Klooster, Vorden and Lochem averaged residuals mostly subceeded 0.10 m, whilst residuals in the higher elevated eastern ridges were larger than 0.50 m following the complex geohydrological situation. Due to the spatial distribution of residuals compared to relevant well-fields, and regional scenario comparative character of the study, uncertainties were found acceptable. Parameter and sensitivity analysis can be found in de Weme et al. (2019).

Concludingly, whilst the accuracy of specific results can be questioned based on individual assumptions, limitations, and uncertainties, the overall results were deemed sufficient to answer the general research questions reliably.

6.2 Discussion of the results

6.2.1 Noteworthy results

Results indicated minimal propagation of groundwater fluctuations to soil moisture or evapotranspiration. This is a commonly identified phenomenon in literature (Jeuken et al., 2015). An essential driver seemed to be regional groundwater depth. As groundwater depths mostly exceeded 2 m (Table 5), improvements induced minimal capillary rise or evapotranspiration changes. Runhaar & Hennekens (2015) found that potential drought stress occurs from 1 – 2 m groundwater depth, depending on soil and vegetation characteristics. This explains why both strategies were unable to enhance hydro-environmental parameters effectively. Groundwater levels under alternative strategies remained significantly below these thresholds. For groundwater-dependent ecosystems, this infers that alternative strategies are only sustainable if they sufficiently reduce groundwater depletion to this threshold value, which often is deemed unfeasible without

unorthodox methods (Gerritsen & Barendregt, 2020). An exception was found in trees, which prefer slightly deeper groundwater tables due to smaller rooted volumes, observed by evapotranspiration rates under both strategies (Oltshoorn, 2003).

Furthermore, studies highlighted the importance of land cover and vegetation on the groundwater system (de Niet et al., 2021; Geertsema et al., 2011; van Huijgevoort et al., 2020). Modelled results under the baseline affirmed these trends for soil moisture and evapotranspiration. Observed differences in evapotranspiration between the baseline and alternative strategies showed conformity to local vegetation characteristics. This hinted at the potential to optimize the effect of alternative extractions by incorporating less-vulnerable vegetation types, as by the example of de Niet et al. (2021). Differences in soil moisture, however, indicated no apparent correlation to landcover, soil, or vegetation. The varying applied volumes per individual location made it hard to judge whether effects differed due to the proportioning or local factors.

6.2.2 Evaluation of the alternative strategies

As decentralization proved beneficial to groundwater levels and soil moisture content, the practicality can be discussed. The minor differences between Sd1, Sd2, and Sd3 demonstrated that a relatively limited number of wells (resp. 16 for Sd1) could induce comparable effects to higher scenarios (resp. 27 for Sd2; 50 for Sd3). Thereby, decentralized extraction can be effective by detaching only large consumers ($> 10,000 \text{ m}^3/\text{yr}$). Additionally, selection only larger consumers would restrict the number of wells, reducing initial and infrastructural costs (Giezen et al., 2017). Even so, economic estimates towards decentral extractions strengthen this consideration; indicating that cost-comparative pumping to current strategies is attained for extractions above $20,000 - 60,000 \text{ m}^3/\text{yr}$ (Hofman-Caris et al., 2019). In general, Giezen et al. (2017) argued that decentral systems are most economically effective in remote regions with lower population densities, which can be attributed to the northern Achterhoek to Dutch standards. However, decentralization minimally reduces costs for current locations, primarily dominated by fixed expenditures, and remains an additional cost (van Alphen et al., 2018; van Alphen & Frijns, 2014).

In contrast to most previous studies on decentralization, which focused on alternative sources (e.g. circular water, rainwater; van Alphen & Frijns, 2014; Van den Berg et al., 2008), this study incorporated groundwater in the strategy. Hereby, water quality is assured more consistently (Giezen et al., 2017; Houtsma, 2015). However, comprehensive treatment equipment and quality monitoring protocols are still required (Hofman-Caris et al., 2019), as water quality and adequate maintenance are non-negotiable demands before considering this strategy (Houtsma, 2015). This again is most practical when considering solely large consumers.

For seasonal extractions this consideration is more challenging. The beneficial effects on groundwater and soil moisture were smaller and noticeable results primarily followed high volumes shifts. To extract these volumes, assessing infrastructural potential is inevitable, particularly in the form of temporal (subsurface)-storage (Jeuken et al., 2015; van der Aa et al., 2015), which still requires explorative research. Yet studies showed the potential cost-effectiveness of similar measures compared to current supply systems (Zuurbier et al., 2019). Furthermore, by maintaining distribution control, water quality can be assured. However, considering the relatively lower benefits, questions can be raised whether this strategy would be worthwhile.

The specific seasonal scenarios minimally improved the sustainable utilization of regional groundwater, soil moisture, or evapotranspiration. As significant infrastructural changes would be required to implement this strategy, the disadvantages are not proportional to the benefits. These two scenarios were therefore deemed not viable.

6.3 Research implications

This research provided a valuable contribution to scientific knowledge on sustainable extractions for the Pleistocene uplands by exploring alternative strategies on a regional scale. Given the topic's novelty, the quantitative approach attested to some insightful theories on hydro-environmental interactions and their relation to extractions. Thereby this explorative study paved the road towards more detailed future studies and provided some rough directions of interest to built-upon. Particular interest lies in the benefits for academics evaluating anthropological-alterations to this complex system, only to increase in relevance by future climatological trends.

The practical implications, however, were bilateral. On one side, findings indicated the effectiveness of decentralized extractions on regional groundwater levels and explored the potential for seasonal extractions. Yet, results also demonstrated that both evaluated strategies would limitedly suffice to reduce hydro-environmental damages. The high-intensity scenarios, Sd3 and St3, implied that even significant measures only slightly mitigated adverse effects. As discussed before, this was in line with scientific literature; but aggravated the need for viable strategies without resorting to drastic measures. The latter already advocated through temporal closure of extractions around vulnerable ecosystems (Waterschap Rijn en IJssel, 2019).

Whilst adverse implications have to be put in perspective, the need for viable sustainable solutions persists in future-orientated policies of Vitens and the Ministry of Infrastructure and Water Management (Bardout et al., 2017; Ministerie van Infrastructuur en Waterstaat, 2021). Increased focus has been put on identifying strategic, or sometimes radical, alternative drinking water sources to mitigate hydro-environmental impacts (Hofman-Caris et al., 2019; Huizer, 2019; Stofberg et al., 2019; Tangena, 2014; van der Aa et al., 2015). However, often research is still in explorative phases, and practicality has not yet been established.

Still, groundwater is the preferred drinking water source for the Pleistocene uplands and remains vital to meet socio-economic demand. Therefore, the most realistic future implication would be a *'best-of-both-worlds'* scenario. Herein incorporating sustainable alternative strategies as baseline to meet demand in a less pressurizing manner, whilst adding supplementary sources (e.g. effluent, riverine water) to achieve a sustainable hydro-environmental situation in the long-term (Kloosterman et al., 2012). However, still significant process has to be made as research towards viable strategies remains explorative.

6.4 Recommendations and future research

Based on the findings of this thesis, future research on sustainable extraction strategies for the Pleistocene uplands could benefit from incorporating the following recommendations:

- It is suggested to study decentralized extractions using higher-resolution data for the spatial and temporal domains. Preferably this would comprise monthly data for individual consumers to include seasonal trends and assure accurate well-placement.
- To better assess local impacts in low quantities, particularly for well-field specific results, it is recommended for future research to apply a 25x25m model resolution. Current data availability accommodates this approach, however, exceeded the scope of this thesis.
- Seasonal extractions were tested as general concept using percentage-based reductions. Future research would benefit from exploring fixed volume changes per individual location (e.g. dependent on practical limitations) to evaluate impacts to local characteristics.
- High practical interest for future research lies in exploring the integrative potential between the developed strategies, and whether, or to what extent, these results would differ from individual implementation.
- Key-sustainability challenges still prevail in the accommodation of changing socio-economic water demand and future meteorological trends in the water balance. Whilst neglected in this thesis; their addition would significantly improve the predictive character of each strategy.
- To achieve a holistic view on the sustainability of both alternative strategies, complementary socio-economic and technological research is required: exploring stakeholder views, economic viability, and infrastructural potential.

Chapter 7 Conclusion

This thesis explored two alternative drinking water extraction strategies for the sandy Pleistocene regions of the Netherlands; pursuing sustainable groundwater management on a regional-scale. Decentralized extractions and seasonal extractions were quantified and evaluated on their hydrological and hydro-environmental impacts. This was done by scenario analysis and the geohydrological model AMIGO v3.1. The northern Achterhoek functioned as case-study.

The implementation of decentralized extractions had an overall positive effect on regional groundwater levels. Drawdown under decentralized scenarios reduced by 0 – 15%, increasing with higher decentralized volumes. Results showed comparable effects for all three scenarios (Sd1, Sd2, Sd3), indicating that disconnecting solely large consumers ($> 10,000 \text{ m}^3/\text{yr}$) would suffice for this strategy to be effective. Both the extent and intensity of positive effects outweighed adverse effects at decentral locations. Seasonal extractions were concluded slightly less effective (0 – 5%), except when applied in extensive volumes (5 – 15%), and showed potential to optimize annual water containment on a regional-scale. Beneficial summer effects consistently exceeded the adverse effects during winter.

Both alternative strategies had a less prominent effect on regional soil moisture content. The regional soil water saturation deficits were reduced by 0 – 5%, with outliers to 10%. Yet, the spatial extent of all significant changes was highly well-field specific and related to fluctuations in groundwater levels. No eminent relation was observed to local characteristics as soil or landcover type. Consequently, the implementation of decentralized or seasonal extraction strategies had a minimal effect on regional evapotranspiration ($< 1\%$). The deep regional groundwater tables prohibited effective interactions between the unsaturated zone and vegetation, and changes in groundwater level. Noticeable effects were only found around forested regions as their deep rootzones profited in earlier stages to minor fluctuation in soil moisture content.

It is therefore concluded that both alternative extraction strategies can only partly contribute to sustainable groundwater management for the Pleistocene uplands. Alternative extractions alone will not suffice in reducing hydro-environmental impacts, but will be required in the short-term to meet socio-economic demand more sustainably. These findings support the need for a multi-directional approach towards sustainable drinking water provision. This explorative work could help water managers by paving the road to more detailed studies and hinting at directions of future sustainability.

Chapter 8 References

- Aeschbach-Hertig, W., & Gleeson, T. (2012). Regional strategies for the accelerating global problem of groundwater depletion. *Nature Geoscience*. <https://doi.org/10.1038/ngeo1617>
- Bakel, P. J. T. van, Blom, M., Hermans, C. M. L., Paulissen, M. P. C. P., Rooij, S. A. M. van, Steingrover, E. G., Stuyt, L. C. P. M., Vos, C. C., & Verbout, A. (2008). *Klimaat effectschetsboek Gelderland*. Alterra. <https://edepot.wur.nl/2577>
- Bartholomeus, R., Louw, P. de, Witte, F., Dam, J. van, Deijl, D. van, Hoefsloot, P., Huijgevoort, M. van, Hunink, J., America, I., Pouwels, J., & Wit, J. de. (2020). *Droogte in zandgebieden van Zuid-, Midden- en Oost-Nederland: Rapportage Fase 1. Ontwikkeling van uniforme werkwijze voor analyse van droogte en tussentijdse bevindingen*. KWR Water Research Institute. <https://library.kwrwater.nl/publication/60038685/>
- Bartholomeus, R., van Weeren, B.-J., & Raat, K. (2021). *Programma Lumbricus: Integrale benadering van een klimaatrobuuste inrichting en beheer van stroomgebieden: een overzicht* (Rapport; 2021-05). Stichting Toegepast Onderzoek Waterbeheer (STOWA). <https://edepot.wur.nl/542286>
- Beersma, J., Hakvoort, H., Jilderda, R., Overeem, A., & Versteeg, R. (2019). *Neerslagstatistiek en -Reeksen voor het Waterbeheer 2019*. <https://www.stowa.nl/neerslagstatistieken>
- Berendsen, H. J. A. (2015). *De vorming van het land: Inleiding in de geologie en de geomorfologie* (6e herz. d). Koninklijke Van Gorcum.
- Berendsen, H. J. A., & Stouthamer, E. (2008). *Landschappelijk Nederland: de fysisch-geografische regio's* (4e herz. d). Koninklijke Van Gorcum.
- Bergkamp, G., & Cross, K. (2006). Groundwater and ecosystem services: towards their sustainable use. *International Symposium on Groundwater Sustainability*, 177–193. <https://api.semanticscholar.org/CorpusID:36446693>
- Bierkens, M. F. P., & Wada, Y. (2019). Non-renewable groundwater use and groundwater depletion: a review. *Environmental Research Letters*, 14(6). <https://doi.org/10.1088/1748-9326/ab1a5f>
- Biondi, D., Freni, G., Iacobellis, V., Mascaro, G., & Montanari, A. (2012). Validation of hydrological models: Conceptual basis, methodological approaches and a proposal for a code of practice. *Physics and Chemistry of the Earth, Parts A/B/C*, 42–44, 70–76. <https://doi.org/10.1016/j.pce.2011.07.037>
- Breman, B. C., Oosterbaan, A., Fontein, R. J., & Doorn, A. M. van. (2013). *Het kansrijke platteland van de Achterhoek, Analyse van ruimtelijke, economische en sociale ontwikkelingen*. Alterra. <https://library.wur.nl/WebQuery/wurpubs/439027>
- Brozović, N., Sunding, D. L., & Zilberman, D. (2010). On the spatial nature of the groundwater pumping externality. *Resource and Energy Economics*, 32(2), 154–164. <https://doi.org/10.1016/j.reseneeco.2009.11.010>
- Brozović, N., Sunding, D., & Zilberman, D. (2006). Optimal Management of Groundwater over Space and Time. In R.-U. Goetz & D. Berga (Eds.), *Frontiers in Water Resource Economics* (pp. 109–135). Springer US. https://doi.org/10.1007/0-387-30056-2_6

- Bruggeman, W., Haasnoot, M., Hommes, S., Te Linde, A., & Van der Brugge, R. (2011). *Deltascenario's*. Deltares. <https://edepot.wur.nl/170665>
- Castilla-Rho, J. C., Rojas, R., Andersen, M. S., Holley, C., & Mariethoz, G. (2019). Sustainable groundwater management: How long and what will it take? *Global Environmental Change*, 58. <https://doi.org/10.1016/j.gloenvcha.2019.101972>
- Chan, P. M., Hofstra, M., Nijburg, C., Jan, G., & Arwin Van Buuren, E. (2014). *Het Deltaplan Hoge Zandgronden Een reflectie op governance*. <http://hdl.handle.net/1765/77178>
- Custodio, E., Kretsinger, V., & Llamas, M. R. (2005). Intensive development of groundwater: concept, facts and suggestions. *Water Policy*, 7(2), 151–162. <https://doi.org/10.2166/wp.2005.0010>
- de Bruin, H. A. R., & Lablans, W. N. (1998). Reference crop evapotranspiration determined with a modified Makkink equation. *Hydrological Processes*, 12(7), 1053–1062. [https://doi.org/10.1002/\(SICI\)1099-1085\(19980615\)12:7%3C1053::AID-HYP639%3E3.0.CO;2-E](https://doi.org/10.1002/(SICI)1099-1085(19980615)12:7%3C1053::AID-HYP639%3E3.0.CO;2-E)
- de Niet, J., van der Toorn, L., Beijer, E., Heijkers, J., & Hoekstra, J. (2021). Hydrologische effecten van het vervangen van naaldbos op de Utrechtse Heuvelrug door loofbos. *H2O Online*. <https://bit.ly/3AJmuMe>
- de Weme, A., Klutman, W., & Huizer, S. (2019). *Vernieuwen Grondwatermodel AMIGO: Waterschap Rijn en IJssel*. <https://bit.ly/3yyMwQo>
- Dinica, V. (2014). Competing societal and ecological demands for groundwater: boundary judgments and convergence mechanisms in the Netherlands. *Environment, Development and Sustainability*, 16(3), 555–573. <https://doi.org/10.1007/s10668-013-9493-6>
- Doorn, A. van, & Jalink, M. H. (2017). *Functiecombinatie waterwinning en natuur, verkenning in drie landschapstypen*. <https://library.kwrwater.nl/publication/55036296/>
- Ehtiat, M., Jamshid Mousavi, S., & Srinivasan, R. (2018). Groundwater Modeling Under Variable Operating Conditions Using SWAT, MODFLOW and MT3DMS: a Catchment Scale Approach to Water Resources Management. *Water Resources Management*, 32(5), 1631–1649. <https://doi.org/10.1007/s11269-017-1895-z>
- Essink, G. H. P. O. (2001). Improving fresh groundwater supply - Problems and solutions. *Ocean and Coastal Management*, 44(5–6), 429–449. [https://doi.org/10.1016/S0964-5691\(01\)00057-6](https://doi.org/10.1016/S0964-5691(01)00057-6)
- Fitts, C. R. (2013). *Groundwater Science*. <https://doi.org/10.1016/C2009-0-62950-0>
- Folmer, I. M., van Herpen, F. C. J., & Krikken, A. (2012a). *Gebiedsdossier Gelderland: Winning 't Klooster*. 51.
- Folmer, I. M., van Herpen, F. C. J., & Krikken, A. (2012b). *Gebiedsdossier Gelderland: Winning Vorden*. 53.
- Gaast, J. W. J. van der, & Massop, H. T. L. (2008). *De hydrologie voor het beheergebied van waterschap Velt en Vecht: een karakterisering op basis van karteerbare kenmerken* (Alterra-Rapport: 1686). Alterra. <https://edepot.wur.nl/24973>

- García-Cáceres, R. G., Castañeda-Galvis, M. T., & Suárez-Fajardo, J. F. (2019). Towards an efficient and sustainable planning of the drinking water supply chain. *Journal of Cleaner Production*, 230, 394–401. <https://doi.org/10.1016/j.jclepro.2019.05.062>
- Geertsema, W., Runhaar, H., Spek, T., & Steingrover, E. G. (2011). *Klimaatadaptatie droge rurale zandgronden - Gelderland*. Programmabureau Kennis voor Klimaat. <https://edepot.wur.nl/194887>
- Gerritsen, J., & Barendregt, L. (2020). *Alleen onorthodoxe plannen helpen tegen extreme droogte: 'Als we niks doen, moeten we de Achterhoek opgeven.'* <https://www.gelderlander.nl/doetinchem/alleen-onorthodoxe-plannen-helpen-tegen-extreme-droogte-als-we-niks-doen-moeten-we-de-achterhoek-opgeven~a78538bc/>
- Giezen, M., Brouwer, S., Roest, K., & Vliet, B. J. M. van. (2017). *De energiesector als lichtend of verblindend voorbeeld?* <https://edepot.wur.nl/425745>
- Glavan, M. O. (2018). *Chapter 10. Safe Drinking Water: Concepts, Benefits, Principles and Standards*. IntechOpen. <https://doi.org/10.5772/intechopen.71352>
- Gleeson, T., Cuthbert, M., Ferguson, G., & Perrone, D. (2020). Global Groundwater Sustainability, Resources, and Systems in the Anthropocene. *Annual Review of Earth and Planetary Sciences*, 48(1), 431–463. <https://doi.org/10.1146/annurev-earth-071719-055251>
- Hasiotis, S. T., Kraus, M. J., & Demko, T. M. (2007). CHAPTER 11 - Climatic Controls on Continental Trace Fossils. In W. MILLER (Ed.), *Trace Fossils* (pp. 172–195). Elsevier. <https://doi.org/10.1016/B978-044452949-7/50137-6>
- Heinen, M., Brouwer, F., Teuling, C., & Walvoort, D. J. J. (2021). *BOFEK2020 - Bodemfysische schematisatie van Nederland: update bodemfysische eenhedenkaart*. Alterra. <https://edepot.wur.nl/541544>
- Hendriks, M. R. (2010). *Introduction to Physical Hydrology*. Oxford University Press.
- Hiemstra, P., & Sluiter, R. (2011). Interpolation of Makkink Evaporation in the Netherlands. *De Bilt, 2011 | Technical Report; TR-327*, 2, 78. <https://library.wur.nl/WebQuery/hydrotheek/1978863>
- Hofman-Caris, R., Cirkel, G., De Waal, L., Huiting, H., & De Bruin, E. (2019). Kleinschalige drinkwaterproductie: wanneer is dat haalbaar? *H2O: Tijdschrift Voor Watervoorziening En Waterbeheer*. <https://library.kwrwater.nl/publication/59832790/>
- Hofman-Caris, R., Stofberg, S., van Alphen, H. J., De Waal, L., & van Huijgevoort, M. (2019). *VO Radicaal nieuwe bronnen voor drinkwater*. <https://library.kwrwater.nl/publication/59958049/>
- Hoogvliet, M., Stuyt, L. C. P. M., Bakel, J. van, Velstra, J., Louw, P. de, Massop, H. T. L., Tolck, L., Kempen, C. van, & Nikkels, M. (2014). *Methode voor het selecteren van lokale zoetwateroplossingen en het afwegen van hun effecten "Fresh Water Options Optimizer"* (Rapport / KvK: 141/014). Programmabureau Kennis voor Klimaat. <https://edepot.wur.nl/329919>
- House of Water and Environment. (n.d.). Chapter Three: Groundwater flow to wells. In *Groundwater Engineering* (p. 92). Birzeit University. <http://www.hwe.org.ps/>
- Houtsma, W. H. (2015). *Decentrale productie drinkwater*. 14. <https://bit.ly/2TB3yyJ>

- Huizer, S. (2019). *Drinkwaterwinning 't Klooster: Verkennende modelstudie naar een klimaatrobuust grondwatersysteem*. <https://doi.org/C03081.000341>
- Hummelman, J., Maljers, D., Menkovic, A., Reindersma, R., Vermes, R., & Stafleu, J. (2019). *Totstandkomingsrapport Hydrogeologisch Model (REGIS II v2.2)*. 95. <https://doi.org/TNO 2019 R11654>
- Jansen, H. C., Sicco Smit, M. E., & van der Bolt, F. J. E. (2004). *Systeemverkenning Schuitembeek LK*. Alterra. <https://edepot.wur.nl/120065>
- Jansen, P. C., Massop, H. T. L., Houten, G. J. van den, Klutman, W. A. J., & Bakx, W. (2013). *Basisafvoer van de Baakse beek: onderzoek naar perspectieven voor aquatische natuur in een laaglandbeek* (Alterra-Rapport: 2383). <https://edepot.wur.nl/283014>
- Jeuken, A., Tolk, L., Stuyt, L. C. P. M., Delsman, J., Louw, P. de, Baaren, E. van, & Paalman, M. (2015). *Zelfvoorzienend in zoetwater: zoek de mogelijkheden: kleinschalige oplossingen voor een robuustere regionale zoetwatervoorziening*. Stichting Toegepast Onderzoek Waterbeheer (STOWA). <https://edepot.wur.nl/365422>
- Khan, S., Mushtaq, S., Hanjra, M. A., & Schaeffer, J. (2008). Estimating potential costs and gains from an aquifer storage and recovery program in Australia. *Agricultural Water Management*, 95(4), 477–488. <https://doi.org/10.1016/j.agwat.2007.12.002>
- Kim, J. H., & Jackson, R. B. (2012). A Global Analysis of Groundwater Recharge for Vegetation, Climate, and Soils. *Vadose Zone Journal*, 11. <https://doi.org/10.2136/vzj2011.0021RA>
- Klijn, F., Velzen, E. van, Maat, J. ter, Hunink, J., Baarse, G., Beumer, V., Boderie, P., Buma, J., Delsman, J., Hoogewoud, J., Hoogvliet, M., Prinsen, G., Bakel, J. van, Mark, R. van der, Ek, R. van, Sligte, R. van, Verheij, H., & Zwolsman, G.-J. (2012). *Zoetwatervoorziening in Nederland: aangescherpte landelijke knelpuntenanalyse 21e eeuw*. Deltares. <https://edepot.wur.nl/430674>
- Kloosterman, R., Kostense, A., Essen, J. van, & Meer, W. van der. (2012). Visie van Vitens op waterinfrastructuur voor de lange termijn. *H2O online*, 45(8), 20–23. <https://edepot.wur.nl/339098>
- KNMI. (n.d.). *KNMI Data Platform*. <https://dataplatform.knmi.nl/>
- Kosow, H., & Gaßner, R. (2008). *Methods of future and scenario analysis: overview, assessment, and selection criteria* (Vol. 39). Deutsches Institut für Entwicklungspolitik. https://www.die-gdi.de/uploads/media/Studies_39.2008.pdf
- Kumar, M. D., Patel, A., Ravindranath, R., & Singh, O. P. (2008). Chasing a Mirage: Water Harvesting and Artificial Recharge in Naturally Water-Scarce Regions. *Economic and Political Weekly*, 43(35), 61–71. <http://www.jstor.org/stable/40278725>
- Langevin, C. D., Hughes, J. D., Banta, E. R., Niswonger, R. G., Panday, S., & Provost, A. M. (2017). Documentation for the MODFLOW 6 Groundwater Flow Model. In *Techniques and Methods*. <https://doi.org/10.3133/tm6A55>
- Larned, S. T. (2012). Phreatic groundwater ecosystems: research frontiers for freshwater ecology. *Freshwater Biology*, 57(5), 885–906. <https://doi.org/10.1111/j.1365-2427.2012.02769.x>

- Lóaiciga, H. A., & Leipnik, R. B. (2001). Theory of sustainable groundwater management: An urban case study. *Urban Water*, 3(3), 217–228. [https://doi.org/10.1016/S1462-0758\(01\)00040-1](https://doi.org/10.1016/S1462-0758(01)00040-1)
- Lowry, C. S., & Loheide, S. P. (2010). Groundwater-dependent vegetation: Quantifying the groundwater subsidy. *Water Resources Research*, 46(6). <https://doi.org/10.1029/2009WR008874>
- Mao, D., Wan, L., Yeh, T.-C. J., Lee, C.-H., Hsu, K.-C., Wen, J.-C., & Lu, W. (2011). A revisit of drawdown behavior during pumping in unconfined aquifers. *Water Resources Research*, 47(5). <https://doi.org/10.1029/2010WR009326>
- Massop, H. T. L. (2019). *Historische data en hydrologie van de Baakse Beek*. 33(1), 61–74. <https://edepot.wur.nl/470882>
- Massop, H. T. L., & Schuiling, C. (2016). *Buisdrainagekaart 2015: update landelijke buisdrainagekaart op basis van de landbouwmetingen van 2012*. Alterra. <https://edepot.wur.nl/370378>
- Mays, L. W. (2013). Groundwater Resources Sustainability: Past, Present, and Future. *Water Resources Management*, 27(13), 4409–4424. <https://doi.org/10.1007/s11269-013-0436-7>
- McDonald, R. I., Green, P., Balk, D., Fekete, B. M., Revenga, C., Todd, M., & Montgomery, M. (2011). Urban growth, climate change, and freshwater availability. *Proceedings of the National Academy of Sciences*, 108(15), 6312–6317. <https://doi.org/10.1073/PNAS.1011615108>
- Ministerie van Infrastructuur en Waterstaat. (2021). *Beleidsnota Drinkwater 2021-2026: Samenwerken aan een toekomstbestendige drinkwatervoorziening*. <https://www.rijksoverheid.nl/documenten/rapporten/2021/04/23/bijlage-beleidsnota-drinkwater-2021-2026>
- Moors, E. J., Dolman, A. J., Bouten, W., & Veen, A. W. L. (1996). *De verdamping van bossen*. 29(16), 462–466. <https://edepot.wur.nl/361947>
- Neuman, S. P. (1972). Theory of flow in unconfined aquifers considering delayed response of the water table. *Water Resources Research*, 8(4), 1031–1045. <https://doi.org/10.1029/WR008i004p01031>
- Oltshoorn, A. F. M. (2003). *Effecten van vernatting in bossen: conclusies en aanbevelingen voor praktijk en beleid*. Expertisecentrum LNV, Ministerie van Landbouw, Natuurbeheer en Visserij. <https://bit.ly/2Vn9CLw>
- Page, D., Bekele, E., Vanderzalm, J., & Sidhu, J. (2018). Managed Aquifer Recharge (MAR) in Sustainable Urban Water Management. In *Water* (Vol. 10, Issue 3). <https://doi.org/10.3390/w10030239>
- Peel, M. C., & Blöschl, G. (2011). Hydrological modelling in a changing world. *Progress in Physical Geography: Earth and Environment*, 35(2), 249–261. <https://doi.org/10.1177/0309133311402550>
- Piratla, K. R., & Goverdhanam, S. (2015). Decentralized Water Systems for Sustainable and Reliable Supply. *Procedia Engineering*, 118, 720–726. <https://doi.org/10.1016/j.proeng.2015.08.506>
- Provincie Gelderland. (2014). *Omgevingsverordening Gelderland: Grondwaterbeschermingsgebieden*. <https://gldanders.planoview.nl/planoview/>

- Przybysz-Jarnut, J. K., Hanea, R. G., Jansen, J.-D., & Heemink, A. W. (2007). Application of the representer method for parameter estimation in numerical reservoir models. *Computational Geosciences*, *11*(1), 73–85. <https://doi.org/10.1007/s10596-006-9035-5>
- Rácz, C., Nagy, J., & Dobos, A. (2013). Comparison of Several Methods for Calculation of Reference Evapotranspiration. *Acta Silvatica et Lignaria Hungarica*, *9*, 9–24. <https://doi.org/10.2478/aslh-2013-0001>
- Ramaker, A. B., Blokker, M., Beuken, R., Van den Berg, G. A., Cirkel, G., Cornelissen, E., Doomen, A., Kappelhof, J., Raterman, B., & Stuyfzand, P. (2006). *Flexwater: Inventarisatie van bronnen, berging, zuivering en infrastructuur*. KWR Water Research Institute. <https://library.kwrwater.nl/publication/51451018/>
- Rambags, F., Raat, K., Zuurbier, K., Berg, G., & Hartog, N. (2013). Aquifer Storage and Recovery (ASR): Design and operational experiences for water storage. *Geochemistry*, *27*, 2435–2452.
- Roelsma, J., Kselik, R. A. L., & de Vos, J. A. (2008). *Watersysteemverkenning Noordelijke Friese Wouden* (Alterra). <http://edepot.wur.nl/31734>
- Roumasset, J. A., & Wada, C. A. (2010). Optimal and sustainable groundwater extraction. *Sustainability*. <https://doi.org/10.3390/su2082676>
- Runhaar, H., & Hennekens, S. M. (2015). *Hydrologische randvoorwaarden natuur : gebruikershandleiding (waternoodapplicatie versie 3)*. Stichting Toegepast Onderzoek Waterbeheer (STOWA). <https://edepot.wur.nl/348632>
- Sachs, J., Schmidt-Traub, G., Kroll, C., Lafortune, G., Fuller, G., & Woelm, F. (2020). The Sustainable Development Goals and COVID-19. In *Sustainable Development Report* (Vol. 2020). <https://unstats.un.org/sdgs/report/2020/>
- Sahoo, S., & Jha, M. K. (2017). Numerical groundwater-flow modeling to evaluate potential effects of pumping and recharge: implications for sustainable groundwater management in the Mahanadi delta region, India. *Hydrogeology Journal*. <https://doi.org/10.1007/s10040-017-1610-4>
- Schipper, P. N. M., Groenendijk, P., Eekeren, N. J. M. van, Zanen, M., Rozemeijer, J., Jansen, G., & Swart, B. (2015). *Goede grond voor een duurzaam watersysteem: verdere verkenningen in de relatie tussen agrarisch bodembeheer, bodemkwaliteit en waterhuishouding* (Rapport: 2015-19). Stichting Toegepast Onderzoek Waterbeheer (STOWA). <https://edepot.wur.nl/348633>
- Sluiter, R. (2009). Interpolation methods for climate data. In *KNMI Intern Report (R&D Information and Observation Technology)*.
- Spek, T., Kiljan, B., Moorman, J., Geertsema, W., & Steingröver, E. G. (2010). *Klimaatverandering op de hoge zandgronden: betekenis van klimaatverandering voor het landelijk gebied in de provincie Gelderland: een uitwerking voor de gebiedsontwikkeling in Baakse Beek en Blauwe Bron*. Provincie Gelderland. <https://edepot.wur.nl/318910>
- Stofberg, S., Hofman-Caris, R., Pronk, G., van Alphen, H.-J., & Putters, B. (2019). Toekomstverkenning: alternatieve bronnen voor drinkwater in Nederland. *H2O Online*, *28 augustus*. <https://edepot.wur.nl/499127>

- Stouthamer, E., Cohen, K., & Hoek, W. Z. (2020). *De vorming van het land. Geologie en geomorfologie* (8e herz. d).
- Sulis, M., Williams, J. L., Shrestha, P., Diederich, M., Simmer, C., Kollet, S. J., & Maxwell, R. M. (2017). Coupling Groundwater, Vegetation, and Atmospheric Processes: A Comparison of Two Integrated Models. *Journal of Hydrometeorology*, 18(5), 1489–1511. <https://doi.org/10.1175/JHM-D-16-0159.1>
- Tabari, H. (2010). Evaluation of Reference Crop Evapotranspiration Equations in Various Climates. *Water Resources Management*, 24(10), 2311–2337. <https://doi.org/10.1007/s11269-009-9553-8>
- Tangena, B. H. (2014). *Behoeftedekking Nederlandse drinkwatervoorziening 2015-2040: Rapport t.b.v. Verkenning grondwatervoorraden voor drinkwater*. Rijksinstituut voor Volksgezondheid en Milieu RIVM. <https://rivm.openrepository.com/handle/10029/557178>
- TNO. (2021). *Dinoloket database en models: REGIS vII.2*. Geologische Dienst Nederland. <https://www.dinoloket.nl/en/subsurface-models>
- van Alphen, H. J., & Frijns, J. (2014). *Praktijk en toekomst van decentrale drinkwaterproductie*. KWR Water Research Institute. <https://library.kwrwater.nl/publication/53149145/>
- van Alphen, H. J., Van Duuren, D., & Koop, S. H. . (2018). *Decentrale watersystemen: potentie, impact en gevolgen voor drinkwaterbedrijven*. <https://library.kwrwater.nl/publication/55752812/>
- van Baaren, E. S., Oude Essink, G. H. P., Janssen, G., De Louw, P. G. B., Heerdink, R., & Goes, B. J. M. (2016). Verzoeting en verzilting freatisch grondwater in de Provincie Zeeland: Rapportage 3D regionaal zoet-zout grondwater model. *Deltares Rapport 1220185-000*, 86. <https://bit.ly/3jPDXwr>
- van Beek, K., van den Berg, G., & Jalink, M. (2007). *Kennisdocument Achterhoek: Winningen 't Klooster en Olde Kaste*. <https://doi.org/30.6512.050>
- van Daele, T., & de Bie, E. (2015). *Leidraad grondwatermodellering voor passende beoordeling: onderbouwing voor wegwijzer 'verdroging/vernatting'*. <https://pureportal.inbo.be/nl/publications/leidraad-grondwatermodellering-voor-passende-beoordeling-onderbouw>
- van den Berg, G., de Rijk, S., Mesman, G., Abrahamse, A., & De Graaf, R. (2008). *Kansen voor decentrale drinkwatervoorziening in Nederland: Flexwater pilot De Draai, Heerhugowaard*. Delft Cluster. <https://bit.ly/3e6gGml>
- van den Meiracker, R., Jansen, S., & Welkers, J. (2021). *Flexibele drinkwaterwinningen - Kennisbasis*. http://publications.deltares.nl/11205767_000.pdf
- van der Aa, N. G. F. M., Tangena, B. H., Wuijts, S., & de Nijs, A. C. M. (2015). *Scenario 's drinkwatervraag 2040 en beschikbaarheid bronnen: Verkenning grondwatervoorraden voor drinkwater*. Rijksinstituut voor Volksgezondheid en Milieu RIVM. <https://rivm.openrepository.com/bitstream/10029/557188/3/2015-0068.pdf>
- van der Gaast, J. W. J., & Massop, H. T. L. (2003). *Spreidingslengte voor het beheersgebied van waterschap Veluwe: een maat voor het bufferzonebeleid* (Alterra-Rapport: 653). Alterra. <https://edepot.wur.nl/43657>

- van der Meer, R. W. (2013). *Watergebruik in de agrarische sector 2001-2011, naar stroomgebied* (Nota / LEI Wageningen UR : 13-092). Landbouw-Economisch Instituut WUR. <https://edepot.wur.nl/283881>
- van Engelenburg, J., de Jonge, M., Rijpkema, S., van Slobbe, E., & Bense, V. (2020). Hydrogeological evaluation of managed aquifer recharge in a glacial moraine complex using long-term groundwater data analysis. *Hydrogeology Journal*, 28(5), 1787–1807. <https://doi.org/10.1007/s10040-020-02145-7>
- van Engelenburg, J., van Slobbe, E., & Hellegers, P. (2019). Towards sustainable drinking water abstraction: an integrated sustainability assessment framework to support local adaptation planning. *Journal of Integrative Environmental Sciences*, 16(1), 89–122. <https://doi.org/10.1080/1943815X.2019.1636284>
- van Engelenburg, J., van Slobbe, E., Teuling, A. J., Uijlenhoet, R., & Hellegers, P. (2021). Sustainability characteristics of drinking water supply in the Netherlands. *Drinking Water Engineering and Science*, 14(1), 1–43. <https://doi.org/10.5194/dwes-14-1-2021>
- van Huijgevoort, M. H. J., Voortman, B. R., Rijpkema, S., Nijhuis, K. H. S., & Witte, J.-P. M. (2020). Influence of Climate and Land Use Change on the Groundwater System of the Veluwe, The Netherlands: A Historical and Future Perspective. In *Water* (Vol. 12, Issue 10). <https://doi.org/10.3390/w12102866>
- van Loon, A. H., Paalman, M., & Jalink, M. (2014). *Voorraadvorming van water door vernatten van de Stippelberg: experimentele verificatie van de effectiviteit van infiltreren*. KWR Water Research Institute. <https://library.kwrwater.nl/publication/52052038/>
- van Sijl, J., & Giesbers, G. (2020). *Watervoorziening Achterhoek*. Vitens.
- van Walsum, P. E. V., Veldhuizen, A. A., & Groenendijk, P. (2014). *SIMGRO 7.2.25: Theory and model implementation*. <https://bit.ly/3hDAKNW>
- Vandenbohede, A., Van Houtte, E., & Lebbe, L. (2009). Sustainable groundwater extraction in coastal areas: A Belgian example. *Environmental Geology*, 57(4), 735–747. <https://doi.org/10.1007/s00254-008-1351-8>
- Vergouwen, L., Vissers, M., Wolthuis, S., & Dik, P. (2016). *Samenwerken aan het drinkwater van de toekomst*.
- Verhagen, F., Krikken, A., van Grootheest, J., Hans, I., Arts, M., Schaap, J., & van Meeteren, M. (2011). *Gebiedsdossier Haarlo - Olden Eibergen*.
- Vermeulen, P. T. M., Roelofsen, F. J., Hunnink, J., Janssen, G. M. C. M., Verastegui, B. R., Engelen, J. van, & Russcher, M. (2020). *iMOD User Manual Version 5.2*. <https://bit.ly/3xBiVWk>
- Vitens. (2021). *Jaarverbruik regionale klanten >3000 m3/jaar* (p. 1). Vitens.
- Wang, B., Ma, Y., Ma, W., Su, B., & Dong, X. (2019). Evaluation of ten methods for estimating evaporation in a small high-elevation lake on the Tibetan Plateau. *Theoretical and Applied Climatology*, 136(3), 1033–1045. <https://doi.org/10.1007/s00704-018-2539-9>
- Wang, C., Fu, B., Zhang, L., & Xu, Z. (2018). Soil moisture–plant interactions: an ecohydrological

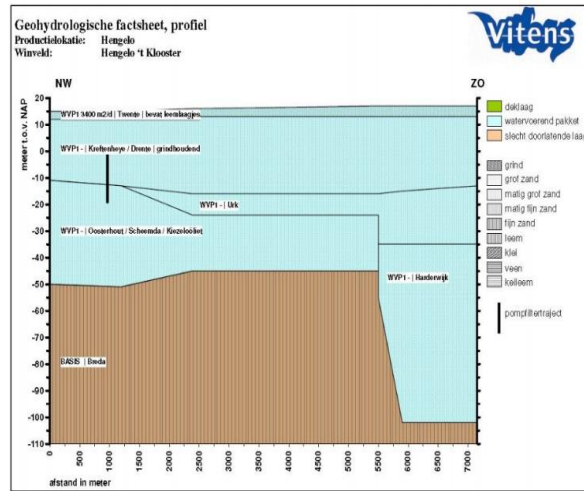
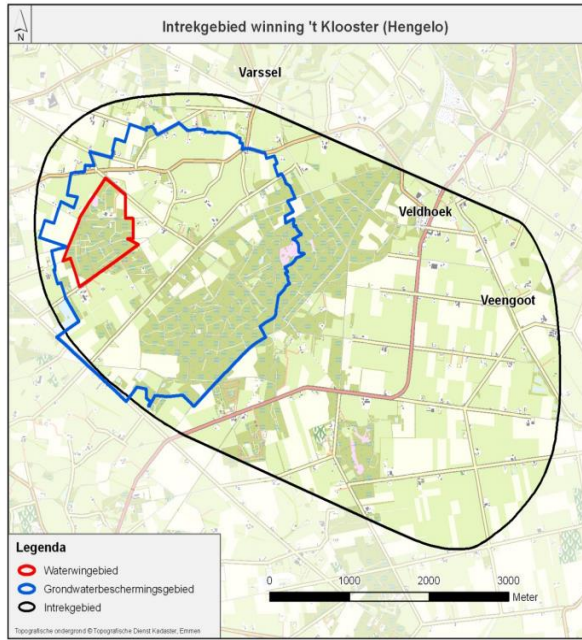
- review. *Journal of Soils and Sediments*, 19(1), 1–9. <https://doi.org/10.1007/s11368-018-2167-0>
- Waterschap Rijn en IJssel. (1998). *Verdrogingsbestrijdingsplan Noordijkerveld*. <https://edepot.wur.nl/260427>
- Waterschap Rijn en IJssel. (2019). *Onttrekkingsverbod vanwege extreme droogte*. <https://www.wrij.nl/@8944/sproeiverbod-vanwege/>
- Wesselingh, F. (n.d.). *Zandlandschap*. Geologie van Nederland; Naturalis. <https://www.geologievannederland.nl/landschap/landschappen/zandlandschap>
- Witte, J., Louw, P. De, Ek, R. Van, & Bartholomeus, R. (2020). *Aanpak droogte vraagt transitie waterbeheer*. 120–131. <https://edepot.wur.nl/538739>
- Wolters, H., Hunink, J., Delsman, J., Lange, G. de, Schasfoort, F., Mark, R. van der, Gert Jan van den Born, E. D., Rijken, B., & Reinhard, S. (2018). *Deltascenarios: Nieuwe blik op de toekomst*. 27. <https://bit.ly/3qQLyfl>
- Zoetwatervoorziening Oost-Nederland. (2017). *Waterbeschikbaarheid op de Hoge Zandgronden: Naar een klimaatbestendige balans in vraag en aanbod van zoetwater*. <https://bit.ly/3AF2ytS>
- Zuurbier, K., Paalman, M., van Loon, A., Stuyfzand, P., & Stofberg, S. (2019). *Ondergrondse waterberging : Deltafact*. Stichting Toegepast Onderzoek Waterbeheer (STOWA). <https://edepot.wur.nl/258351>

Chapter 9 Appendices

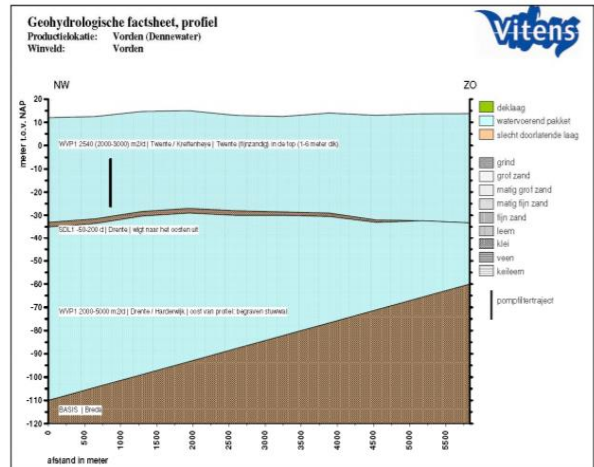
Appendix A.

Supplementary information on individual extraction locations: site-specifics and geohydrology.

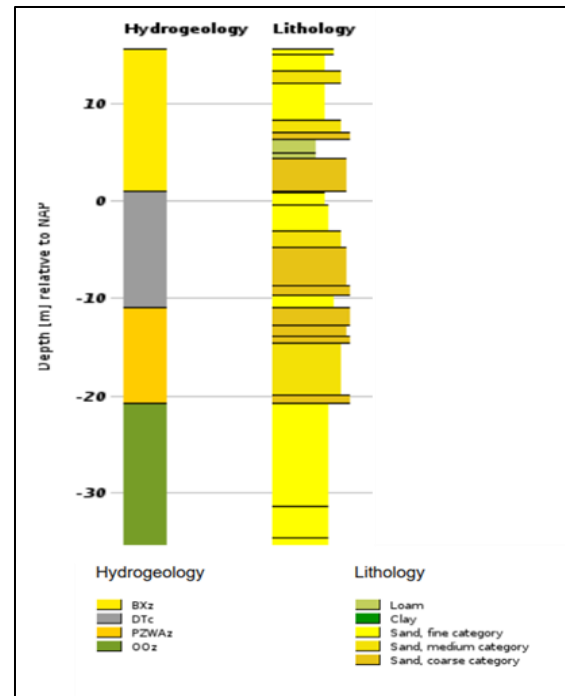
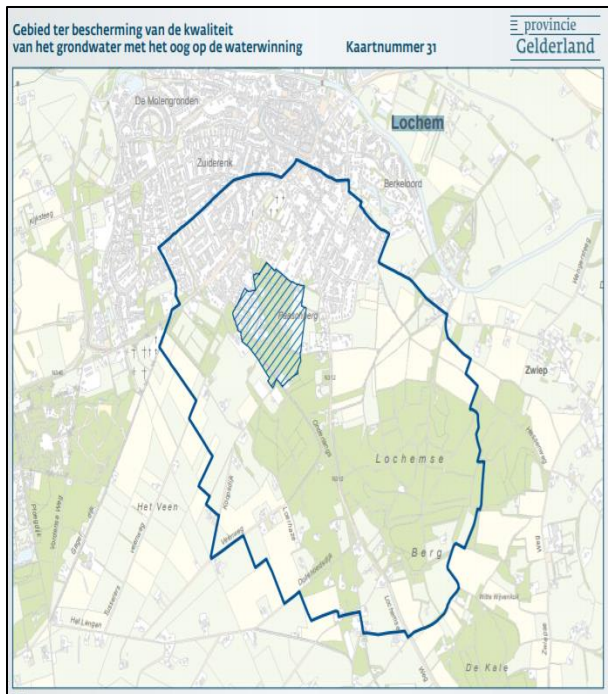
1. 't Klooster (Folmer et al., 2012a)



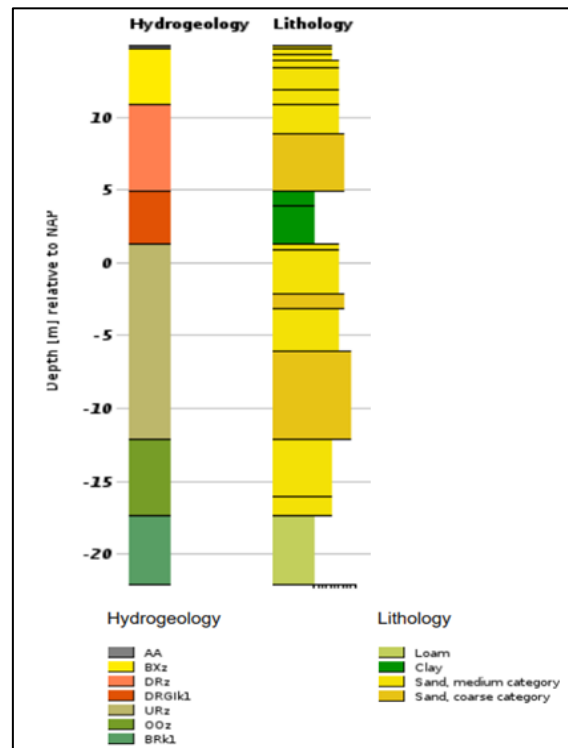
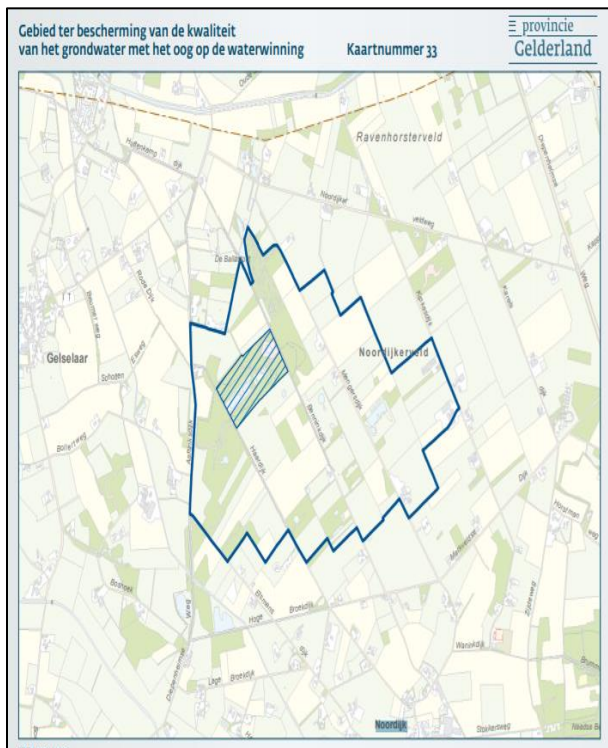
2. Vorden (Folmer et al., 2012b)



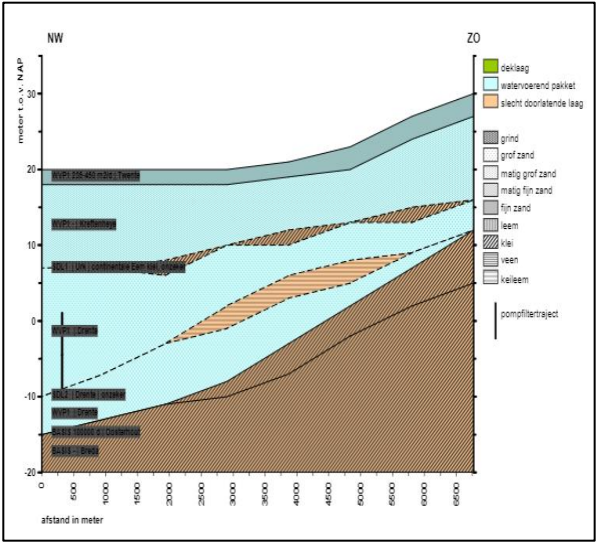
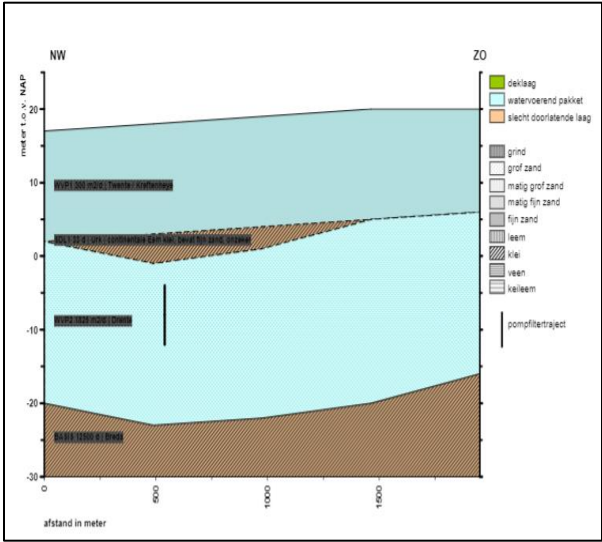
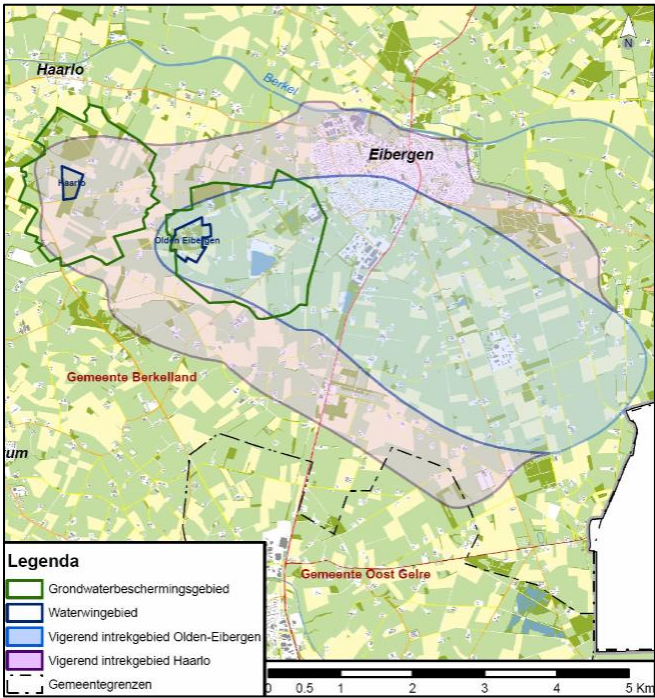
3. Lochem (Provincie Gelderland, 2014; TNO, 2021)



4. Noordijk (Provincie Gelderland, 2014; TNO, 2021)

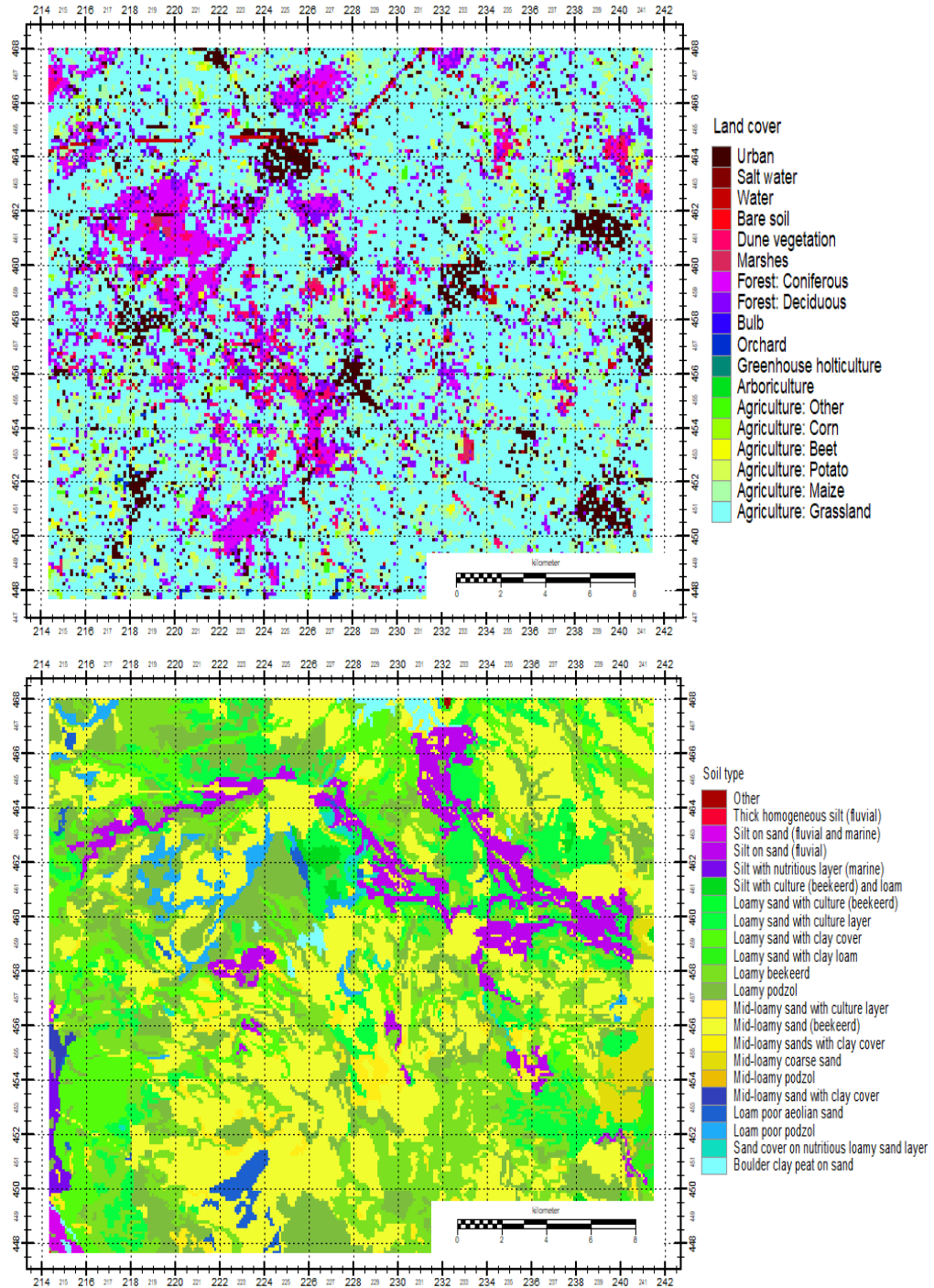


5. Haarlo & Eibergen (Vergouwen et al., 2016; Verhagen et al., 2011)



Appendix B

Appendix B.1 Land cover (WUR LGN/CORINE) and soil type classification (BOFEK2012) input maps; localized for the northern Achterhoek (de Weme et al., 2019).



Appendix B.2 Utilized packages and modules within iMOD (de Weme et al., 2019; Vermeulen et al., 2020).

Parameter / Package	Module	Time dependency	Unit	Description (based on Vermeulen et al. (2020))
Boundary Conditions	BND	Steady	-	Boundary specification per individual subsurface layer: fixated heads (value < 0), excluded (value = 0), transient heads (value > 0).
Starting Head	SHD	Steady	m [+NAP]	Initial head specification at the start of the simulation. Distinction per cell and individual subsurface layer.
Geological layering	TOP & BOT	Steady	m [+ NAP]	Top and bottom boundaries of all individual geological layers within the modelled area. Confines to the permeable section of each layer.
Transmissivity	KDW	Steady	m ³ /d/m	Defines the aquifers' transmissivity per cell and subsurface layer.
Vertical Resistance	VCW	Steady	m/d	Defines the vertical resistance per subsurface layer. Differentiated in both factor (FCT) and Angle (ANG).
Confined Storage Coefficients	STO	Steady	-	Defines the confined specific storage coefficients (i.e. capacity of aquifers to release groundwater; also storativity) per individual layer.
Anisotropy	ANI	Steady	-	Defines the vertical anisotropy per individual model layer.
Horizontal Flow Barrier	HFB	Steady	-	Characterization of the regional impermeable or semi-impermeable barriers, faults, and obstructions for hydrological flow for each model layer.
MetaSWAP	CAP	Transient	-	Defines input parameters for computations concerning unsaturated zone hydrology. Contains a singular layer with meteorological stations (MST), soil type (SLT), land use (LUS), rootzone-depth (RTZ), ponding-depths (PxA), infiltrative capacity (IxU), and runoff resistance (RxA).
Wells	WEL	Transient	- m m m ³ /d	Describes the location (x,y), depth, and screen length of each extraction wells per subsurface layer. Additionally, extraction volume per time unit can be added.
Drainage	DRN	Transient	m m ² /d	Characterization of the drainage pipe system, including the elevation and the conductance. Contains two individual layers for the top model layer. Drainage in urban areas has been excluded to prevent discontinuities.
River	RIV	Transient	- m ² /d m m	Defines river occurrence by four specifying layers: (1) location, (2) conductance, (3) bottom boundary, and (4) water level. Distinction is made between major rivers, regional waterways, and local streams.
Recharge	RCH	Transient	mm/d	Defines the fraction of precipitation that infiltrates and percolates to recharge groundwater.
Overland Flow	OLF	Transient	m	The input of the boundary elevation to which groundwater outflow to the land surface and surface water occurs for the top layer

Appendix B.3 AMIGO v3.1 runfile example: baseline scenario script lines 0 – 243 of 409,597.

```

'Z:\-----\STAGE_JASPER\AMIGO\RUNFILES\IMOD_USER\MODELS\BASELINE_100M'
  15  15  5753  0  1  0  0  1  0  0  1
Z:\-----\stage_jasper\AMIGO\DBase\Observation\ts_observation.ipf,2,1,2,3,4,5
1,0,0,0,1
500,15,0.100000E-02,0.100000E+02,0.995000E+00,1
  214337.000,  447686.000,  245057.000,  468053.000,  100.000,  1000.00
ACTIVE MODULES
1,0 (BND)
1,0 (KDW)
1,0 (VCW)
1,10,1,2,3,4,5,6,7,8,9,10 (SHD)
1,0 (STO)
1,0 (ANI)
1,0 (HFB)
1,1,1 (CAP)
1,1,1 (DRN)
1,0 (OLF)
1,1,1 (RIV)
1,0 (WEL)
'Z:\-----\stage_jasper\AMIGO\DBASE\AMIGO31\MODELGRENZEN\MODELGRENZEN.IDF'
MODULES FOR EACH LAYER
015,(BND) Boundary Condition
  1, 1.000000 , 0.000000 ,Z:\-----\stage_jasper\AMIGO\DBASE\AMIGO31\MODELGRENZEN\MODELGRENZEN.IDF'
  2, 1.000000 , 0.000000 ,Z:\-----\stage_jasper\AMIGO\DBASE\AMIGO31\MODELGRENZEN\MODELGRENZEN.IDF'
  3, 1.000000 , 0.000000 ,Z:\-----\stage_jasper\AMIGO\DBASE\AMIGO31\MODELGRENZEN\MODELGRENZEN.IDF'
  4, 1.000000 , 0.000000 ,Z:\-----\stage_jasper\AMIGO\DBASE\AMIGO31\MODELGRENZEN\MODELGRENZEN.IDF'
  5, 1.000000 , 0.000000 ,Z:\-----\stage_jasper\AMIGO\DBASE\AMIGO31\MODELGRENZEN\MODELGRENZEN.IDF'
  6, 1.000000 , 0.000000 ,Z:\-----\stage_jasper\AMIGO\DBASE\AMIGO31\MODELGRENZEN\MODELGRENZEN.IDF'
  7, 1.000000 , 0.000000 ,Z:\-----\stage_jasper\AMIGO\DBASE\AMIGO31\MODELGRENZEN\MODELGRENZEN.IDF'
  8, 1.000000 , 0.000000 ,Z:\-----\stage_jasper\AMIGO\DBASE\AMIGO31\MODELGRENZEN\MODELGRENZEN.IDF'
  9, 1.000000 , 0.000000 ,Z:\-----\stage_jasper\AMIGO\DBASE\AMIGO31\MODELGRENZEN\MODELGRENZEN.IDF'
 10, 1.000000 , 0.000000 ,Z:\-----\stage_jasper\AMIGO\DBASE\AMIGO31\MODELGRENZEN\MODELGRENZEN.IDF'
 11, 1.000000 , 0.000000 ,Z:\-----\stage_jasper\AMIGO\DBASE\AMIGO31\MODELGRENZEN\MODELGRENZEN.IDF'
 12, 1.000000 , 0.000000 ,Z:\-----\stage_jasper\AMIGO\DBASE\AMIGO31\MODELGRENZEN\MODELGRENZEN.IDF'
 13, 1.000000 , 0.000000 ,Z:\-----\stage_jasper\AMIGO\DBASE\AMIGO31\MODELGRENZEN\MODELGRENZEN.IDF'
 14, 1.000000 , 0.000000 ,Z:\-----\stage_jasper\AMIGO\DBASE\AMIGO31\MODELGRENZEN\MODELGRENZEN.IDF'
 15, 1.000000 , 0.000000 ,Z:\-----\stage_jasper\AMIGO\DBASE\AMIGO31\MODELGRENZEN\MODELGRENZEN.IDF'
015,(KDW) Transmissivity
  1, 1.000000 , 0.000000 ,Z:\-----\stage_jasper\AMIGO\DBASE\AMIGO31\kd-waarden\KD_1.IDF'
  2, 1.000000 , 0.000000 ,Z:\-----\stage_jasper\AMIGO\DBASE\AMIGO31\kd-waarden\KD_2.IDF'
  3, 1.000000 , 0.000000 ,Z:\-----\stage_jasper\AMIGO\DBASE\AMIGO31\kd-waarden\KD_3.IDF'
  4, 1.000000 , 0.000000 ,Z:\-----\stage_jasper\AMIGO\DBASE\AMIGO31\kd-waarden\KD_4.IDF'
  5, 1.000000 , 0.000000 ,Z:\-----\stage_jasper\AMIGO\DBASE\AMIGO31\kd-waarden\KD_5.IDF'
  6, 1.000000 , 0.000000 ,Z:\-----\stage_jasper\AMIGO\DBASE\AMIGO31\kd-waarden\KD_6.IDF'
  7, 1.000000 , 0.000000 ,Z:\-----\stage_jasper\AMIGO\DBASE\AMIGO31\kd-waarden\KD_7.IDF'
  8, 1.000000 , 0.000000 ,Z:\-----\stage_jasper\AMIGO\DBASE\AMIGO31\kd-waarden\KD_8.IDF'
  9, 1.000000 , 0.000000 ,Z:\-----\stage_jasper\AMIGO\DBASE\AMIGO31\kd-waarden\KD_9.IDF'
 10, 1.000000 , 0.000000 ,Z:\-----\stage_jasper\AMIGO\DBASE\AMIGO31\kd-waarden\KD_10.IDF'
 11, 1.000000 , 0.000000 ,Z:\-----\stage_jasper\AMIGO\DBASE\AMIGO31\kd-waarden\KD_11.IDF'
 12, 1.000000 , 0.000000 ,Z:\-----\stage_jasper\AMIGO\DBASE\AMIGO31\kd-waarden\KD_12.IDF'
 13, 1.000000 , 0.000000 ,Z:\-----\stage_jasper\AMIGO\DBASE\AMIGO31\kd-waarden\KD_13.IDF'
 14, 1.000000 , 0.000000 ,Z:\-----\stage_jasper\AMIGO\DBASE\AMIGO31\kd-waarden\KD_14.IDF'
 15, 1.000000 , 0.000000 ,Z:\-----\stage_jasper\AMIGO\DBASE\AMIGO31\kd-waarden\KD_15.IDF'
014,(VCW) Vertical Resistance
  1, 1.000000 , 0.000000 ,Z:\-----\stage_jasper\AMIGO\DBASE\AMIGO31\C-WAARDEN\LAAGK1-C-K.IDF'
  2, 1.000000 , 0.000000 ,Z:\-----\stage_jasper\AMIGO\DBASE\AMIGO31\C-WAARDEN\LAAGK2-C-K.IDF'
  3, 1.000000 , 0.000000 ,Z:\-----\stage_jasper\AMIGO\DBASE\AMIGO31\C-WAARDEN\LAAGK3-C-K.IDF'
  4, 1.000000 , 0.000000 ,Z:\-----\stage_jasper\AMIGO\DBASE\AMIGO31\C-WAARDEN\LAAGK4-C-K.IDF'
  5, 1.000000 , 0.000000 ,Z:\-----\stage_jasper\AMIGO\DBASE\AMIGO31\C-WAARDEN\LAAGK5-C-K.IDF'
  6, 1.000000 , 0.000000 ,Z:\-----\stage_jasper\AMIGO\DBASE\AMIGO31\C-WAARDEN\LAAGK6-C-K.IDF'
  7, 1.000000 , 0.000000 ,Z:\-----\stage_jasper\AMIGO\DBASE\AMIGO31\C-WAARDEN\LAAGK7-C-K.IDF'
  8, 1.000000 , 0.000000 ,Z:\-----\stage_jasper\AMIGO\DBASE\AMIGO31\C-WAARDEN\LAAGK8-C-K.IDF'
  9, 1.000000 , 0.000000 ,Z:\-----\stage_jasper\AMIGO\DBASE\AMIGO31\C-WAARDEN\LAAGK9-C-K.IDF'
 10, 1.000000 , 0.000000 ,Z:\-----\stage_jasper\AMIGO\DBASE\AMIGO31\C-WAARDEN\LAAGK10-C-K.IDF'
 11, 1.000000 , 0.000000 ,Z:\-----\stage_jasper\AMIGO\DBASE\AMIGO31\C-WAARDEN\LAAGK11-C-K.IDF'
 12, 1.000000 , 0.000000 ,Z:\-----\stage_jasper\AMIGO\DBASE\AMIGO31\C-WAARDEN\LAAGK12-C-K.IDF'
 13, 1.000000 , 0.000000 ,Z:\-----\stage_jasper\AMIGO\DBASE\AMIGO31\C-WAARDEN\LAAGK13-C-K.IDF'
 14, 1.000000 , 0.000000 ,Z:\-----\stage_jasper\AMIGO\DBASE\AMIGO31\C-WAARDEN\LAAGK14-C-K.IDF'
015,(SHD) Starting Heads
  1, 1.000000 , 0.000000 ,Z:\-----\stage_jasper\AMIGO\DBASE\AMIGO31\startstijghoogten\head_20160331_L1.IDF'
  2, 1.000000 , 0.000000 ,Z:\-----\stage_jasper\AMIGO\DBASE\AMIGO31\startstijghoogten\head_20160331_L2.IDF'
  3, 1.000000 , 0.000000 ,Z:\-----\stage_jasper\AMIGO\DBASE\AMIGO31\startstijghoogten\head_20160331_L3.IDF'
  4, 1.000000 , 0.000000 ,Z:\-----\stage_jasper\AMIGO\DBASE\AMIGO31\startstijghoogten\head_20160331_L4.IDF'
  5, 1.000000 , 0.000000 ,Z:\-----\stage_jasper\AMIGO\DBASE\AMIGO31\startstijghoogten\head_20160331_L5.IDF'
  6, 1.000000 , 0.000000 ,Z:\-----\stage_jasper\AMIGO\DBASE\AMIGO31\startstijghoogten\head_20160331_L6.IDF'
  7, 1.000000 , 0.000000 ,Z:\-----\stage_jasper\AMIGO\DBASE\AMIGO31\startstijghoogten\head_20160331_L7.IDF'
  8, 1.000000 , 0.000000 ,Z:\-----\stage_jasper\AMIGO\DBASE\AMIGO31\startstijghoogten\head_20160331_L8.IDF'
  9, 1.000000 , 0.000000 ,Z:\-----\stage_jasper\AMIGO\DBASE\AMIGO31\startstijghoogten\head_20160331_L9.IDF'
 10, 1.000000 , 0.000000 ,Z:\-----\stage_jasper\AMIGO\DBASE\AMIGO31\startstijghoogten\head_20160331_L10.IDF'
 11, 1.000000 , 0.000000 ,Z:\-----\stage_jasper\AMIGO\DBASE\AMIGO31\startstijghoogten\head_20160331_L11.IDF'
 12, 1.000000 , 0.000000 ,Z:\-----\stage_jasper\AMIGO\DBASE\AMIGO31\startstijghoogten\head_20160331_L12.IDF'
 13, 1.000000 , 0.000000 ,Z:\-----\stage_jasper\AMIGO\DBASE\AMIGO31\startstijghoogten\head_20160331_L13.IDF'
 14, 1.000000 , 0.000000 ,Z:\-----\stage_jasper\AMIGO\DBASE\AMIGO31\startstijghoogten\head_20160331_L14.IDF'
 15, 1.000000 , 0.000000 ,Z:\-----\stage_jasper\AMIGO\DBASE\AMIGO31\startstijghoogten\head_20160331_L15.IDF'
015,(STO) Confined Storage Coefficient

```

```

1, 1.000000 , 0.000000 ,0.1500000
2, 1.000000 , 0.000000 ,0.1000000E-03
3, 1.000000 , 0.000000 ,0.1000000E-03
4, 1.000000 , 0.000000 ,0.1000000E-03
5, 1.000000 , 0.000000 ,0.1000000E-03
6, 1.000000 , 0.000000 ,0.1000000E-03
7, 1.000000 , 0.000000 ,0.1000000E-03
8, 1.000000 , 0.000000 ,0.1000000E-03
9, 1.000000 , 0.000000 ,0.1000000E-03
10, 1.000000 , 0.000000 ,0.1000000E-03
11, 1.000000 , 0.000000 ,0.1000000E-03
12, 1.000000 , 0.000000 ,0.1000000E-03
13, 1.000000 , 0.000000 ,0.1000000E-03
14, 1.000000 , 0.000000 ,0.1000000E-03
15, 1.000000 , 0.000000 ,0.1000000E-03
004,(ANI) Anisotropy
3, 1.000000 , 0.000000 ,Z:\-----\stage_Jasper\AMIGO\DBASE\AMIGO31\ANISOTROPIE\anisotropiefactor.IDF'
4, 1.000000 , 0.000000 ,Z:\-----\stage_Jasper\AMIGO\DBASE\AMIGO31\ANISOTROPIE\anisotropiefactor.IDF'
5, 1.000000 , 0.000000 ,Z:\-----\stage_Jasper\AMIGO\DBASE\AMIGO31\ANISOTROPIE\anisotropiefactor.IDF'
6, 1.000000 , 0.000000 ,Z:\-----\stage_Jasper\AMIGO\DBASE\AMIGO31\ANISOTROPIE\anisotropiefactor.IDF'
3, 1.000000 , 0.000000 ,Z:\-----\stage_Jasper\AMIGO\DBASE\AMIGO31\ANISOTROPIE\anisotropiehoek.IDF'
4, 1.000000 , 0.000000 ,Z:\-----\stage_Jasper\AMIGO\DBASE\AMIGO31\ANISOTROPIE\anisotropiehoek.IDF'
5, 1.000000 , 0.000000 ,Z:\-----\stage_Jasper\AMIGO\DBASE\AMIGO31\ANISOTROPIE\anisotropiehoek.IDF'
6, 1.000000 , 0.000000 ,Z:\-----\stage_Jasper\AMIGO\DBASE\AMIGO31\ANISOTROPIE\anisotropiehoek.IDF'
004,(HFB) Horizontal Flow Barrier
3, 0.1000000E-02, 0.000000 ,Z:\-----\stage_Jasper\AMIGO\DBASE\AMIGO31\ANISOTROPIE\kleischotten.gen'
4, 0.1000000E-02, 0.000000 ,Z:\-----\stage_Jasper\AMIGO\DBASE\AMIGO31\ANISOTROPIE\kleischotten.gen'
5, 0.1000000E-02, 0.000000 ,Z:\-----\stage_Jasper\AMIGO\DBASE\AMIGO31\ANISOTROPIE\kleischotten.gen'
6, 0.1000000E-02, 0.000000 ,Z:\-----\stage_Jasper\AMIGO\DBASE\AMIGO31\ANISOTROPIE\kleischotten.gen'
030,(CAP) MetaSwap
1.000000 , 0.000000 ,Z:\-----\stage_Jasper\AMIGO\DBASE\AMIGO31\MODELGRENZEN\MODELGRENZEN.IDF'
1.000000 , 0.000000 ,Z:\-----\stage_Jasper\AMIGO\DBASE\AMIGO31\METASWAP\grd\Landgebruik.IDF'
1.000000 , 0.000000 ,Z:\-----\stage_Jasper\AMIGO\DBASE\AMIGO31\METASWAP\grd\Wortelzone.IDF'
1.000000 , 0.000000 ,Z:\-----\stage_Jasper\AMIGO\DBASE\AMIGO31\METASWAP\grd\Bodemkaart.IDF'
1.000000 , 0.000000 ,Z:\-----\stage_Jasper\AMIGO\DBASE\AMIGO31\METASWAP\grd\metestation.idf
1.000000 , 0.000000 ,Z:\-----\stage_Jasper\AMIGO\DBASE\AMIGO31\MAAIVELD\MV25_FILL.IDF'
0.000000 , 0.000000 ,Z:\-----\stage_Jasper\AMIGO\DBASE\AMIGO31\METASWAP\grd\beregening_locatie.idf
0.000000 , 0.000000 ,Z:\-----\stage_Jasper\AMIGO\DBASE\AMIGO31\METASWAP\grd\beregening_modellaag.idf
1.000000 , 0.000000 ,.25.00000
1.000000 , 0.000000 ,Z:\-----\stage_Jasper\AMIGO\DBASE\AMIGO31\METASWAP\grd\WTA_v30.IDF'
1.000000 , 0.000000 ,Z:\-----\stage_Jasper\AMIGO\DBASE\AMIGO31\METASWAP\grd\UBA_v30.IDF'
1.000000 , 0.000000 ,.999.0000
1.000000 , 0.000000 ,.1.000000
1.000000 , 0.000000 ,.1.000000
1.000000 , 0.000000 ,.1.000000
1.000000 , 0.000000 ,.1.000000
1.000000 , 0.000000 ,.1.000000
1.000000 , 0.000000 ,.1.000000
1.000000 , 0.000000 ,.1.000000
1.000000 , 0.000000 ,.1.000000
1.000000 , 0.000000 ,.1.000000
1.000000 , 0.000000 ,.1.000000
1.000000 , 0.000000 ,.1.000000
1.000000 , 0.000000 ,.1.000000
1.000000 , 0.000000 ,.1.000000
Z:\-----\stage_Jasper\AMIGO\DBASE\AMIGO31\METASWAP\inp\fact_svat.inp
Z:\-----\stage_Jasper\AMIGO\DBASE\AMIGO31\METASWAP\inp\luse_svat.inp
Z:\-----\stage_Jasper\AMIGO\DBASE\AMIGO31\METASWAP\inp\mete_grid.inp
Z:\-----\stage_Jasper\AMIGO\DBASE\AMIGO31\METASWAP\inp\para_sim.inp
Z:\-----\stage_Jasper\AMIGO\DBASE\AMIGO31\METASWAP\inp\tpop_sim.inp
Z:\-----\stage_Jasper\AMIGO\DBASE\AMIGO31\METASWAP\inp\init_svat.inp
Z:\-----\stage_Jasper\AMIGO\DBASE\AMIGO31\METASWAP\inp\sel_key_svat_per.inp
Z:\-----\stage_Jasper\AMIGO\DBASE\AMIGO31\METASWAP\inp\metaswap.sim
PACKAGES FOR EACH LAYER AND STRESS-PERIOD
00001, 1.0000000,20040401,1,20040402
3,(DRN) Drainage
1, 1.000000 , 0.000000 ,Z:\-----\stage_Jasper\AMIGO\DBASE\AMIGO31\DRAINAGE\conductance_duitsland.IDF'
1, 1.000000 , 0.000000 ,Z:\-----\stage_Jasper\AMIGO\DBASE\AMIGO31\DRAINAGE\conductance_buisdrainage.IDF'
1, 1.000000 , 0.000000 ,Z:\-----\stage_Jasper\AMIGO\DBASE\AMIGO31\OPPERVLAKTEWATER\ONTGRONDINGEN\conductance_ontgrondingen.IDF'
1, 1.000000 , 0.000000 ,Z:\-----\stage_Jasper\AMIGO\DBASE\AMIGO31\DRAINAGE\peil_duitsland.IDF'
1, 1.000000 , 0.000000 ,Z:\-----\stage_Jasper\AMIGO\DBASE\AMIGO31\DRAINAGE\peil_buisdrainage.IDF'
1, 1.000000 , 0.000000 ,Z:\-----\stage_Jasper\AMIGO\DBASE\AMIGO31\OPPERVLAKTEWATER\ONTGRONDINGEN\peil_ontgrondingen.IDF'
1,(OLF) Overland Flow
1, 1.000000 , 0.5000000E-01,Z:\-----\stage_Jasper\AMIGO\DBASE\AMIGO31\MAAIVELD\MV25_FILL.IDF'
9,(RIV) Rivers
1, 1.000000 , 0.000000 ,Z:\-----\stage_Jasper\AMIGO\DBASE\AMIGO31\OPPERVLAKTEWATER\RIVIER\Conductance_ISG_AMIGO.IDF'
1, 1.000000 , 0.000000 ,Z:\-----\stage_Jasper\AMIGO\DBASE\AMIGO31\OPPERVLAKTEWATER\LEGGER\conductance_legger_zomer.IDF'
1, 1.000000 , 0.000000 ,Z:\-----\stage_Jasper\AMIGO\DBASE\AMIGO31\OPPERVLAKTEWATER\TOP10\Conductance_TOP10_BREED_BUITEN.IDF'
1, 1.000000 , 0.000000 ,Z:\-----\stage_Jasper\AMIGO\DBASE\AMIGO31\OPPERVLAKTEWATER\TOP10\Conductance_TOP10_BREED_WRIJ.IDF'
1, 1.000000 , 0.000000 ,Z:\-----\stage_Jasper\AMIGO\DBASE\AMIGO31\OPPERVLAKTEWATER\TOP10\Conductance_TOP10_NORMAAL_BUITEN.IDF'
1, 1.000000 , 0.000000 ,Z:\-----\stage_Jasper\AMIGO\DBASE\AMIGO31\OPPERVLAKTEWATER\TOP10\Conductance_TOP10_NORMAAL_WRIJ.IDF'
1, 1.000000 , 0.000000 ,Z:\-----\stage_Jasper\AMIGO\DBASE\AMIGO31\OPPERVLAKTEWATER\TOP10\Conductance_TOP10_SMAL_BUITEN.IDF'
1, 1.000000 , 0.000000 ,Z:\-----\stage_Jasper\AMIGO\DBASE\AMIGO31\OPPERVLAKTEWATER\TOP10\Conductance_TOP10_SMAL_WRIJ.IDF'
1, 1.000000 , 0.000000 ,Z:\-----\stage_Jasper\AMIGO\DBASE\AMIGO31\OPPERVLAKTEWATER\TWENTE_KANAAL\Conductance_TWKANAL.IDF'
1, 1.000000 , 0.000000 ,Z:\-----\stage_Jasper\AMIGO\DBASE\AMIGO31\OPPERVLAKTEWATER\RIVIER\maandgem\STAGE_20040401.IDF'
1, 1.000000 , 0.000000 ,Z:\-----\stage_Jasper\AMIGO\DBASE\AMIGO31\OPPERVLAKTEWATER\LEGGER\peil_legger_zomer.IDF'
1, 1.000000 , 0.000000 ,Z:\-----\stage_Jasper\AMIGO\DBASE\AMIGO31\OPPERVLAKTEWATER\TOP10\Peil_TOP10_BREED_BUITEN.IDF'
1, 1.000000 , 0.000000 ,Z:\-----\stage_Jasper\AMIGO\DBASE\AMIGO31\OPPERVLAKTEWATER\TOP10\Peil_TOP10_BREED_WRIJ.IDF'
1, 1.000000 , 0.000000 ,Z:\-----\stage_Jasper\AMIGO\DBASE\AMIGO31\OPPERVLAKTEWATER\TOP10\Peil_TOP10_NORMAAL_BUITEN.IDF'
1, 1.000000 , 0.000000 ,Z:\-----\stage_Jasper\AMIGO\DBASE\AMIGO31\OPPERVLAKTEWATER\TOP10\Peil_TOP10_NORMAAL_WRIJ.IDF'
1, 1.000000 , 0.000000 ,Z:\-----\stage_Jasper\AMIGO\DBASE\AMIGO31\OPPERVLAKTEWATER\TOP10\Peil_TOP10_SMAL_BUITEN.IDF'
1, 1.000000 , 0.000000 ,Z:\-----\stage_Jasper\AMIGO\DBASE\AMIGO31\OPPERVLAKTEWATER\TOP10\Peil_TOP10_SMAL_WRIJ.IDF'

```


Appendix C

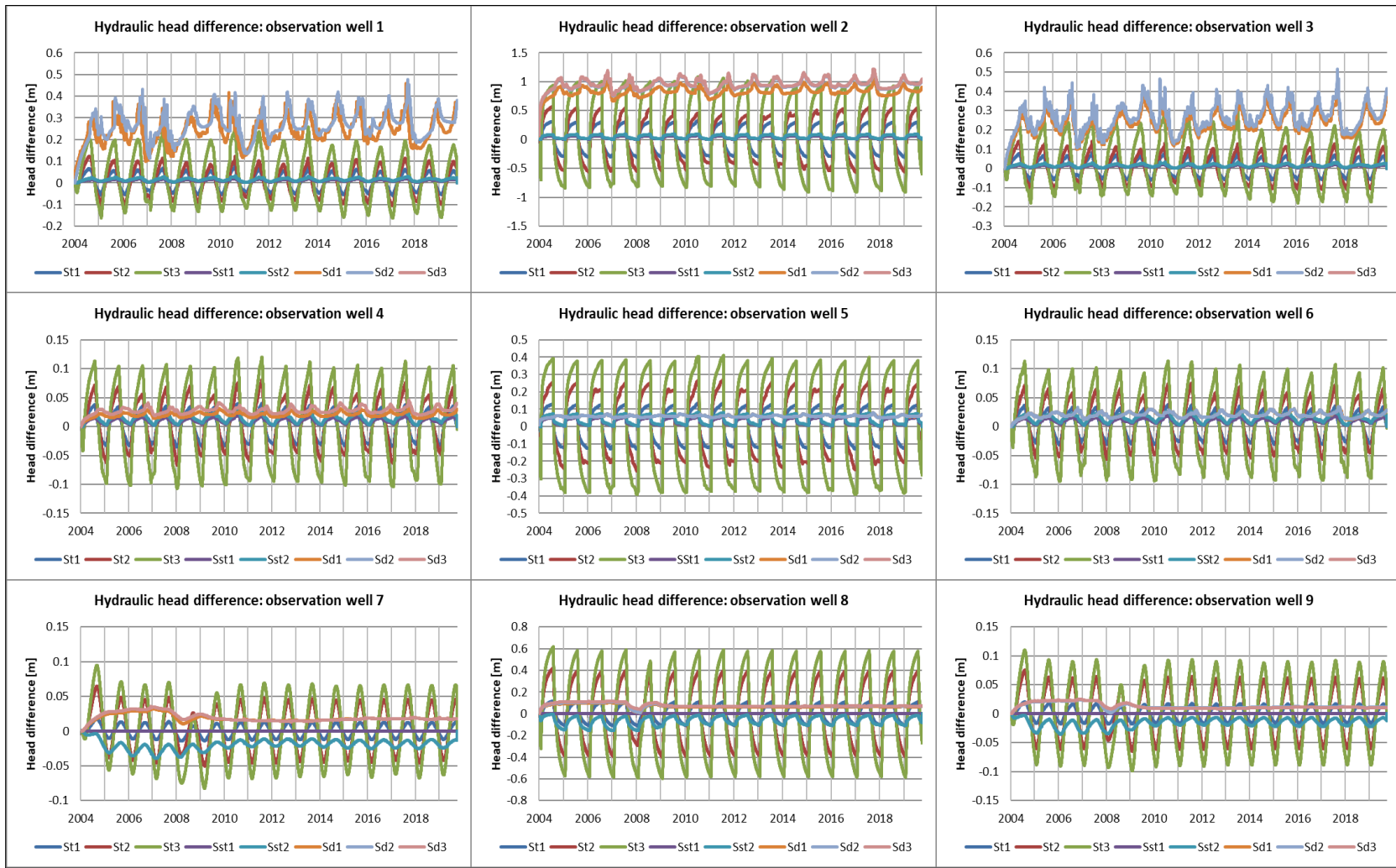
Complemented datafile decentralized consumers (resp. 2020) per supply system (Vitens, 2021).

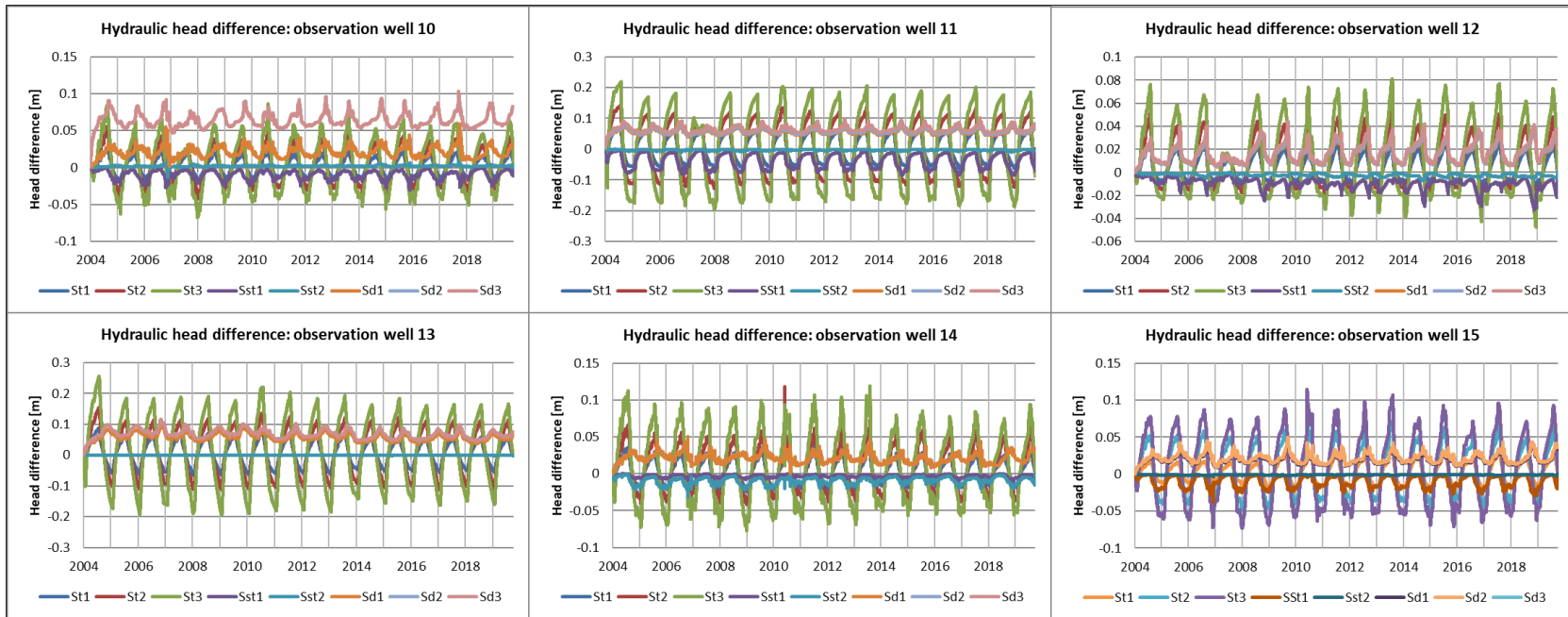
Nummer	Balansgebied	Postcode	x [RD]	y [RD]	Jaarverbruik [m ³ /yr]	Dagverbruik [m ³ /d]	Filterdiepte [m]	Geologische laag winning
1	't Klooster				754962.00	2097.12	-3.49 -- -14.82	4
2	't Klooster				405906.00	1127.52	-3.49 -- -14.82	4
3	't Klooster				109175.00	303.26	-3.19 -- -15.23	4
4	't Klooster				57675.00	160.21	-3.49 -- -14.82	4
5	't Klooster				8390.00	23.31	-3.49 -- -14.82	4
6	't Klooster				7994.00	22.21	-3.49 -- -14.82	4
7	't Klooster				7678.00	21.33	-3.19 -- -15.23	4
8	't Klooster				6476.00	17.99	-3.49 -- -14.82	4
9	't Klooster				5776.00	16.04	-3.49 -- -14.82	4
10	't Klooster				5408.00	15.02	-3.19 -- -15.23	4
11	't Klooster				5117.00	14.21	-3.49 -- -14.82	4
12	't Klooster				4307.00	11.96	-3.49 -- -14.82	4
13	't Klooster				4135.00	11.49	-3.49 -- -14.82	4
14	't Klooster				333900	9.28	-3.19 -- -15.23	4
15	Vorden				55140.00	153.17	-7.47 -- -19.72	4
16	Vorden				15370.00	42.69	-7.47 -- -19.72	4
17	Vorden				11726.00	32.57	-7.47 -- -19.72	4
18	Vorden				10848.00	30.13	-6.62 -- -21.61	4
19	Vorden				10490.00	29.14	-7.47 -- -19.72	4
20	Vorden	PRIVATIZED	PRIVATIZED	PRIVATIZED	4989.00	13.86	-6.62 -- -21.61	4
21	Vorden	PRIVATIZED	PRIVATIZED	PRIVATIZED	4717.00	13.10	-7.47 -- -19.72	4
22	Vorden	PRIVATIZED	PRIVATIZED	PRIVATIZED	4638.00	12.88	-7.47 -- -19.72	4
23	Vorden	PRIVATIZED	PRIVATIZED	PRIVATIZED	3962.00	11.01	-7.47 -- -19.72	4
24	Vorden	PRIVATIZED	PRIVATIZED	PRIVATIZED	3751.00	10.42	-7.47 -- -19.72	4
25	Vorden	PRIVATIZED	PRIVATIZED	PRIVATIZED	3725.00	10.35	-7.47 -- -19.72	4
26	Vorden				3481.00	9.67	-6.62 -- -21.61	4
27	Vorden				3421.00	9.50	-7.47 -- -19.72	4
28	Vorden				3072.00	8.53	-7.47 -- -19.72	4
29	Vorden				3064.00	8.51	-7.47 -- -19.72	4
30	Vorden				3012.00	8.37	-7.47 -- -19.72	4
31	Eibergen				167738.00	465.94	-3.42 -- -14.83	8
32	Eibergen				47480.00	131.89	-3.42 -- -14.83	8
33	Eibergen				26679.00	74.11	-3.42 -- -14.83	8
34	Eibergen				26380.00	73.28	-3.42 -- -14.83	8
35	Eibergen				12999.00	36.11	-3.42 -- -14.83	8
36	Eibergen				12673.00	35.20	-3.42 -- -14.83	8
37	Eibergen				10181.00	28.28	-3.42 -- -14.83	8
38	Eibergen				9596.00	26.66	-3.42 -- -14.83	8
39	Eibergen				7517.00	20.88	-3.42 -- -14.83	8
40	Eibergen				7313.00	20.31	-3.42 -- -14.83	8
41	Eibergen				5882.00	16.34	-3.42 -- -14.83	8
42	Eibergen				4989.00	13.86	-4.05 -- -13.67	8
43	Eibergen				4836.00	13.43	-3.42 -- -14.83	8

44	Eibergen		4662.00	12.95	-4.05 – -13.67	8
45	Eibergen		4528.00	12.58	-3.42 – -14.83	8
46	Eibergen		4151.00	11.53	-3.42 – -14.83	8
47	Eibergen		3388.00	9.41	-4.05 – -13.67	8
48	Eibergen		3311.00	9.20	-3.42 – -14.83	8
49	Eibergen		3204.00	8.90	-3.42 – -14.83	8
50	Eibergen		3068.00	8.52	-3.42 – -14.83	8

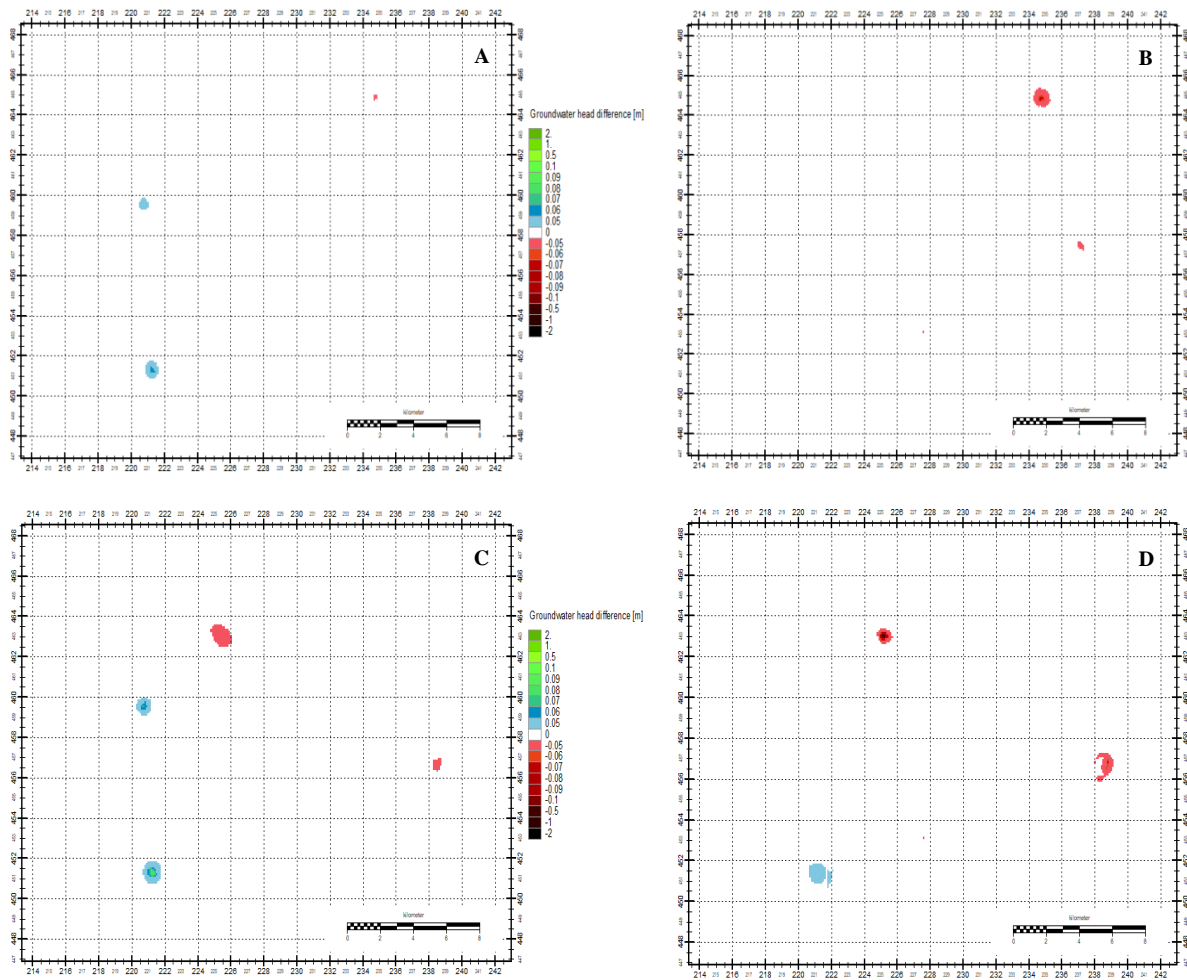
Appendix D

Appendix D.1 Timeseries showing the net differences in total phreatic groundwater head [m] between decentralized and seasonal scenarios to the baseline for all relevant observations wells. Positive difference values indicate an increased head under alternative scenarios. Negative values indicate a reversed situation.



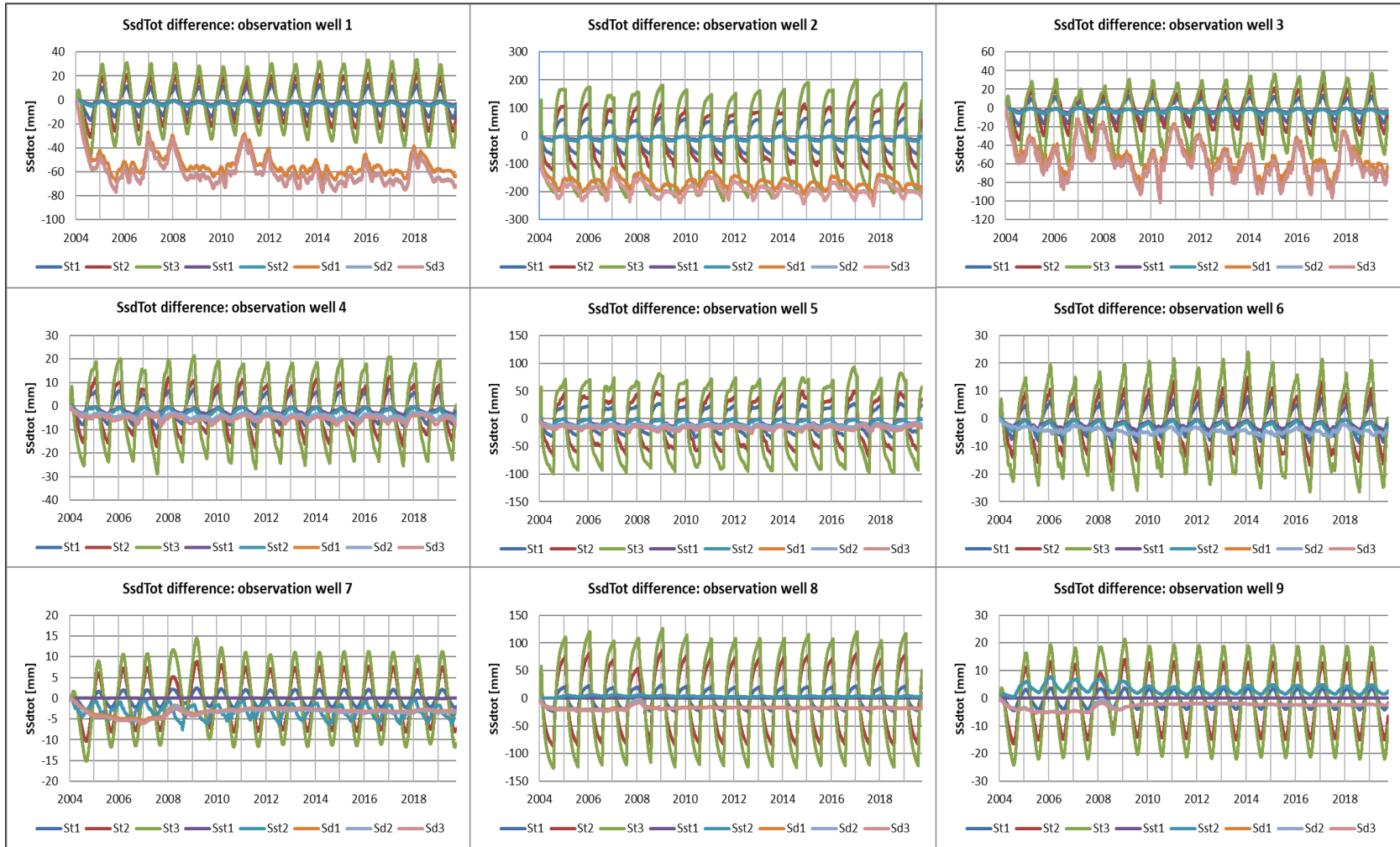


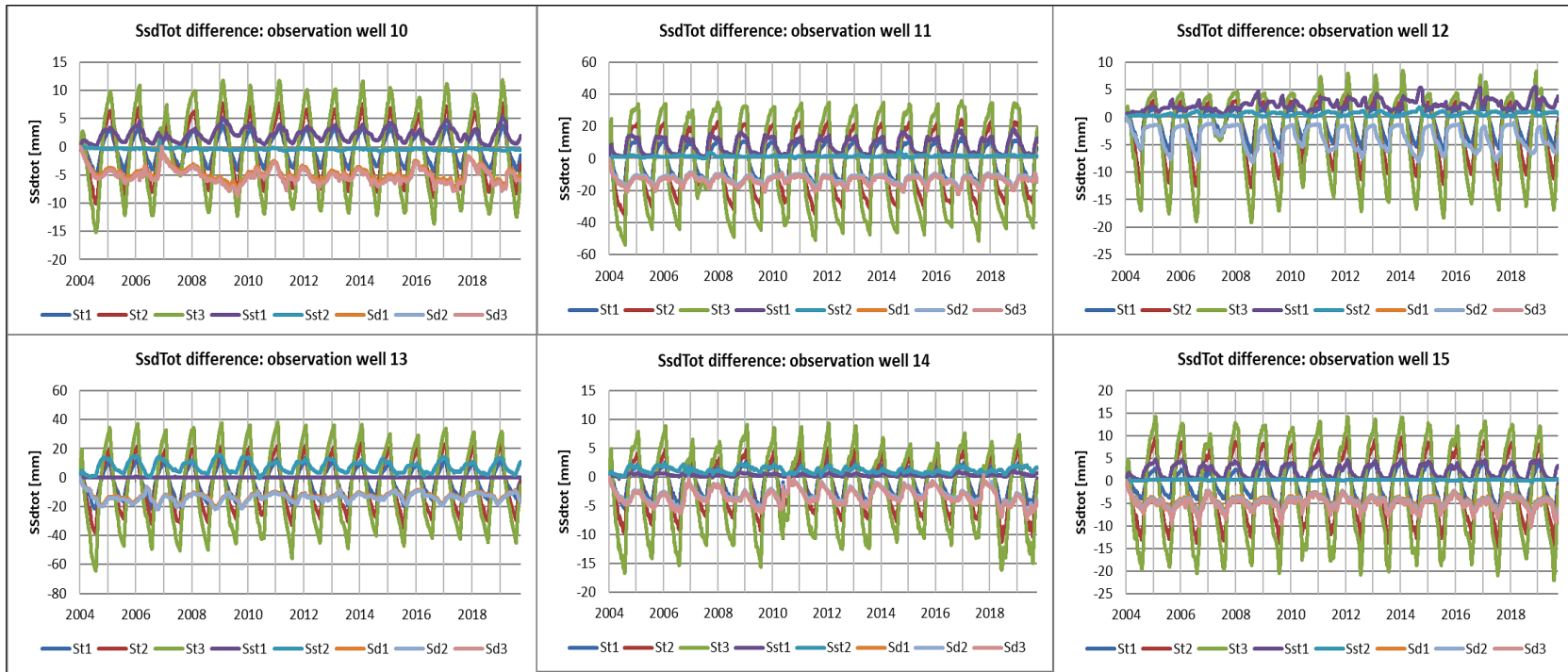
Appendix D.2 Regional daily difference maps showing the spatial extent of phreatic groundwater head changes [m] for the remaining seasonal scenarios compared to the baseline for both summer and winter. Difference maps in respective order: a) Sst1 summer, b) Sst1 winter, c) Sst2 summer, d) Sst2 winter.



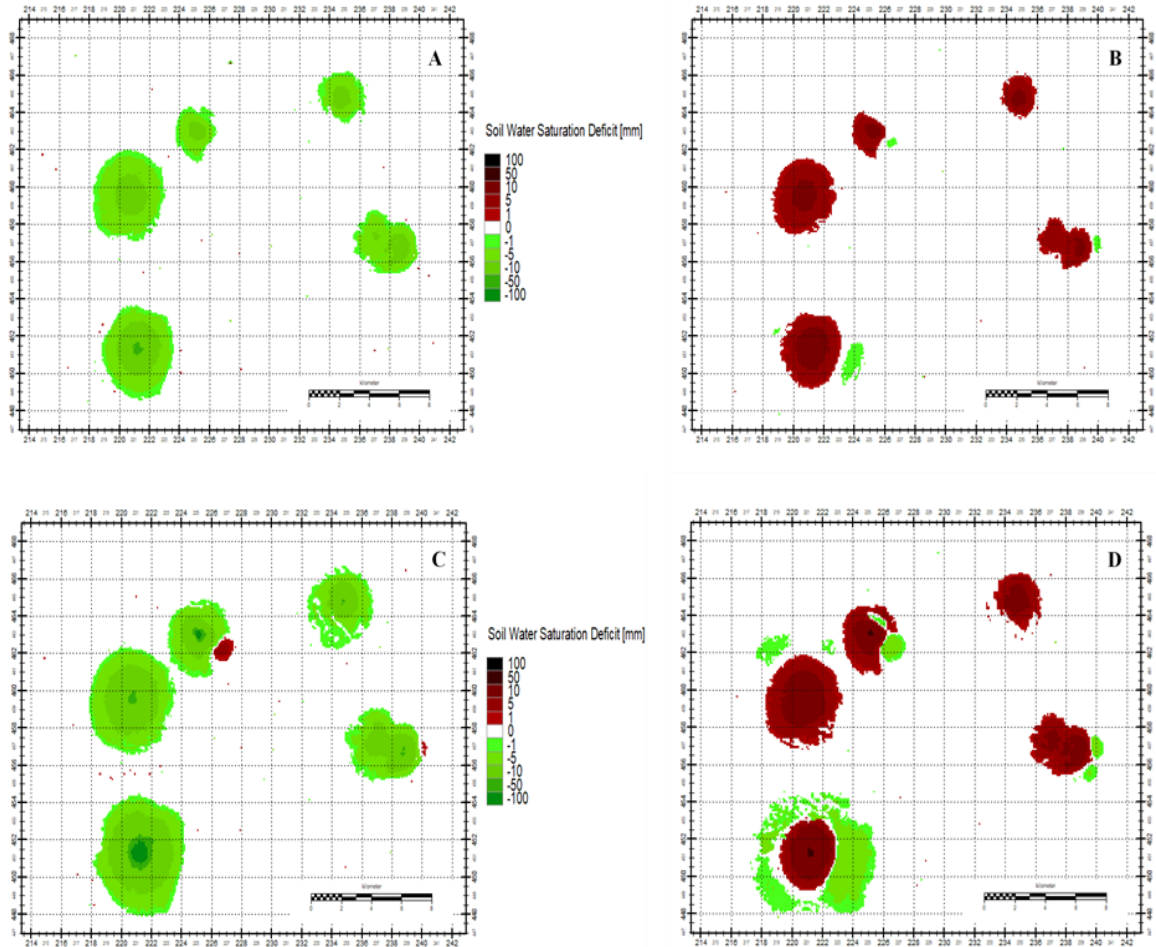
Appendix E

Appendix E.1 Timeseries showing the differences in total soil moisture saturation deficit [mm] between decentralized and seasonal scenarios to the baseline for all relevant observations wells. Negative difference values indicate a decrease in soil moisture deficits. Positive values indicate a reversed situation.



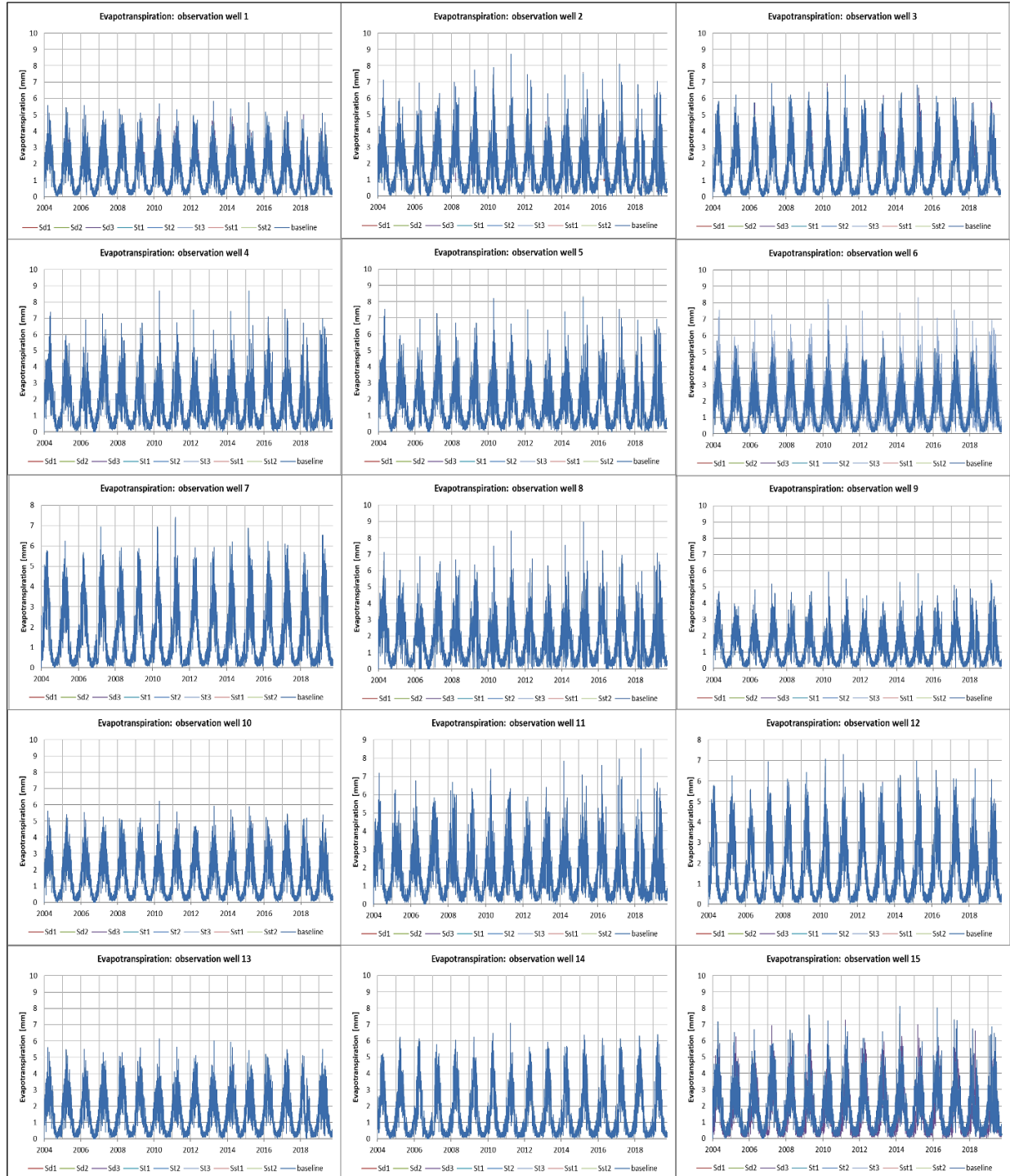


Appendix E.2 Regional daily difference maps showing the spatial extent of the soil water saturation deficit [mm] for the remaining seasonal scenarios compared to the baseline for both summer and winter. Difference maps in respective order: a) St1 summer, b) St1 winter, c) St3 summer, d) St3 winter.



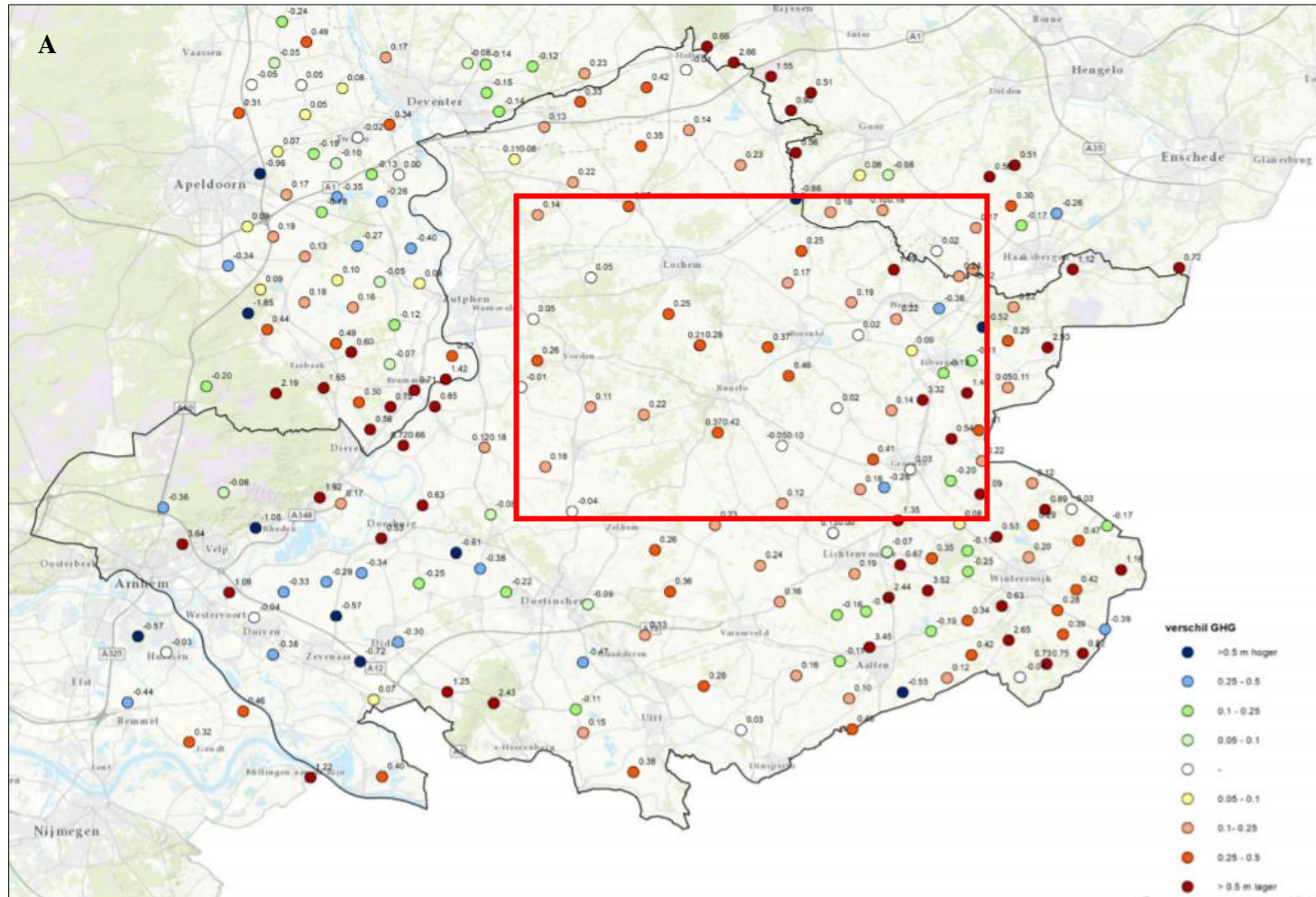
Appendix F

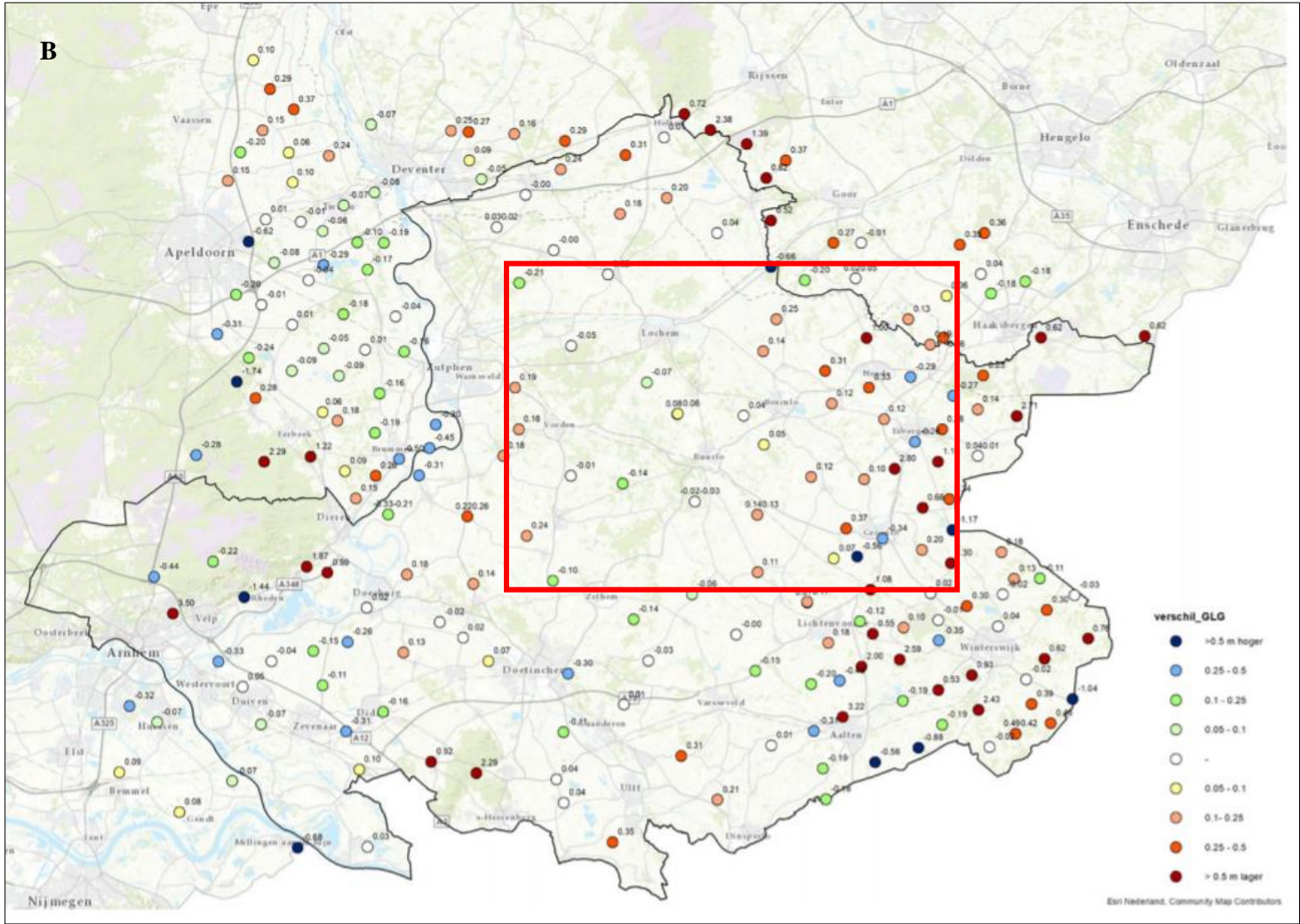
Time graphs of actual evapotranspiration rates [mm] for baseline and alternative scenarios over the entire simulation period for all relevant observation wells. Note that net differences between scenarios were minimal, resulting in an unavoidable overlay of lines with top visibility of the baseline scenario.



Appendix G

Uncertainty analysis of the validated AMIGO model. In respective order: a) Uncertainty dot-map GHG compared to measured data, b) Uncertainty dot-map GLG compared to measured data, c) Statistical uncertainty analysis of the validated model (de Weme et al., 2019). Red borders approximated the model cut-out.





C

